

Summer 8-2011

# Attenuated Total Reflection Infrared Spectroscopy (ATR-IR) as an In Situ Technique for Dissolution Studies

Abe S. Kassis  
*Seton Hall University*

Follow this and additional works at: <http://scholarship.shu.edu/dissertations>

 Part of the [Biochemistry Commons](#)

---

## Recommended Citation

Kassis, Abe S., "Attenuated Total Reflection Infrared Spectroscopy (ATR-IR) as an In Situ Technique for Dissolution Studies" (2011).  
*Seton Hall University Dissertations and Theses (ETDs)*. Paper 1432.

---

**Attenuated Total Reflection Infrared Spectroscopy (ATR-IR)  
as an *In Situ* Technique for Dissolution Studies**

by  
**Abe S. Kassis**

**Ph.D. DISSERTATION**

Submitted in partial fulfillment of the requirements for the degree of Doctor of Philosophy in  
the Department of Chemistry and Biochemistry of Seton Hall University


**Seton Hall University**  
Department of Chemistry and Biochemistry  
400 South Orange Avenue  
South Orange, New Jersey 07079  
**August 2011**

---

## DISSERTATION COMMITTEE APPROVALS

We certify that we have read this thesis and that in our opinion it is sufficient in scientific scope and quality as a dissertation for the degree of Doctor of Philosophy

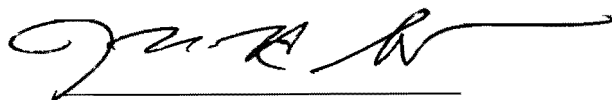
APPROVED BY:



---

John R. Sowa, Jr., Ph.D.

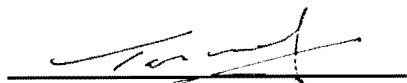
Advisor, Seton Hall University



---

Nicholas H. Snow, Ph.D.

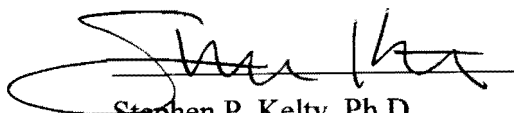
Member of Dissertation Committee, Seton Hall University



---

Tarun Patel, Ph.D.

Member of Dissertation Committee, Novartis Pharmaceuticals Corporation



---

Stephen P. Kelty, Ph.D.

Chair, Department of Chemistry and Biochemistry, Seton Hall University

---

*“Although nature commences with reason and ends in experience it is necessary for us to do the opposite, that is to commence with experience and from this to proceed to investigate the reason.”*

**-Leonardo da Vinci**

---

## **Abstract**

### **Attenuated Total Reflection Infrared Spectroscopy (ATR-IR) as an *in situ* Technique for Dissolution Studies**

Dissolution studies are critical tests for measuring the performance, or rate of release, of a drug product. There are many variables that affect the dissolution rate of the drug. Such variables may include characteristics of the active pharmaceutical ingredient (API) (e.g., particle size, crystal form, and bulk density), drug product composition (e.g., drug loading, and the identity, type, and levels of excipients), the drug product manufacturing process (e.g., compression forces, equipment), and the effects of stability storage conditions (e.g., temperature, humidity). Since dissolution has the ability to detect these variables, the regulatory agencies (i.e. FDA and EMEA) have placed great emphasis on the test. Moreover, the regulatory agencies have increased the monitoring and auditing of the dissolution test.

A novel technique using *in situ* attenuated total reflection-infrared spectroscopy (ATR-IR) to monitor dissolutions of pharmaceutical drug products was developed. The accuracy of this technique is  $\pm 3\%$  relative to HPLC. Salicylic acid calibrator tablets were studied and two over-the-counter (OTC) formulations containing acetaminophen, and/or acetylsalicylic acid were tested during the research. This novel approach was also used to analyze multiple components in a single tablet. For example, dissolution of the individual components of caffeine-free version of Excedrin® tablets, acetaminophen and acetylsalicylic acid were easily distinguished.

---

Furthermore, the system has the capability of monitoring the drug transformations during dissolution. For instance, this technique was used to monitor the dissolution and hydrolysis of aspirin to salicylic acid. The ATR-IR system was found to have good sensitivity and can analyze samples as low as 0.03 mg/mL ( $2 \times 10^{-4}$  M) based on the limit of detection (“LOD”) studies. This will be discussed in details in chapter four. This technique allows deeper insight into spectroscopy, reaction analysis, kinetics and dynamics of the dissolution of active components in a pharmaceutical formulation.

In addition, this novel system was used to support research related to the BP oil spill that occurred in the Gulf of Mexico during April 20th – June 3rd, 2010. Specifically, the system was used to study dispersion of oil in the presence of dishwashing soaps as preliminary models for commercial dispersants. Dawn® dishwashing soap was used because of its powerful claim to clean wildlife affected by oil spills. Dawn® specifically uses anionic surfactants, such as alkyl dimethyl amine oxide, to break down oil samples. These surfactants reduce the surface tension of water and can weaken the barrier that automatically forms between oil and water, allowing them to unnaturally mix.

Furthermore, in recognition of the potential of this technique to be widely used in the pharmaceutical industry for drug dissolution studies, an instrument was designed and the design is presented as a chapter in this dissertation. Overall, this work has discovered and validated the use of ATR-IR as a technique for monitoring to dissolution and dissolution/hydrolysis reactions of pharmaceutical formulations. It has excellent potential for studies of the dissolution of tablets especially multi-component tablets and tablets with ingredients that undergo subsequent hydrolysis.

---

## **Acknowledgments**

During my graduate career at Seton Hall University, I have had the privilege and opportunity to develop myself as a research scientist and strategic thinker. This would not have been possible without the support I received from my great employer Novartis Pharmaceuticals Corporation, for giving me the financial support and opportunity to obtain my doctorate degree. Moreover, I would like to give special thanks to Cynthia Cetani, Andre Wyss, Colleen Ruegger, Steffen Lang, Lynne Delisi and many others for their support and mentorship. Also, I would like to give special thanks to my research advisor Dr. John R. Sowa, Jr. for his valuable guidance, expertise, encouragement, and his dear friendship. Dr. Sowa inspires me to become a better scientist and individual.

I would also like to acknowledge Dr. Sowa's research group as well as the faculty members of the Department of Chemistry and Biochemistry at Seton Hall University. Specifically, I would like to give special appreciation to; Dr. Snow for encouraging, motivating and supporting my research ambitions, Dr. Kazakevich for his great guidance and teachings in HPLC, Dr. Kelty, Dr. Murphy, Dr. Fadeev and Dr. Marzabadi. I would also like to acknowledge Dr. Tarun Patel from the Novartis Pharmaceuticals Corporation for his guidance and mentoring throughout my studies. I will forever be indebted to those who have supported me through the years in this endeavor. It is with great appreciation that I offer my gratitude to all.

To my Dad and Mom, Sam and Nina Kassis for opening the door to science and motivating me to reach further in life. To my dear sisters, family and close friends.

---

Finally, I want to thank my wife, Cindy for her unwavering support. Also, I want to thank my daughter Amber and my son Neil for their support and understanding. Without them none of this would have been possible.

I would like to acknowledge Wes Walker and Jane Riley from Mettler-Toledo for technical support for the iC<sub>10</sub>IR Instrument.



---

## Table of contents

Table of contents .....	viii
List of figures .....	xii
List of tables .....	xviii
1 Introduction and Literature Overview .....	1
1.1 History .....	5
1.2 Infrared Spectroscopy .....	28
1.3 Literature background: in situ ATR-IR and dissolution.....	32
2 Dissolution of salicylic acid, acetylsalicylic acid and acetaminophen using <i>In Situ</i> ATR-IR spectroscopy .....	35
2.1 Experimental section .....	38
2.1.1 Chemical and materials .....	38
2.1.2 Instrumentation .....	39
2.1.3 Buffered solutions .....	40
2.1.4 Dissolution experiments.....	40
2.1.5 HPLC analysis.....	41
2.1.6 ATR-IR analysis .....	42
2.2 Results and discussion .....	44
2.2.1 Single-component analysis .....	44
2.2.2 Dissolution results for salicylic acid using pH 7.4 phosphate buffer ...	47

---

2.2.3	Multi-tablet analysis.....	50
2.2.4	Multi-component analysis.....	54
2.3	Chapter summary.....	60
3	Kinetics of drug hydrolysis of common over-the-counter (OTC) drugs via ATR-IR spectroscopy .....	61
3.1	Background and history of Aspirin .....	62
3.2	Experimental section .....	64
3.2.1	Chemical and materials.....	64
3.2.2	Instrumentation .....	66
3.2.3	Buffered solutions.....	66
3.2.4	Hydrolysis Experiments.....	67
3.2.5	ATR-IR analysis .....	67
3.3	Results and discussion.....	71
3.3.1	Hydrolysis of aspirin to salicylic acid in test tubes.....	71
3.3.2	Hydrolysis of aspirin to salicylic acid using aspirin tablet as the starting ingredient .....	74
3.3.3	Hydrolysis of aspirin to salicylic acid using aspirin powder as the starting ingredient .....	77
3.3.4	Hydrolysis data: comparison between tablet and powder formulations .....	79
3.3.5	Kinetic rates observed during hydrolysis experimentation.....	84

---

3.4	Chapter summary .....	87
4	Instrument Development Proposal: "Solv-IR" as an <i>In-Situ</i> ATR-IR Instrument for Solvation Chemistry .....	89
4.1	Background.....	89
4.2	Broader impacts from the proposed activities .....	92
4.3	Limit of detection (LOD) and limit of quantitation (LOQ) data .....	93
4.4	Instrument design .....	101
4.5	System components .....	104
4.5.1	Radiation source.....	104
4.5.2	Interferometer.....	104
4.5.3	Two Six-device Multiplexors.....	104
4.5.4	Six ATR Probes.....	104
4.5.5	Detector .....	105
4.5.6	Six Solvation Vessels.....	105
4.6	Instrument Control/ Acquisition/ Processing .....	109
4.7	Anticipated technical difficulties.....	109
4.8	Chapter summary.....	109
5	Analysis of the BP Gulf oil spill by Attenuated Total Reflection-Infrared Spectroscopy and Dissolution .....	112
5.1	Research with React-IR.....	114
5.2	Experimental section .....	117

---

5.2.1	Chemical and materials .....	117
5.2.2	Instrumentation .....	121
5.2.3	Dispersant stock solution .....	123
5.2.4	Crude oil sample preparation .....	123
5.2.5	ATR-IR analysis .....	124
5.3	Results .....	124
5.3.1	Standards and expected absorption values.....	125
5.3.2	Venice oil samples dispersed using Joy soap.....	130
5.3.3	Venice oil samples dispersed using Dawn® soap.....	133
5.3.4	Analysis by UV-Vis Spectroscopy .....	137
5.4	Chapter summary .....	142
6	Research conclusions .....	143
7	Appendix [A]: <i>In situ</i> ATR-IR Spectroscopy and Dissolution Data.....	146
8	Appendix [B]: Studying drug kinetics via ATR-IR Spectroscopy.....	163
9	Appendix [C]: New Instrument Design (“Solv-IR”) attachments.....	167
10	Appendix [D]: BP Gulf oil research attachments.....	168

---

## List of figures

Figure 1-1	Dissolution apparatus: Noyes and Whitney (Ref 1) (Figure reproduced from bottle figure in article).....	6
Figure 1-2	Dissolution process .....	13
Figure 1-3	Importance of sink conditions in dissolution: dissolution of benzoic acid at low concentrations: Underwood and Cadwallader (Ref 8) (Figure reproduced from figure-1 in article).....	16
Figure 1-4	Importance of sink conditions in dissolution: dissolution of benzoic acid at higher concentrations: Underwood and Cadwallader (Ref 8) (Figure reproduced from figure-3 in article).....	17
Figure 1-5	Schematic illustration of Apparatus 1 and Apparatus 2 (Reproduced from USP General Chapter on Dissolution <711>) .....	22
Figure 1-6	USP Apparatus 1 Specifications (Reproduced from USP General Chapter on Dissolution <711>).....	24
Figure 1-7	USP Apparatus 2 specifications (Reproduced from USP General Chapter on Dissolution <711>).....	25
Figure 1-9	FT-IR system schematic (Ref 23) .....	31
Figure 2-1	Salicylic acid spectra at different concentrations in pH 7.4 phosphate buffered solution. ....	45

---

Figure 2-2	Comparison of <i>in situ</i> ATR-IR and HPLC methods for dissolution of a salicylic acid tablet.....	48
Figure 2-3	Calibration curves of acetaminophen standards at pH 5.8: UV/Vis absorbance at 296 nm and IR peak intensity at 1246 cm <sup>-1</sup> .....	51
Figure 2-4	Simultaneous dissolution of acetaminophen and salicylic acid tablets: <i>in situ</i> ATR-IR vs. HPLC .....	53
Figure 2-5	ATR-IR spectra of Excedrin® caplets at different time-points during dissolution in pH 7.4 phosphate buffered solution .....	55
Figure 2-6	Dissolution of acetylsalicylic acid and acetaminophen in Excedrin® caplets: <i>in situ</i> ATR-IR vs. HPLC .....	56
Figure 2-7	Compounds studied/of interest for future work .....	59
Figure 3-1	Structures of acetylsalicylic acid (aspirin).....	62
Figure 3-2	Synthesis of aspirin-late 1800's.....	63
Figure 3-3	Chemical structures studied .....	65
Figure 3-4	Ferric chloride color test- control samples.....	72
Figure 3-5	Waterfall plot of aspirin tablet dissolution.....	75
Figure 3-6	Hydrolysis of Aspirin Tablets (325 mg) in pH 1.2 SGF Solution (n=2).....	76
Figure 3-7	Ferric chloride color test for salicylic acid (tablet dissolution) .....	76
Figure 3-8	Hydrolysis of acetylsalicylic acid powder to salicylic acid hydrosylate in pH 1.2 solution .....	78

Figure 3-9	Release profile of Salicylic Acid (“SA”) during hydrolysis in SGF (pH1.2): powder vs. tablet.....	81
Figure 3-10	Release profile of acetylsalicylic acid (aspirin) during hydrolysis: powder vs. tablet .....	82
Figure 3-11	Release profile of acetylsalicylic acid (aspirin) and salicylic acid hydrosylate during hydrolysis: powder vs. tablet .....	83
Figure 3-12	Typical calculation plot of rate from dissolution .....	86
Figure 3-13	Rate of dissolution for Aspirin (based on slope of dissolution plot) ....	86
Figure 4-1	Limit of detection of ATR-IR system .....	95
Figure 4-2	Fiber optic probes specifications (ref 56) .....	96
Figure 4-3	Calculated LOD and LOQ values .....	97
Figure 4-4	LOD/LOQ Sample Calculation Sheet- DiComp Probe Results-1 .....	98
Figure 4-5	LOD/LOQ Sample Calculation Sheet- Flow Cell Probe Results-1 ....	100
Figure 4-6	Diagram of proposed Solv-IR Instrument.....	103
Figure 4-7	Sketch of ATR crystal embedded in the side wall of the 1 L glass vessel. The area directly under the stir shaft is known to have poor mixing and as indicated by the term “dead zone”.....	106
Figure 4-8	Top plate of constant rpm stirring assembly showing motor, main gear and minor gears which drive the stir shafts in each vessel .....	108
Figure 5-1	Photo of oil rig similar to Deepwater Horizon.....	113
Figure 5-2	Aerial view: location of BP Gulf oil samples .....	118

---

Figure 5-3	Zoom view: location of BP Gulf oil samples [Both samples were collected near the UNO site].....	119
Figure 5-4	Ocean depth diagram showing location of BP Gulf oil samples (reproduced and modified from Ref 71) .....	120
Figure 5-5	Instrument photo: ATR-IR and dissolution apparatus .....	121
Figure 5-6	Gulf oil vs. blank (ocean water) standard spectra .....	127
Figure 5-7	Baseline corrected: ATR-IR scans of BP oil and Ocean Water samples.....	128
Figure 5-8	Photo of vessels at different time points during the dispersion experiments .....	129
Figure 5-9	ATR-IR scans of Venice oil and 50 mL of Joy soap .....	131
Figure 5-10	ATR-IR scans of 50 mL of Joy soap only (Blank solution) .....	132
Figure 5-11	ATR-IR scans of Venice oil and 50 mL of Dawn® soap .....	134
Figure 5-12	ATR-IR scans of 50 mL of Dawn® soap only (Blank solution) .....	135
Figure 5-13	Visible spectra of chlorophyll a and b .....	139
Figure 5-14	Chemical structure of chlorophyll a (Chem. Draw).....	140
Figure 5-15	Chemical structure of chlorophyll b (Chem. Draw) .....	140
Figure 5-16	UV/Vis spectra of BP oil samples in different solvents: 1 mm cell: spectrophotometer fully covered from outside lighting.....	141
Figure 7-1	Linearity of salicylic acid in pH 7.4 phosphate buffer (corresponds to Figure 2-1 in Chapter 2).....	153



---

Figure 7-2	Linear regression chart for salicylic acid .....	154
Figure 7-3	Dissolution results for salicylic acid in pH 7.4 phosphate buffer: HPLC vs. IR data (corresponds to Figure 2-2 in Chapter 2).....	155
Figure 7-4	ATR-IR System photo.....	156
Figure 7-5	Mettler Toledo ATR-IR/ Dissolution Systems .....	157
Figure 7-6	Flow Cell Fiber Optic Probe:.....	158
Figure 7-7	K4 Fiber Optic Probe .....	159
Figure 7-8	HPLC analysis for Salicylic Acid calibrator tablets .....	160
Figure 7-9	HPLC Method Parameters: Single Component and Multi Component Experiments.....	161
Figure 7-10	Typical Excedrin® experiment spectra.....	162
Figure 7-11	Excedrin® HPLC Data .....	162
Figure 8-1	Salicylic Acid standard spectra.....	163
Figure 8-2	Acetylsalicylic Acid standard spectra .....	164
Figure 8-3	Rate Order Formulas and Equations (Reproduced from Wikipedia website on Rate Order) .....	166
Figure 9-1	ATR-IR Technique Diagram (courtesy of Jian Wang, Ph.D., Mettler Toledo) .....	167
Figure 10-1	Detergents used during BP Gulf oil research.....	168
Figure 10-2	IR Spectra of Gulf Oil from Riser: Pre- April 20, 2010 .....	169
Figure 10-3	Thermo Nicolet 4700: % Transmittance of OIL samples .....	171

---

Figure 10-4	Thermo Nicolet 4700: Absorbance of OIL samples ..... 172
-------------	--

---

## List of tables

Table 1-1	Dissolution apparatus in the pharmaceutical industry .....	20
Table 1-2	Absorption bands (Ref 21) (Reproduced from table of frequencies found on CSU Website link).....	29
Table 2-1	Phosphate buffer preparations as per United States Pharmacopeia (USP).....	40
Table 2-2	Method development summary for Salicylic Acid (Linearity and Dissolution results) .....	46
Table 2-3	% Dissolved of salicylic acid: Absolute % dissolved difference between ATR-IR and HPLC results.....	49
Table 2-4	Dissolution of acetylsalicylic acid (aspirin) and acetaminophen in Excedrin® caplets: ATR-IR raw data .....	57
Table 2-5	Dissolution of acetylsalicylic acid (aspirin) and acetaminophen in Excedrin® caplets: HPLC raw data .....	58
Table 2-6	% Dissolved of acetaminophen: Difference between ATR-IR and HPLC results .....	58
Table 2-7	% Dissolved acetylsalicylic acid (aspirin) analysis: Difference between ATR-IR and HPLC results.....	58
Table 3-1	Hydrochloric acid buffer preparations as per United States Pharmacopeia (USP) .....	67
Table 3-2	Ferric chloride color test concentrations .....	73

---

Table 3-3	Ferric chloride color test observations [added 2mg /ml Fe (III) solution] .....	73
Table 3-4	Kinetic rates for hydrolysis of aspirin in acidic medium .....	85
Table 4-1	LOD/LOQ Sample Calculation Sheet- DiComp Probe Result-2 .....	99
Table 5-1	Chemicals used in commercial dispersants (COREXIT 9500 and 9527) .....	116
Table 5-2	Experimental details and sample information.....	122
Table 5-3	Expected FT-IR stretching values for crude oil and sulfonated soaps.....	126
Table 5-4	Amount of Dawn® in solution.....	136
Table 5-5	Amount of BP oil in solution .....	136
Table 5-6	% Dispersant calculated .....	136
Table 8-1	Aspirin FT-IR Frequencies of Interest.....	165
Table 10-1	Amount of Dawn® dishwashing detergent added .....	170

---

## Abbreviations

ATR	Attenuated Total Reflection
ATR-IR	Attenuated Total Reflection-Infrared Spectroscopy
API	Active Pharmaceutical Ingredient
ASA	Acetylsalicylic acid
BA	Bioavailability
BE	Bioequivalence
Disso	Dissolution
EPA	Environmental Protection Agency
FDA	Food and Drug Administration
GI	Gastrointestinal
HCl	Hydrochloric Acid
HPLC	High Performance Liquid Chromatography
HPMC	Hydroxypropylmethylcellulose
IR	Infrared Spectroscopy
LOD	Limit of Detection
LOQ	Limit of Quantitation
MDL	Method Detection Limit
MCT	Mercury-Cadmium-Telluride
NSF	National Science Foundation
OTC	Over the Counter
PEG	Poly (ethylene glycol)
RPM	Revolutions per Minute
SA	Salicylic acid
SGF	Simulated Gastric Fluid
TFA	Trifluoroacetic acid
USP	United States Pharmacopeia
UV	Ultra-Violet
Vis	Visible

## 1 Introduction and Literature Overview

Dissolution is a critical test for measuring the performance of a pharmaceutical formulation. The overall performance of the drug pertains to the rate of release of the drug. There are many variables that affect the dissolution rate of the drug. Recently, the importance of the dissolution test has increased substantially as indicated by the high level of regulations imposed on the industry by the various health agencies around the world. Dissolution testing plays several important roles in the pharmaceutical industry. First, the test is a quality control tool that measures change in composition of the formulation. Some of the relevant changes the dissolution test is able to detect include changes caused by temperature, humidity and photosensitivity. Second, the test is also important for formulation development. During development of a drug product, the formulators use the dissolution test to distinguish between different variations of the drug product. Such variations may include characteristics of the active pharmaceutical ingredient (API) (e.g., particle size, crystal form, and bulk density), drug product composition (e.g., drug loading, and the identity, type, and levels of excipients) and the drug product manufacturing process (e.g., compression forces, equipment). In the pharmaceutical industry it is important to produce several variations of the drug product since these are needed to assess the drugs' performance in clinical trials. From the clinical trials, the efficacy of the variants are distinguished and obtained. Third, once *in vivo* (clinical trials) data has been established for the drug product, a correlation between *in vivo* (human blood data)/*in vitro* (lab dissolution results) is made using the dissolution studies.

Dissolution, as per the IUPAC, is defined as the mixing of two phases with the formation of one new homogeneous (i.e. the solution) phase and is pharmaceutically defined as the rate of mass transfer from a solid surface into the dissolution medium or solvent under standardized conditions of liquid/solid interface, temperature and solvent composition.<sup>1</sup> It is a dynamic property that changes with time and explains the process by which a homogenous mixture of a solid or a liquid can be obtained in a solvent. It happens to chemically occur by the crystal break down into individual ions, atoms or molecules and their transport into the solvent.<sup>2</sup> Dissolution is controlled by the affinity between the solid substance and the solvent. Moreover, the dissolution rate plays an important role in the understanding the chemistry of solvation. The dissolution rate is defined as the amount of drug substance that goes into solution per unit time under standardized conditions of liquid/solid interface, temperature and solvent composition.

In order for drug molecules to be transported into solution, they must detach from the solid surface and form solvated molecules. This phenomenon is known as solvation. Regardless of whether a solid is crystalline or amorphous, neighboring molecules are closely associated with each other through intermolecular forces. The dissolution process involves two main steps: the first step is the interaction between the solid and solvent molecules (solvation). The second step is the mass transport of solvated molecules to the bulk solution. Solubility controls the first step while transport controls the second. The first step of dissolution is considered a physico-chemical reaction. The solvation process is reversible, and solubility is

---

<sup>1</sup> IUPAC, Compendium of Chemical Terminology, 2nd ed. (the "Gold Book") (1997). Online corrected version: (2006–) "dissolution".

<sup>2</sup> Dressman, J. J.; Kramer, J. K., Eds. *Pharmaceutical Dissolution Testing*; Taylor and Francis: Florida, 2005.

reached when the reaction reaches equilibrium. The dissolution process can also be described by the Gibbs free energy equation shown below:

**(Equation 1)**

$$\Delta G = \Delta H - T\Delta S$$

This reaction involves the breaking and formation of new intermolecular interactions. The net entropy is usually positive in dissolution since dissolution favors disorder. Moreover, the net enthalpy plays a crucial role in this equation. Dissolution is usually determined by the net enthalpy change. If the net enthalpy is less than or equal to zero, then the reaction will occur until all solid particles are dissolved. However, if the net enthalpy is positive, the reaction will occur until equilibrium is reached. In addition, the reaction rates in dissolution could be described kinetically by the following equations:

**(Equation 2)**

$$V = K_1[Drug][Solvent]$$

**(Equation 3)**

$$K_1 = Ae^{-Ea/RT}$$

Where V is the reaction rate, Ea is the activation energy, R is a constant and T is temperature. The rate of dissolution is governed by the slower step of the two step process mentioned earlier. Therefore, at room temperature, the rate of solvation is so fast that equilibrium is



typically instantaneous. The mass transport step is usually much slower and becomes the rate limiting step in the dissolution process.<sup>3</sup>

Next, this chapter of the thesis will focus on describing the history of dissolution testing which has led to many types of pharmaceutical dosage forms as well as different types of apparatus systems. Even though there is increased interest in this area, the techniques used for studying dissolution rates remain fairly constant. In fact, there are only a handful of instruments used to analyze and understand the dissolution rates of drugs. This chapter will also discuss the current techniques used for dissolution testing.

Last but not least, a thorough literature search into the use of ATR-IR spectroscopy as a dissolution technique was made and will be discussed in this chapter. The research has found that FTIR imaging and NIR spectroscopy have been used to study dissolution testing. Although FTIR imaging utilizes the same spectroscopic region as the proposed research, it is more of a qualitative test than a quantitative one. Furthermore, NIR was used to study dissolving reactions. The major weakness of the NIR region is that the absorption bands occurring there are the overtones of the fundamental bands residing in the mid-IR region. As a result, they are relatively weak and not clearly delineated. This makes quantitative calculations complex and calibration procedures quite laborious and not transferable from one instrument to another. This research focuses on the mid-IR region. The mid-IR spectral region is where most of the fundamental structural information is produced. Also, because molecules differ from each other by having different combinations of functional groups, their mid-IR spectra can be used to identify them and characterize their structure.

---

<sup>3</sup> Hanson, R; Gray, V. Handbook of Dissolution Testing, 3rd ed., *Dissolution Technologies*: Delaware, 2004.

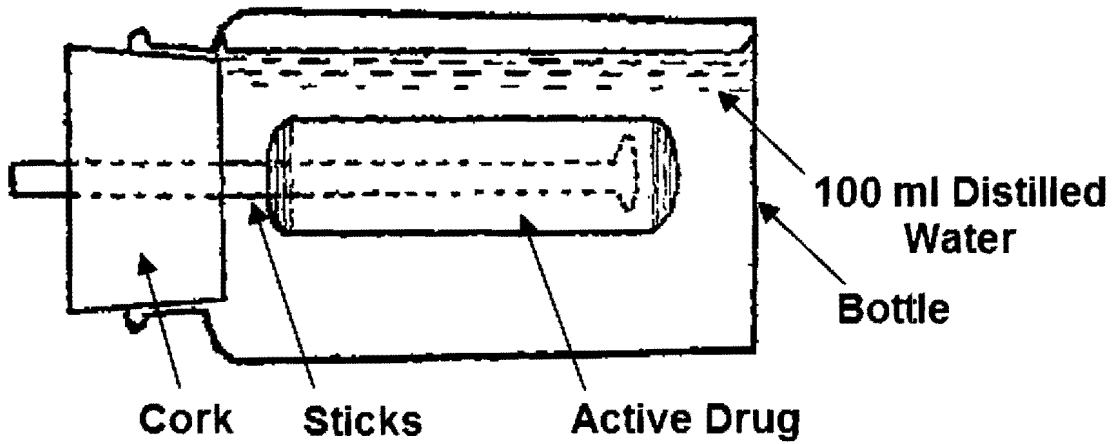
## 1.1 History

The earliest theories of the dissolution were based on physicochemical properties. The earliest reference to dissolution dates back to 1897 when Noyes and Whitney published an article entitled, "The Rate of Solution of Solid Substances in Their Own Solution."<sup>4</sup> Noyes and Whitney investigated the phenomenon of dissolution by using two slightly soluble substances; benzoic acid and lead chloride. They developed a rotating bottle technique coupled with a titration method to determine the dissolution rates of these two active drugs. Refer to Figure 1-1 for a schematic diagram of the first dissolution apparatus.

---

<sup>4</sup> Noyes, Arthur A.; Whitney, Willis R. The rate of solution of solid substances in their own solutions. *Journal of the American Chemical Society* **1897**, *19(12)*, 930-934.

Figure 1-1 Dissolution apparatus: Noyes and Whitney (Ref 1) (Figure reproduced from bottle figure in article).



**BOTTLE INSERTED IN THERMOSTATED BATH**

Noyes and Whitney determined that the velocity of the solution is proportional to the difference between the concentration of the saturated solution and that of the solution present at the moment in question. They determined the following dissolution rate equation as shown in the equation 4 below:

**(Equation 4)**

$$\frac{dx}{dt} = C (S - x)$$

where S represents the solubility of the substance (mg/mL), x the concentration (usually mg or mmol) at the expiration of the time t (seconds) and C is a constant. Integration of the equation above gives equation 5:

**(Equation 5)**

$$C = \frac{1}{T} \log_e \frac{S}{(S - x)}$$

In order to obtain values for C in the equation, the solubility or S of the substance must be known. In addition, Noyes and Whitney found that the dissolution rate is controlled by a thin layer of saturated solution that forms instantly around a solid particle. Also, the rate at which a solid substance dissolves in its own solution is proportional to the difference between the concentration of the solution and the concentration of the saturated solution.

In 1904, Nernst and Brunner modified the Noyes-Whitney equation by applying Fick's law of diffusion.<sup>5</sup> They were able to show a relationship between the dissolution rate constant and

---

<sup>5</sup> Nernst, W.; Brunner, E. Velocity of Reaction in Non-Homogeneous System. *Physical Chemistry* **1904**, *47*, 56-102.

the diffusion coefficient. Refer to equation 6. The equation for Fick's law of diffusion is shown below:

**(Equation 6)**

$$k = \frac{DS}{Vh}$$

where D represents the diffusion coefficient (cm<sup>2</sup>/s), S is surface area (cm<sup>2</sup>) of the diffusion layer, V the solution volume (mL) and h is the diffusion layer thickness (μm). By applying Fick's law, equation 7 was derived as shown below where k is the intrinsic dissolution rate constant:

**(Equation 7)**

$$\frac{dx}{dt} = k \left( \frac{DS}{Vh} \right) (C_s - C_t)$$

Based on the equations discussed earlier, it is evident that certain properties of the drug are important when determining dissolution. These properties include the solubility, physical form, media and pH of the media.

In the 1950's the emphasis shifted from studying the effects of physicochemical properties of drugs on dissolution to correlation of dissolution to bioavailability (BA) of dosage forms. Oral bioavailability is a key pre-requisite for any orally administered drug to be systemically effective. The United States Food and Drug Administration (FDA) defines bioavailability according to 21 CFR 320 (§ 320.1)<sup>6</sup> as: *the rate and extent to which the active ingredient or active moiety is absorbed from a drug product and becomes available at the site of action.* For drug products that are not intended to be absorbed into the bloodstream, bioavailability

---

<sup>6</sup> Bioavailability and Bioequivalence Requirements. Code of Federal Regulations, Part 320, Title 21, 2003.

may be assessed by measurements intended to reflect the rate and extent to which the active ingredient or active moiety becomes available at the site of action. This definition focuses on the processes by which the active ingredients or moieties are released from an oral dosage form and move to the site of action.<sup>7</sup> The definition above focuses on the process by which the active drugs or ingredients are released from an oral dosage form and move to the site of action in the human body. As noted in the guidance document, bioavailability is documented by developing a systemic exposure profile. This profile can be achieved by measuring the concentration of active ingredients and its active metabolites over time in samples collected from the systemic circulation. Systemic circulation describes the part of the cardiovascular system within the human body which carries oxygenated blood away from the heart and returns deoxygenated blood back to the heart.<sup>8</sup> Bioequivalence (BE) also plays an important role when considering dissolution. As per the FDA, bioequivalence is defined in § 320.1 as: the absence of a significant difference in the rate and extent to which the active ingredient or active moiety in pharmaceutical equivalents or pharmaceutical alternatives becomes available at the site of drug action when administered at the same molar dose under similar conditions in an appropriately designed study. Both bioequivalence and bioavailability focus on the release of a drug substance from a drug product and subsequent absorption in the system circulation. Moreover, this is the basis for pharmacokinetics.

Pharmacokinetics may be simply defined as what the body does to the drug. It attempts to study the mechanisms of absorption and distribution of the administered drug, the rate at

---

<sup>7</sup> Guidance for Industry: Bioavailability and Bioequivalence Studies for Orally Administered Drug Products- General Considerations 2003. U.S. Department of Health and Human Services, FDA [Online], <http://www.fda.gov/cder/guidance/index.htm> (accessed May 1, 2011).

which the drug begins and duration of the effect. Bioavailability and bioequivalence rely on pharmacokinetics measurements such as AUC and Cmax that reflect the systemic exposure. AUC is the area under the plasma/serum/blood concentration-time curve from time zero to time t, where t is the last time point with measurable concentration for individual formulation. Cmax measures the peak exposure by measuring the peak drug concentration obtained directly from the data without interpolation.<sup>9</sup>

In the 1950's, the scientific community focused its interests on dissolution as the rate process for controlling the absorption of active drugs into the bloodstream. In 1951 L.J. Edwards suggested that the analgesic activity of aspirin tablets can be manipulated by its rate of dissolution within the GI tract.<sup>10</sup> Edwards studied the kinetics of the dissolution of aspirin in water at different pH's but over the same temperature range. The solubilities of aspirin were measured and diffusion rates were recorded at several concentrations. He determined that the diffusion coefficients are not independent of the concentration. Edwards suggested that the dissolution of an aspirin tablet in the stomach and intestine is the rate process controlling the absorption of the aspirin into the bloodstream.

In 1960, Levy and Hayes used a beaker and a three blade stirrer to demonstrate that the incidence of GI irritation of different brands of aspirin is dependent on the dissolution rates of

---

<sup>8</sup> Wilding, I. Bioequivalence testing for locally acting gastrointestinal products: what role for gamma scintigraphy? *Journal of Clinical Pharmacology* 2002, 42(11), 1200-1210.

<sup>9</sup> Guidance for Industry: Bioavailability and Bioequivalence Studies for Orally Administered Drug Products- General Considerations 2003. U.S. Department of Health and Human Services, FDA [Online], <http://www.fda.gov/cder/guidance/index.htm> (accessed May 1, 2011).

<sup>10</sup> Edwards, L. J. Solution and diffusion of aspirin in aqueous media. *Transactions of the Faraday Society* 1951, 47, 1191-1210.

the dosage forms.<sup>11</sup> In other words, the dissolution rates were critical for the release of aspirin into the body and causing irritation. Thus, if the release profile is controlled then the irritation levels are controlled. During this period it was recognized that although disintegration was a critical process, de-aggregation was also essential for bioavailability. Disintegration is the process by which an object breaks down or loses its cohesive ability. De-aggregation<sup>12</sup> is the dispersion of particles and dislodgment of the granules. Usually, surfactant in solution helps in the de-aggregation process. Figure 1-2 is an illustration of where disintegration and de-aggregation occur in the dissolution process. The dissolution process occurs in three phases. In Phase I, the rate of dissolution is very slow as during this process solvent diffuses into the solid material (e.g., the pill) via a process called wetting. The initial period is called "mechanical lag". Also, during this phase the solid particles undergo disintegration and deaggregation. In Phase II, the solid particles are well dispersed into the solvent and the rate of dissolution is more rapid. This rate follows a zero order kinetics profile ( $\text{rate} = dx/dt=k$ ). This is followed by Phase III in which 1-2 % of the active ingredient is dissolved at a much slower rate. The slower rate is caused by particles that have not been properly wetted and have not been de-aggregated. In this simulated diagram, approximately 5 % of the active ingredient does not dissolve. While, this level of incomplete dissolution is unlikely to occur in a well formulated pill, this section of the diagram nicely represents a process by which some of the active ingredient never dissolves. Two primary factors preventing complete dissolution are occlusion and saturation. In occlusion, the active ingredient is so well aggregated that it is

---

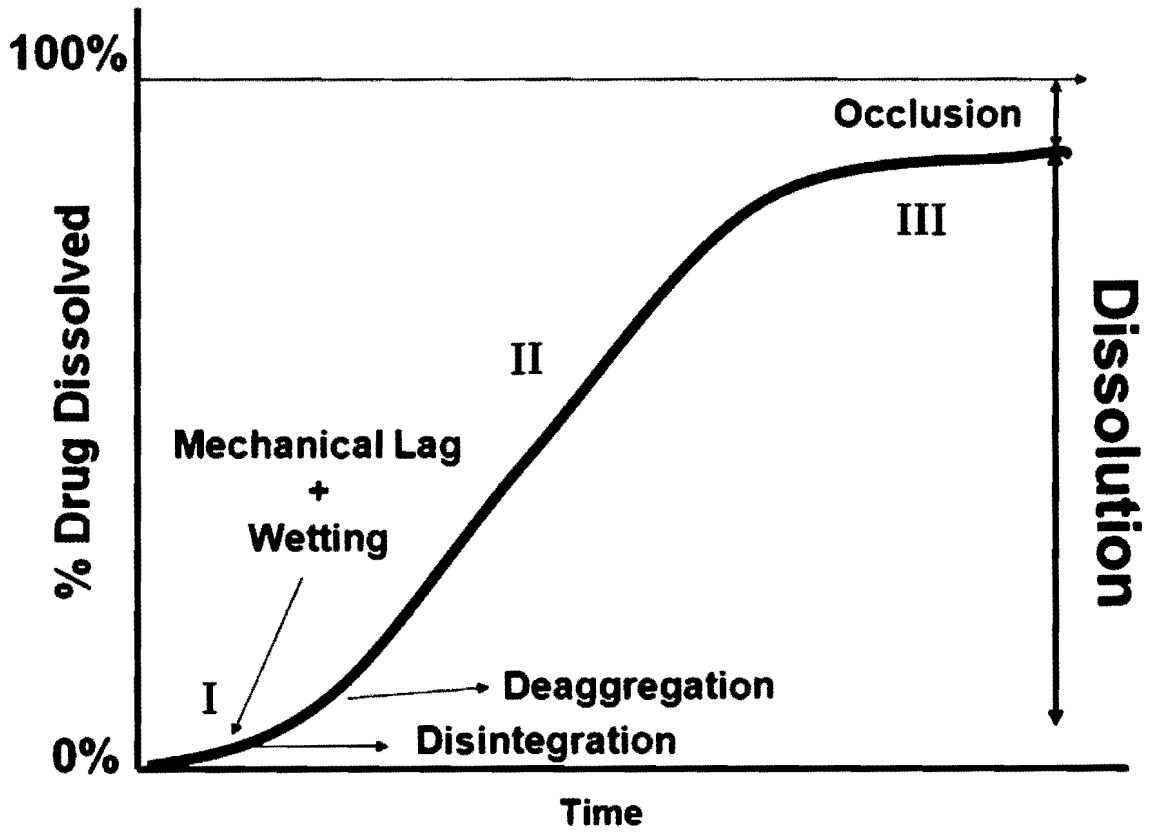
<sup>11</sup> Levy, G.; Hayes, B. A., Physiochemical basis of the buffered acetylsalicylic acid controversy, *New England Journal of Medicine*, **1960**, *21*, 1053-1058.

<sup>12</sup> Liu, J.; Stewart, P. J. Deaggregation during the dissolution of benzodiazepines in interactive mixtures. *Journal of Pharmaceutical Sciences* **1998**, *87*(12), 1632-1638.



poorly wetted that dissolution is not accomplished during the time of the experiment. Alternatively, saturation may have occurred whereby the active ingredient has reached its thermodynamic limit of solubility which prevents complete dissolution. Equilibrium suggests that complete dissolution is difficult to achieve. Equilibrium is the condition of the system in which competing influences are balanced.

Figure 1-2 Dissolution process



In 1978, Underwood and Cadwallader<sup>13</sup> modified the Noyes-Whitney equation to take into consideration sink conditions. They showed that solubility plays an important role in dissolution. Sink conditions exist when the volume of the dissolution medium is three to ten times larger than the volume required to make a saturated solution of the solute. Thus, sink conditions exist when the concentration (C) of active drug in the medium at time t is much smaller than the saturation concentration (Cs). They revised the Noyes Whitney equation accordingly. "M" represents the mass of substance remaining to be dissolved, "A" represents the surface area of the drug exposed to the dissolution medium and "k" represents the intrinsic dissolution rate constant (dissolution constant).

**(Equation 8)**

$$\frac{dM}{dt} = -kA (Cs - C)$$

Moreover, as the concentration of the solution increases, the equation predicts that dM/dt decreases. When the concentration of the saturated solution is much larger than the concentration of the drug ( $C_s \gg C$ ) in the solvent at time t, then equation 9 is obtained.

**(Equation 9)**

$$\frac{dM}{dt} = -kACs$$

Underwood and Cadwallader concluded that the overall dissolution rate increases with increasing dissolution rate constant (k), increased surface area (A) and increased solubility

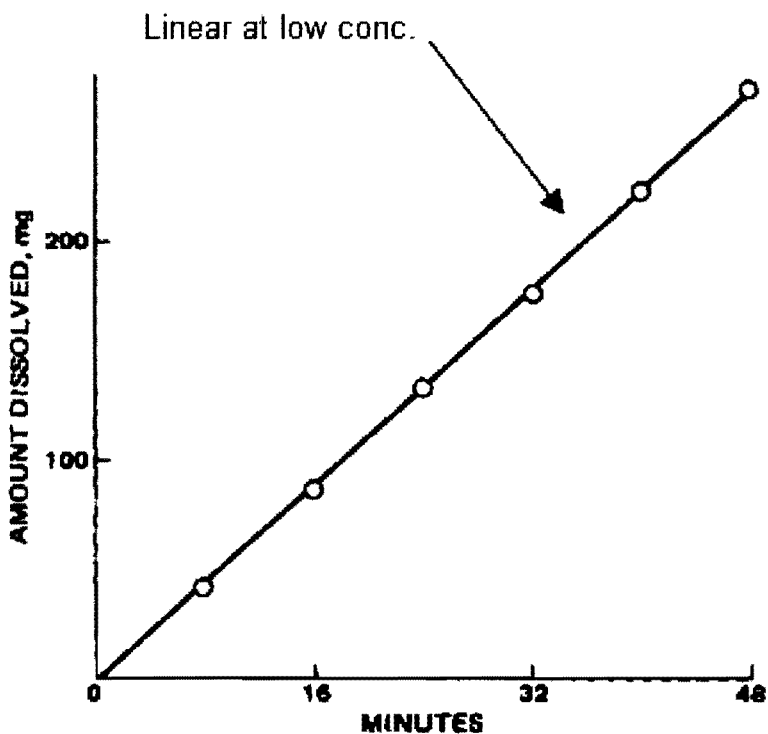
---

<sup>13</sup> Underwood, F. L.; Cadwallader, D. E. Automated potentiometric procedure for studying dissolution kinetics of acidic drugs under sink conditions, *Journal of Pharmaceutical Sciences* **1978**, *67*(8), 1163-1167.

( $C_s$ ). Therefore, by maintaining  $A$  and  $C_s$  as constants, the dissolution rate constant can be conveniently measured.

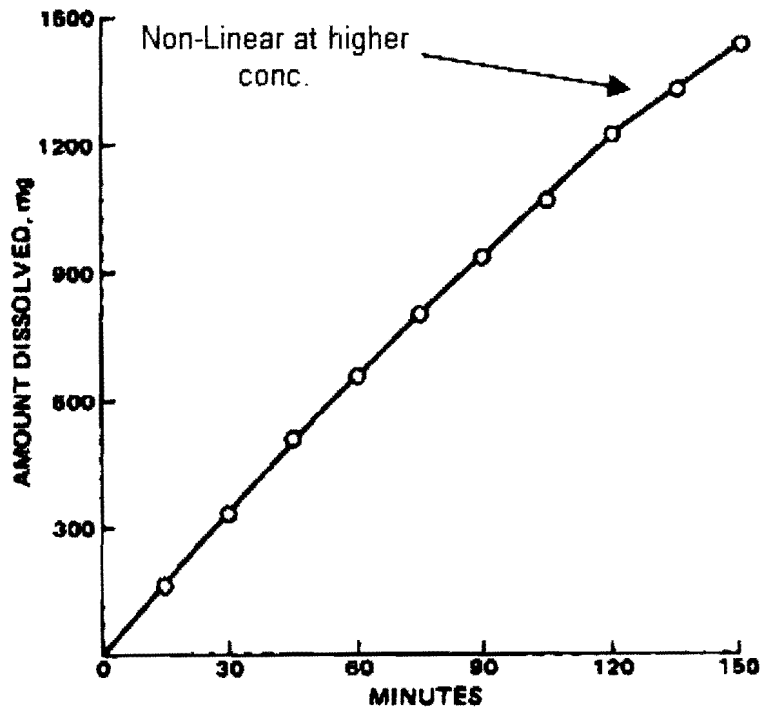
Furthermore, they stated that the dissolution rate of a drug from a constant surface area under sink conditions should follow zero-order kinetics. For zero-order kinetics, a linear plot of [drug concentration] vs. time can be used to determine the rate ( $k$ ). This value can be interpolated from the slope. However, when there is a much higher level of a solute such as of benzoic acid in solution, the dissolution rate decreased slightly as shown in Figure 1-3 and Figure 1-4 below. Underwood and Cadwallader document that a possible reason for this decrease is that the concentration of the buffering compounds in the dissolution medium could retard the dissolution of the solute, i.e., benzoic acid. As the concentration of benzoic acid in solution increases, there is competition for solvent. Also, the buffer pH decreased slightly as the benzoic acid dissolves, which could have decreased the pH of the diffusion layer adjacent to the solid benzoic acid particles and caused a decrease in the dissolution rate.

Figure 1-3 Importance of sink conditions in dissolution: dissolution of benzoic acid at low concentrations: Underwood and Cadwallader (Ref 8)  
(Figure reproduced from figure-1 in article)



*-Dissolution of benzoic acid from a nondisintegrating disk in distilled water (pH-stat 6.2) at 37° and 100 rpm.*

Figure 1-4 Importance of sink conditions in dissolution: dissolution of benzoic acid at higher concentrations: Underwood and Cadwallader (Ref 8)  
(Figure reproduced from figure-3 in article)



*-Dissolution of benzoic acid from a nondisintegrating disk in buffer (pH 6.2) at 37° and 100 rpm.*

As a consequence of the research that had occurred from late 1800's to mid 1900's, in 1970 the first official dissolution test appeared in USP XVIII. The United States Pharmacopeia or USP<sup>14</sup> is a non-governmental, official public standards-setting authority for prescription and over-the-counter medicines and other healthcare products manufactured or sold in the United States. USP also sets widely recognized standards for food ingredients and dietary supplements. They set standards for the quality, purity, strength, and consistency of these products which are critical to the public health.

Increased interest in dissolution regulations continue to grow well into the 1970's. In fact, in 1978 the FDA published the document entitled, "*Guidelines for Dissolution Testing.*"<sup>15</sup> The intention behind this publication was to combine and streamline the systems and processes of different laboratories. This was due to the fact that dissolution results were observed to have high variability and minor changes in the equipment parameters increased variability. The FDA realized that they needed more controls on the tolerances of the dissolution equipment so that results are more reproducible. Additionally, the FDA and USP introduced the idea of calibrator tablets. In 1978 the USP launched three calibrator tablets: Prednisone, Salicylic Acid and Nitrofurantoin. These calibrator tablets were used during the calibration of the instrument to validate that the dissolution bath is working as indicated. The calibrator tablets have known specification limits and the calibrations of the instruments have to be within

---

<sup>14</sup> United States Pharmacopeia, Home Page. <http://www.usp.org/> (accessed May 1, 2011)

<sup>15</sup> Guidance for Industry: Dissolution Testing of Immediate Release Solid Oral Dosage Forms 1997. U.S. Department of Health and Human Services, FDA [Online], <http://www.fda.gov/cder/guidance/index.htm> (accessed May 1, 2011).

those limits. To gain an appreciation of the complexity of the dissolution system and equipment parameters, an overview of the technology will be given in the next section.

In 1995, the USP assigned unique numbers to the different dissolution apparatus that were available to the scientific community. Specifically, there are seven different types of dissolution equipment generally used. These are listed below in Table 1-1.

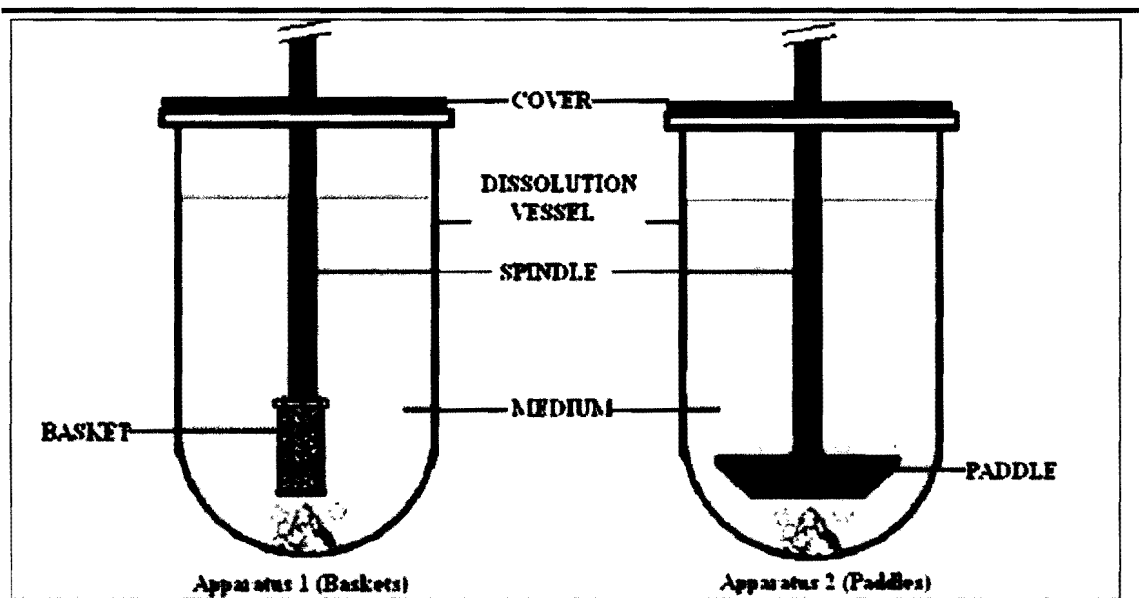


**Table 1-1      Dissolution apparatus in the pharmaceutical industry**

<b>Dissolution Apparatus Number</b>	<b>Dissolution Apparatus Name</b>
Apparatus 1	Basket
Apparatus 2	Paddle
Apparatus 3	Reciprocating Cylinder
Apparatus 4	Flow Through Cell
Apparatus 5	Paddle over Disk
Apparatus 6	Cylinder
Apparatus 7	Reciprocating Disk

Apparatus 1 and 2 are most widely used in the pharmaceutical industry. As shown above the first instrument uses baskets method while the second one uses paddles. Figure 1-5 is a schematic illustration of these two apparatuses. The apparatuses are comprised of a covered vessel, a metallic drive shaft, a motor to spin the shaft, a cylindrical basket (Apparatus 1) or a paddle (Apparatus 2), and a water bath or heated jacket capable of maintaining the temperature of the vessels at  $37^{\circ} \pm 0.5^{\circ}\text{C}$ .

Figure 1-5 Schematic illustration of Apparatus 1 and Apparatus 2 (Reproduced from USP General Chapter on Dissolution <711>)



Although the figures above appear simple in design, there are strict regulations for the specifications of each component of the apparatus and tolerances for each component are specified by USP <711>.<sup>16</sup> Refer to Figure 1-6 and Figure 1-7 for schematic diagrams of the specifications set by the USP for Apparatus 1 and Apparatus 2, respectively.

As a result of these regulations of the past fifty years, the number of USP monographs including dissolution monographs has exponentially increased. As shown in Figure 1-8, in 1970, there were only twelve monographs. In May of 2011, there were 740 dissolution USP monographs.<sup>17 18 19</sup>

---

<sup>16</sup> US Pharmacopoeia & National Formulary- USP General Chapter <711>: Dissolution, USP [Online], <http://www.usp.org/> (accessed May 1, 2011).

<sup>17</sup> Cohen, J; Hubert, B; Leeson, L; Rhodes, C; Robinson, J; Roseman, T; Shefter, E. The Development of USP Dissolution and Drug Release Standards. *Pharmaceutical Research* **1990**, 7(10), 983-987.

<sup>18</sup> Dokoumetzidis, A; Macheras, P. A century of dissolution research: From Noyes and Whitney to the Biopharmaceutics Classification System. *International Journal of Pharmaceutics* **2006**, 321, 1-11.

<sup>19</sup> US Pharmacopoeia & National Formulary- USP Monographs including dissolution (2011 summary), <http://www.usp.org/> (accessed May 1, 2011).

**Figure 1-6 USP Apparatus 1 Specifications (Reproduced from USP General Chapter on Dissolution <711>)**

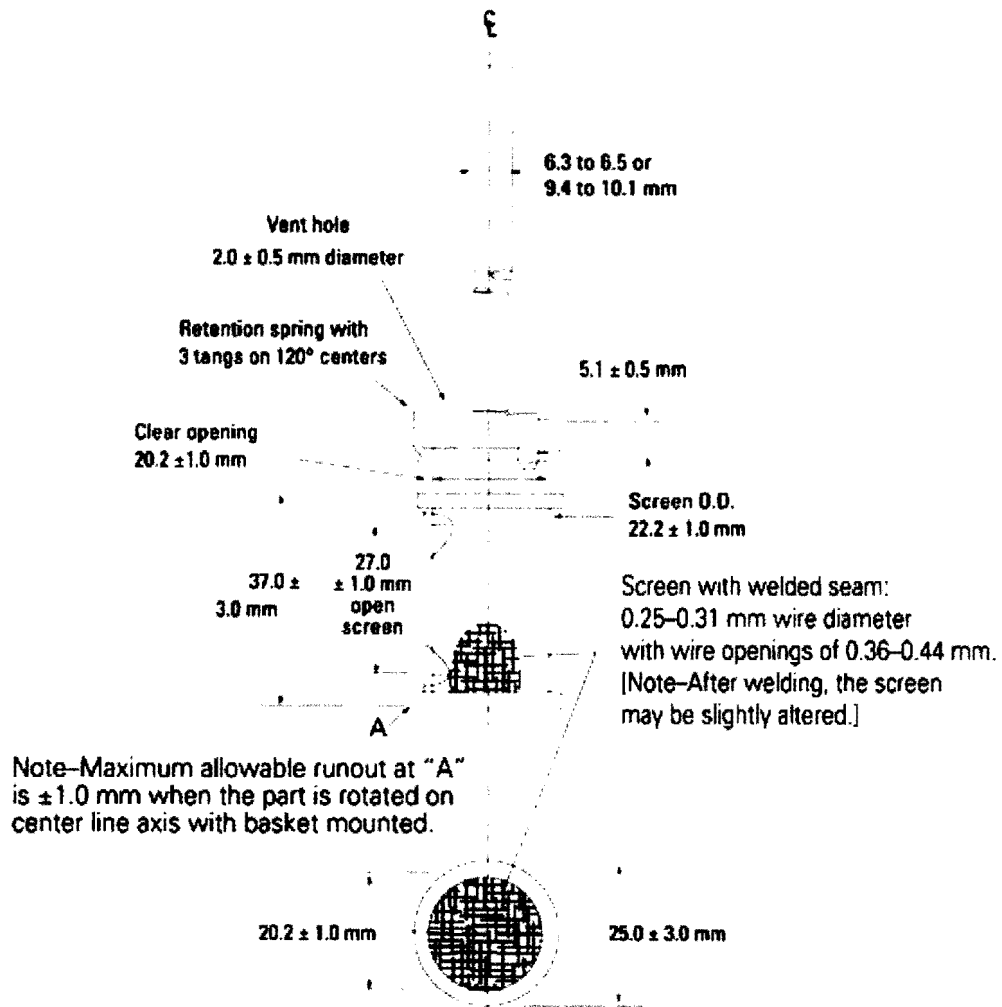


Figure 1-7 USP Apparatus 2 specifications (Reproduced from USP General Chapter on Dissolution <711>)

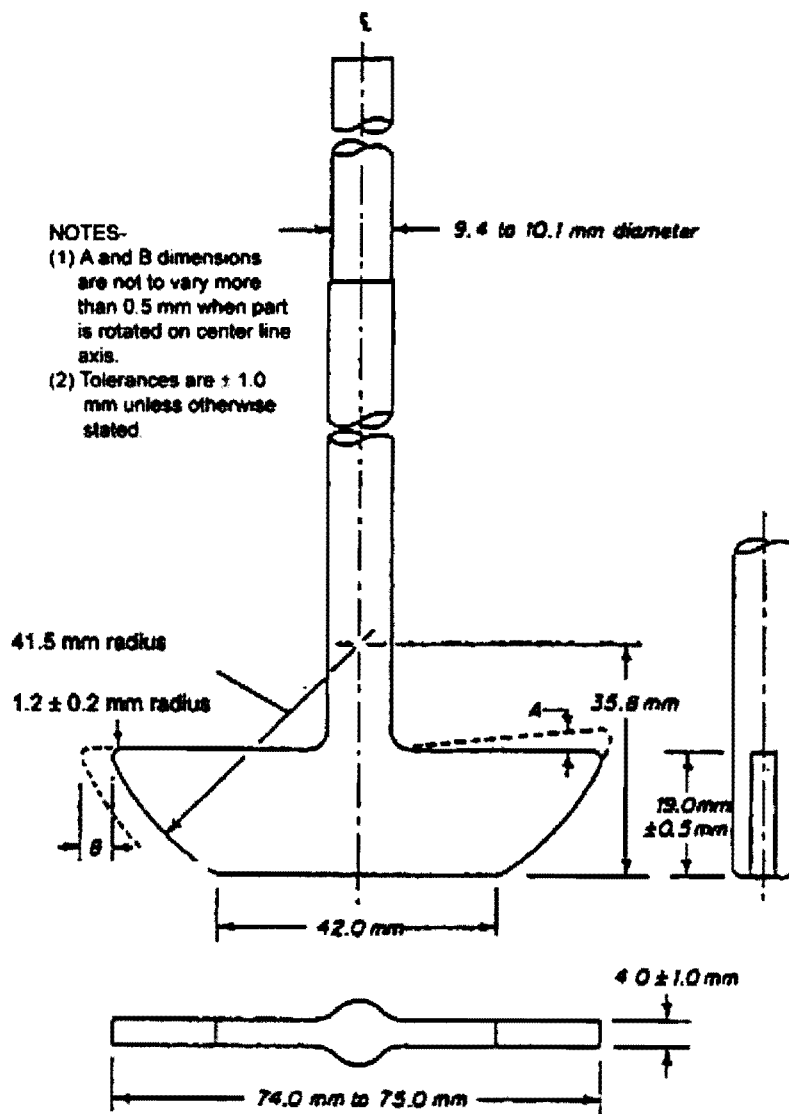
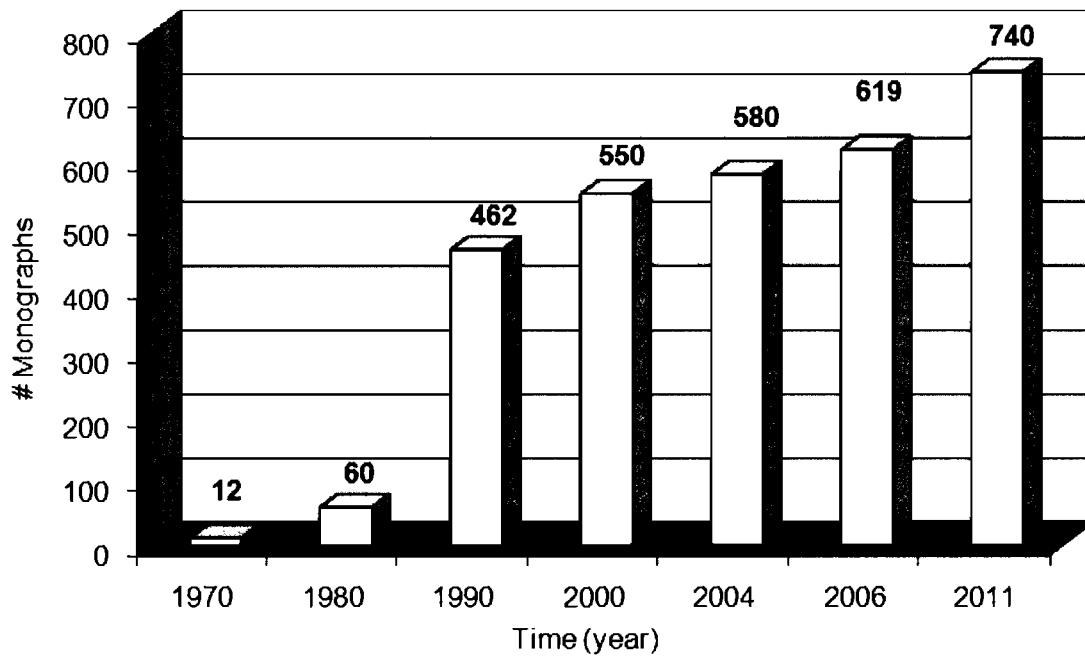


Figure 1-8 Monographs including dissolution in the United States Pharmacopeia (USP)



As a result of the high regulations and increased number of USP monographs including dissolution, this research will improve dissolution testing. Conventional ways of testing have been used for many years by the industry. Specifically, the UV/Vis and HPLC systems have gone through several stages of evolution but continue to be used as the standards. This research and technique will attempt to improve dissolution testing in several ways. First, this technique will allow for in-situ analysis which is very important when dealing with sensitive drug formulations. These sensitive formulations are susceptible to more sampling error when samples are withdrawn from the dissolution vessel. Second, FTIR spectroscopy can be advantageous to dissolution testing. Unlike UV/Vis spectroscopy which gives a single peak per active drug, FTIR spectroscopy can be used to monitor drug release via monitoring of numerous functional groups. Moreover, FTIR spectroscopy can be used to track chemical transformations within the vessel. This will be discussed in chapter three of this thesis. Lastly, FTIR can be used to study multi-component drug formulations.



## 1.2 Infrared Spectroscopy

A brief overview is warranted. Infrared spectroscopy is the spectroscopy that deals with the infrared region,  $14000\text{ cm}^{-1}$  (714 nm) to  $10\text{ cm}^{-1}$  ( $1 \times 10^6$  nm), of the electromagnetic spectrum. Moreover, the IR portion of the electromagnetic spectrum is divided into three regions; near-infrared, mid-infrared and far-infrared. The near-infrared<sup>20</sup> energy, approximately in the region between  $14000\text{--}4000\text{ cm}^{-1}$ , can excite overtone or harmonic vibrations. The mid-infrared<sup>21</sup> energy, approximately in the region between  $4000\text{ cm}^{-1}$  (2500 nm) to  $400\text{ cm}^{-1}$  (25000 nm), can be used to study the fundamental vibrations of structures. The far-infrared region, approximately in the region between  $400\text{--}10\text{ cm}^{-1}$ , can be used to study to rotations of structures. With IR spectroscopy, different functional groups adsorb at different IR bands or regions as shown in Table 1-2.<sup>22</sup> Thus, this technique can help identify and even quantify organic and inorganic molecules.

---

<sup>20</sup> J. Workman Jr. Interpretive spectroscopy for near-infrared, *The Handbook of Organic Compounds*; Academic Press: California, 2001; pp 143-182.

<sup>21</sup> Heise, H. M.; Küpper, L.; Butvina, L. N. Attenuated total reflection mid-infrared spectroscopy for clinical chemistry applications using silver halide fibers. *Sensors and Actuators B: Chemical* **1998**, 51(1-3), 84-91.

<sup>22</sup> Images and frequencies obtained from: <http://wwwchem.csustan.edu/tutorials/infrared.htm>. (accessed May 1, 2011).

**Table 1-2 Absorption bands (Ref 22) (Reproduced from table of frequencies found on CSU Website link)**

<b>Bond</b>	<b>Compound Type</b>	<b>Frequency range, cm<sup>-1</sup></b>
<b>C-H</b>	Alkanes	2960-2850(s) stretch
	CH <sub>3</sub> Umbrella Deformation	1470-1350(v) scissoring and bending 1380(m-w) - Doublet - isopropyl, <i>t</i> -butyl
<b>C-H</b>	Alkenes	3080-3020(m) stretch 1000-675(s) bend
	Aromatic Rings	3100-3000(m) stretch
<b>C-H</b>	Phenyl Ring Substitution Bands	870-675(s) bend
	Phenyl Ring Substitution Overtones	2000-1600(w) - fingerprint region
<b>C-H</b>	Alkynes	3333-3267(s) stretch 700-610(b) bend
	Alkenes	1680-1640(m.w) stretch
<b>C≡C</b>	Alkynes	2260-2100(w.sh) stretch
<b>C=C</b>	Aromatic Rings	1600, 1500(w) stretch
<b>C-O</b>	Alcohols, Ethers, Carboxylic acids, Esters	1260-1000(s) stretch
<b>C=O</b>	Aldehydes, Ketones, Carboxylic acids, Esters	1760-1670(s) stretch
<b>O-H</b>	Monomeric -- Alcohols, Phenols	3640-3160(s.br) stretch
	Hydrogen-bonded -- Alcohols, Phenols	3600-3200(b) stretch
	Carboxylic acids	3000-2500(b) stretch
<b>N-H</b>	Amides	3500-3300(m) stretch
	Amides	1650-1580 (m) bend
<b>C-N</b>	Amides	1340-1020(m) stretch
<b>C≡N</b>	Nitriles	2260-2220(v) stretch
<b>NO<sub>2</sub></b>	Nitro Compounds	1660-1500(s) asymmetrical stretch
		1390-1260(s) symmetrical stretch

The infrared spectrum of a sample can be obtained by passing a beam of infrared light through the sample. A Fourier transform instrument<sup>23</sup> can be used to measure how much energy was absorbed by the sample over the entire wavelength range. The interferometer is a fundamentally different piece of equipment than a monochromator. The light passes through a beamsplitter, which sends the light in two directions at right angles. One beam goes to a stationary mirror then back to the beamsplitter. The other goes to a moving mirror. The motion of the mirror makes the total path length variable versus that taken by the stationary-mirror beam. When the two meet up again at the beamsplitter, they recombine, but the difference in path lengths creates constructive and destructive interference: an interferogram: A mathematical function called a Fourier transform converts an intensity-vs.-time spectrum into an intensity-vs.-frequency spectrum. Refer to equation 10.  $A(r)$  and  $X(k)$  are the frequency domain and time domain points, respectively, for a spectrum of  $N$  points.

**(Equation 10)**

$$A(r) = \sum X(k) \exp(-2\pi \frac{irk}{N})$$

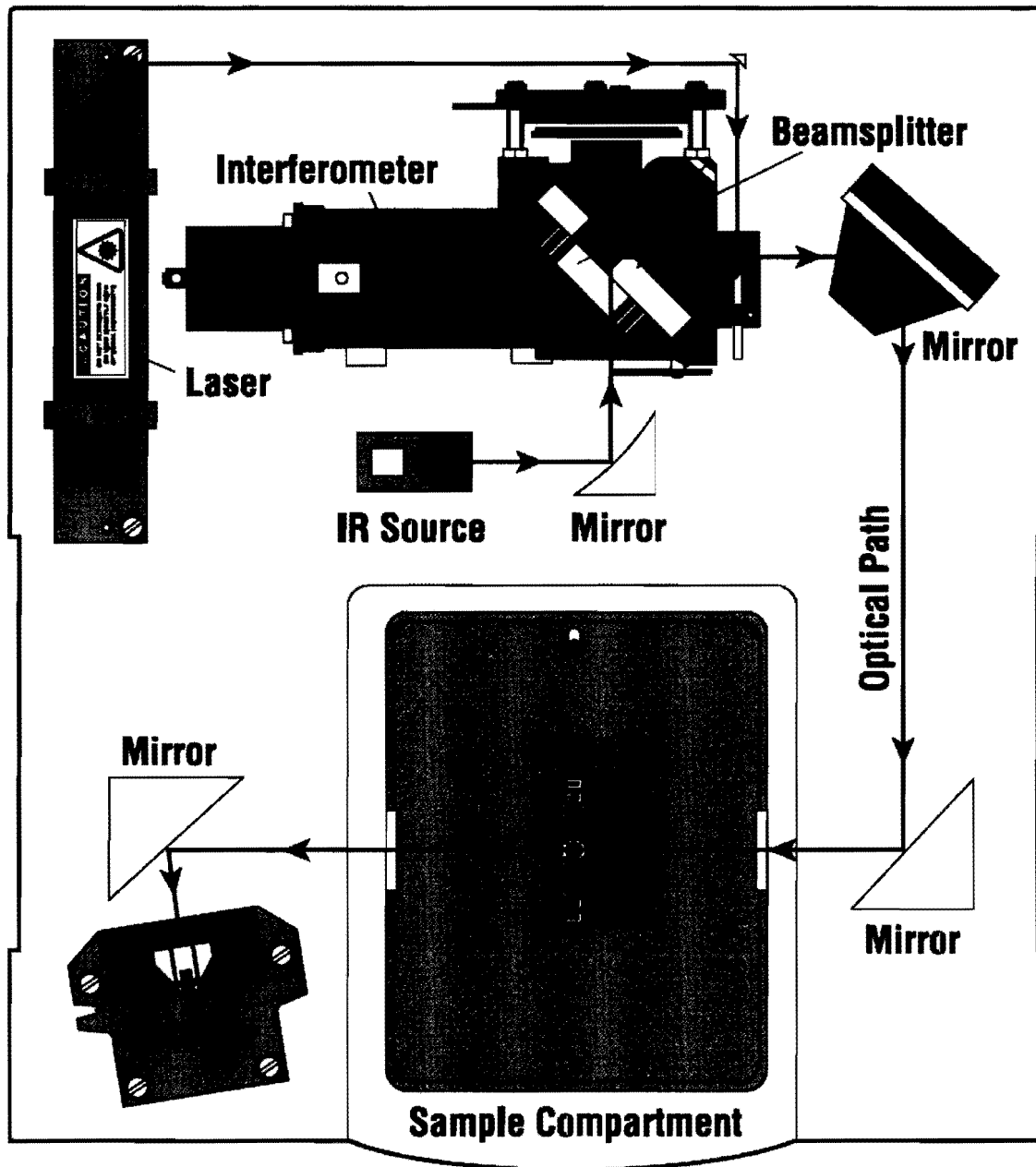
The FT-IR system can produce both transmittance and absorbance spectrum. Refer to Figure 1-9 for an illustration of the FT-IR system.<sup>24</sup> The interferogram represents the light output as a function of mirror position. The FT-IR raw data is processed to give the actual spectrum of light output as a function of wavenumber.

---

<sup>23</sup> Smith, B.C. Fundamentals of Fourier Transform Infrared Spectroscopy; CRC Press: London, 1996; Chapter 4.

<sup>24</sup> Image obtained from <http://mmrc.caltech.edu/FTIR/FTIRintro.pdf> (accessed July 1, 2011).

Figure 1-9 FT-IR system schematic (Ref 24)



### 1.3 Literature background: in situ ATR-IR and dissolution

In the pharmaceutical industry there are two main oral dosage forms: tablets and capsules. These are immersed in an aqueous solution, and the concentration of the active ingredient is monitored as a function of time.<sup>25</sup> Unfortunately, dissolution testing provides limited information on chemical processes that take place within a dissolution vessel. This is due to the limited capabilities of the techniques that are used during dissolution. For instance, most dissolution analysis is carried out using Ultraviolet (UV)/ Visible (Vis) spectroscopy which only gives concentration as a function of time. HPLC is used to separate multi-component drugs but still utilizes UV/Vis detectors as the backbone. One of the challenges the industry is faced with is to increase an understanding of the mechanisms governing dissolution. The current approach relies heavily on a data-driven approach. The health authorities have challenged the pharmaceutical industry to understand dissolution and make the dissolution test more biologically relevant.<sup>26,27</sup> To have a better understanding of dissolution, dissolution chemists need to explore other instruments and experiments that could give insight into what is happening inside of the vessel. Our research focuses on using ATR mid-infrared spectroscopy as an *in situ* technique to monitor and study the dissolution of pharmaceutical tablets. Moreover, this research will give more insight into the science behind dissolution. Specifically, this research will attempt to not only monitor dissolution profiles using FTIR but

---

<sup>25</sup> a) Dressman, J. J.; Kramer, J. K., Eds. *Pharmaceutical Dissolution Testing*; Taylor and Francis: Florida, 2005; b) Hanson, R.; Gray, V. Handbook of Dissolution Testing, 3rd ed., *Dissolution Technologies*: Delaware, 2004.

<sup>26</sup> Tong, C.; D'Souza, S.S.; Parker, J.E.; Mirza, T. Commentary on AAPS workshop - Dissolution testing for the twenty-first century: Linking critical quality attributes and critical process parameters to clinically relevant dissolution. *Pharmaceutical Research* 2007, 24, 1603-1607.

<sup>27</sup> Tong, C.; Lozano, R.; Mao, Y., Mirza, T., Ldbenberg, R.; Nickerson, B.; Gray, V.; Wang, Q. The value of in Vitro dissolution in drug development: A position paper from the AAPS in Vitro release and dissolution focus group. *Pharmaceutical Technology* 2009, 33, 52-64.

also try to explain certain reactions (i.e. transformation of a drug from one form to another-hydrolysis) that are otherwise missed with UV/Vis spectroscopy. Literature research on this topic shows that attempts have been made to study dissolution using near-infrared spectroscopy and infrared imaging.

Attempts have been made to improve the characterization of the controlled release formulations by FT-IR imaging in ATR-IR mode.<sup>28</sup> Van der Weerd and colleagues described the design and implementation of a new cell, which allows the study of drug release from tablets by macro-FT-IR ATR imaging with a diamond ATR accessory. The tablet formulation can be compacted directly on the ATR crystal. The authors explain that various components in the tablet can be determined FT-IR imaging. The described cell was applied to study a model tablet consisting of hydroxypropyl methylcellulose (HPMC) and caffeine. The study by Van der Weerd and co-workers demonstrate that the amount of drug rapidly decreases due to diffusion. Direct observation of this well know phenomenon is unattainable by dissolution techniques, but FT-IR imaging in ATR mode provides a means to achieve this.

Moreover, Van der Weerd and Kazarian explored FT-IR imaging as a useful application for studying the distribution of different components in the tablet, e.g., drug, polymer and water as a function of time. It was shown that the release profile obtained by FT-IR imaging is comparable to that obtained by the flow-through dissolution test with UV spectroscopic

---

<sup>28</sup> a) Van der Weerd, J.; Kazarian, S. G. Combined approach of FTIR imaging and conventional dissolution tests applied to drug release. *Journal Controlled Release* **2004**, *98*, 295-305. b) Van der Weerd, J.; Chan, K. L. A.; Kazarian, S.G. An innovative design of compaction cell for in situ FT-IR imaging of tablet dissolution. *Vibrational Spectroscopy* **2004**, *35*(1-2), 9-13.

detection. In addition, FT-IR imaging was also used to investigate the release of a poorly soluble drug from pharmaceutical tablets.<sup>29</sup>

Blanco<sup>30</sup> and co-workers investigated the use of near-infrared as a tool to study the dissolution profiles in pharmaceutical tablets. Their determination was based on the application of Partial Least-Squares 2 (PLS2) multivariate calibration models to NIR spectra for individual tablets. Marcelo and his colleagues documented that the proposed NIR method provides accurate predictions of dissolution profiles. In fact, the coefficient of correlation between the dissolution profiles obtained with it and a reference method exceeded 0.99 (r) in all cases, and calibration and prediction errors fell within acceptable ranges (6-7%). They conclude that the method allows the entire dissolution profile of intact pharmaceutical tablets to be determined in a simple, clean, expeditious manner without the need to use any reagents or solvents, or the production of any waste.

In addition, Chan<sup>31</sup> and co-workers investigated the use of FT-IR imaging as a tool to study formulations of ibuprofen in poly(ethylene glycol) (PEG) enabled characterization of the distribution of both polymer and drug in the tablet. The authors attempted to study the mechanism of dissolution and drug release for two tablet preparation methods: mechanical mixing and melt extrusion. The mechanisms of dissolution were compared using this spectroscopic imaging approach and found it to be very informative.

---

<sup>29</sup> a) Van der Weerd, J.; Kazarian S. G. Release of poorly soluble drugs from HPMC tablets studied by FTIR imaging and flow-through dissolution tests. *Journal of Pharmaceutical Science* **2005**, 94, 2096-2109. b) Van der Weerd, J.; Kazarian, S.G. Validation of macroscopic attenuated total reflection-Fourier transform infrared imaging to study dissolution of swelling pharmaceutical tablets. *Applied Spectroscopy* **2004**, 58(12), 1413-1419.

<sup>30</sup> Blanco, M.; Alcalá, M.; González, J. M.; Torras, E. Determination of dissolution profiles in intact pharmaceutical tablets by NIR spectroscopy. *The Journal of Process Analytical Technology* **2006**, 3(5), 25-29.

<sup>31</sup> Chan, K. L. A.; Kazarian, S.G. Dissolution of solid dispersions of ibuprofen studied by Fourier Transform infrared imaging. *Polymeric Drug Delivery* **2006**, 203-214.

## **2 Dissolution of salicylic acid, acetylsalicylic acid and acetaminophen using *In Situ* ATR-IR spectroscopy**

This chapter focuses on describing the application of *in situ* attenuated total reflectance-infrared spectroscopy (ATR-IR) as a technique for measuring and studying dissolution of pharmaceutical formulations products. The majority of the methods for monitoring dissolutions utilize UV-Vis spectroscopy. For example, aliquots are manually withdrawn and analyzed by UV-Vis spectroscopy or HPLC with UV-Vis detection. However, the sampling process is disruptive to the dissolution profile since removal of aliquots from the vessel disturbs the solution. In addition, there are instruments that allow real-time analysis using *in situ* UV-Vis probes. For example, fiber optic dissolution testing is used in the industry to monitor pharmaceutical drug product release. Fiber optic dissolution is also used for formulation development.<sup>32</sup> Formulators are using *in situ* UV/Vis systems to profile and develop drugs faster. Instead of relying on conventional techniques where dissolutions are conducted manually and analyzed offline, the advantage of the fiber optic system is that it allows for real-time data analysis.

There is interest in the development of new methods that do not require manual sampling. Also, for multi-component formulations it is important to be able to observe the dissolution profile of each active pharmaceutical ingredient (API). Thus, there is also interest in the development of new spectroscopic methods that enable observation of multiple components. The use ATR-IR for analyzing aqueous samples is limited by the relatively high concentration

---

<sup>32</sup> Mirza, T.; Liu, Q.; Vivilecchia, R.; Joshi, Y. Comprehensive validation scheme for *in situ* fiber optics dissolution method for pharmaceutical drug product testing. *Journal Pharmaceutical Science* **2009**, *98*, 1086-1094.



of analyte required for detection.<sup>33</sup> Hence, this research investigated the use of ATR-IR as a technique for monitoring and understanding dissolution. Limit of detection (LOD) and limit of quantitation (LOQ) will play important roles in determining the sensitivity of the system. The LOD and LOQ values will be discussed in detail in chapter four of this thesis. Refer to equation 11 and 12 for the limit of detection and limit of quantitation calculations:

**(Equation 11)**

$$LOD = 3 \times \left( \frac{S_{xy}}{b} \right)$$

**(Equation 12)**

$$LOQ = 10 \times \left( \frac{S_{xy}}{b} \right)$$

ATR spectroscopy is a sampling technique that is based on molecular vibration and the curvature of light beams when passing through different mediums. An ATR spectrum is generated by transmitting radiation, which can be IR (from  $0.1 \times 10^{-5}$  cm to  $7.5 \times 10^{-5}$  cm), VIS (from  $7.0 \times 10^{-5}$  to  $4.0 \times 10^{-5}$  cm), or UV (from  $4.0 \times 10^{-5}$  cm to  $2.2 \times 10^{-5}$  cm), through an optical crystal in contact with a sample and then determining what portion of the incident radiation is attenuated by the sample at a particular wavelength.

With ATR sampling the IR beam is directed into a crystal of relatively higher refractive index. The IR beam reflects from the internal surface of the crystal and creates an evanescent wave, which projects orthogonally into the sample in intimate contact with the ATR crystal. Some of the energy of the evanescent wave is absorbed by the sample and the reflected

---

<sup>33</sup> Regan, F.; Meaney, M.; Vos, J. G.; Macraith, B. D.; Walsh, J. E. Determination of pesticides in water using [36]

radiation (some now absorbed by the sample) is returned to the detector. The refractive indices of the crystal and sample are important considerations in the ATR sampling technique.

Refer to equation 13:

**(Equation 13)**

$$\theta_c = \sin^{-1} \left( \frac{n_2}{n_1} \right)$$

where  $n_2$  is the refractive index of the sample,  $n_1$  is the refractive index of the crystal and  $\theta_c$  is the critical angle. ATR spectrometry is used extensively in clinical assays, medical diagnostics, and laboratory testing.<sup>34</sup> Since the depth of penetration for the evanescent wave in ATR spectrometry is shallow, there is a low incidence of Fresnel Reflection. Thus, reliable spectral analysis of murky, semisolid, turbid, and optically dense solutions is possible with ATR spectroscopy. Moreover, the ATR crystal is a relatively chemically resistant Zn-Se crystal that can be coated with an additional chemically resistant material which enables IR spectroscopy to be performed in aqueous solution.

Therefore, *in situ* ATR-IR spectroscopy has the unique potential to simultaneously address problems associated with manual sampling and multi-component analysis discussed above. This is a potentially useful method for dissolution testing. Modern infrared instruments can be equipped with fiber optic probes containing ATR crystals that are chemically robust, provide excellent sensitivity and, with respect to *in situ* UV-Vis, are not affected by turbidity. In addition, since IR is very sensitive to specific functional groups, it has greater versatility in

---

ATR-FTIR spectroscopy on PVC/chloroparaffin coatings. *Analytical Chimica Acta* **1996**, 334, 85-92.

<sup>34</sup> Bynum, K.; Kassis, A. ATR Crystal Device. U.S. Patent 6,841,792, March 10, 2002.

differentiating components in a multi-component mixture than UV-Vis spectroscopy.<sup>35</sup> In this chapter, the successful development of dissolution tests using *in situ* ATR-IR spectroscopy to analyze single and multi-component mixtures is described.

Since dissolution testing has evolved into a highly regulated activity in the pharmaceutical industry, health agencies have placed a greater emphasis on regulating dissolution methods. The dissolution test is the only one that can give an *in vitro* snapshot of how the drug product may behave *in vivo*. Because of this function, the number of dissolution methods in the United States Pharmacopeia (USP) has grown substantially. Furthermore, the U.S. Food and Drug Administration (FDA) has placed greater importance on the dissolution test. The FDA official website is full of material related to dissolution testing from guidance documents to warning letters.<sup>36</sup> Thus, the potential impact of a new analytical technique that permits *in situ* analysis of multiple active ingredients is large.

## **2.1 Experimental section**

### **2.1.1 Chemical and materials**

Acetaminophen reference material (batch no. 104K0154) was purchased from Sigma-Aldrich (St. Louis, MO, USA). Salicylic acid reference material (batch no. 04708HE) was purchased from Sigma-Aldrich (St. Louis, MO, USA). Acetaminophen tablets (Tylenol® batch no. SLA175) were purchased from a local pharmacy. Excedrin® Caplets (Back and Body Brand, Lot #10067371: Acetaminophen 250 mg, Aspirin 250 mg) were purchased from a local pharmacy. Salicylic acid calibrator tablets (USP batch no. Q0D200) were purchased from the

---

<sup>35</sup> Skoog, D.; Holler J.; Crouch S. *Principles of Instrumental Analysis, 6th ed.*; Thomson Books, 2007; pp. 455-480.

<sup>36</sup> United States Food and Drug Administration Home Page. <http://www.fda.gov/> (accessed May 1, 2011)

USP. Methanol, acetone and acetonitrile (HPLC grades) were purchased from Pharmaco-Aaper. Sodium hydroxide (batch no. 064214BH), used to prepare the pH buffered solutions, was purchased from Sigma-Aldrich (St. Louis, MO, USA). These analytes were selected because of their immediate release properties and high solubilities in phosphate buffers. Potassium phosphate monobasic (batch no. 103K0060), used to prepare the pH buffered solutions, was purchased from Sigma-Aldrich. Glacial acetic acid was purchased from Sigma Aldrich (St. Louis, MO, USA). All solutions were prepared using water treated by a Milli-Q Millipore purification system. All purified water aliquots have resistivity of not less than 18 MOhm-cm<sup>-1</sup>.

### **2.1.2 Instrumentation**

Samples were tested using Mettler Toledo's iC10 FT-IR system using a fiber optic probe equipped with a 1 mm diamond coated ATR probe. The IR system was operated by Mettler Toledo's iC IR version 3.0 or 4.0 software. pH determinations were carried out using a pH meter from VWR (model no. Symphony SB70P). HPLC analysis was carried out using two systems: Hewlett Packard 1050 (operated by ChemStation) and Waters 2695 (operated by Empower). All UV measurements were carried out using a Hewlett Packard UV instrument (model no. 8452A diode array). The UV instrument was operated using HP's Softer-Olis Spectralworks. All manual dissolutions were tested using a Vankel Dissolution Bath (model no. 700). All analytical weight measurements were carried out using Mettler Toledo's DeltaRange and AG204 DeltaRange top loading balance.

### 2.1.3 Buffered solutions

The pH 5.8 (200 mM) and 7.4 (50 mM) phosphate buffered solutions were prepared with monobasic potassium phosphate in accordance with the USP. As described in the USP, the detailed procedure for preparing these buffers is shown below.<sup>37,38</sup>

#### Phosphate Buffered Solution:

The volumes shown in the table are for 200 mL of buffer solution. Note: Where water is specified for solution or dilution of test substances in pH determinations, use carbon dioxide-free water.

- Sodium Hydroxide Solution (0.2 M) - Dissolve 4.0 g of sodium hydroxide in water to make 100 mL.
- Monobasic Potassium Phosphate Solution (0.2 M) - Dissolve 27.22 g of monobasic potassium phosphate ( $\text{KH}_2\text{PO}_4$ ) in water, and dilute with water to 1000 mL.

**Table 2-1 Phosphate buffer preparations as per United States Pharmacopeia (USP)**

Composition of Standard Buffer Solutions												
<i>Phosphate Buffer</i>												
Place 50 mL of the monobasic potassium phosphate solution in a 200-mL volumetric flask, add the specified volume of the sodium hydroxide solution, then add water to volume.												
pH	5.8	6.0	6.2	6.4	6.6	6.8	7.0	7.2	7.4	7.6	7.8	8.0
0.2 M NaOH, mL	3.6	5.6	8.1	11.6	16.4	22.4	29.1	34.7	39.1	42.4	44.5	46.1

### 2.1.4 Dissolution experiments

Single component analysis: 300 mg salicylic acid tablets were tested in pH 7.4 phosphate buffered solutions. Dissolution was conducted using a vessel volume of 500 mL and at ambient temperature. All dissolutions were conducted using USP Apparatus II (paddles) with an agitation speed of 100 rpm. The dissolution run time was seven hours and thirty minutes.

<sup>37</sup> US Pharmacopoeia & National Formulary- USP Monograph: Salicylic Acid Tablets, USP [Online], <http://www.usp.org/> (accessed May 1, 2011).

Multi-tablet analysis: 300 mg salicylic acid and 500 mg acetaminophen tablets were tested in pH 5.8 phosphate buffered solutions. Dissolution was conducted using a vessel volume of 500 mL and at ambient temperature. All dissolutions were conducted using USP Apparatus II (paddles) with an agitation speed of 50 rpm (a slower rpm was chosen to enable a slower rate of dissolution to help distinguish the components). The dissolution run time was six hours.

Multi-component analysis: Three Excedrin® tablets, each composed of 250 mg aspirin (acetylsalicylic acid) and 250 mg acetaminophen were tested in pH 7.4 phosphate buffered solutions. Dissolution was conducted using a vessel volume of 500 mL and at ambient temperature. All dissolutions were conducted using USP Apparatus II (paddles) with an agitation speed of 100 rpm. The dissolution run time was one hour and thirty minutes.

### **2.1.5 HPLC analysis**

The single-component analysis experiment was performed using the following HPLC parameters: HP 1050 HPLC, Waters Symmetry 300 C18 5  $\mu$ m column (4.6 x 50 mm), mobile phase was 60/40/1 (water/ methanol/glacial acetic acid), flow rate was 2.0 mL/min, isocratic mode, injection volume was 5  $\mu$ L and absorbance was set at 296 nm.

The multi-tablet analysis experiment was analyzed using the following HPLC parameters: Waters 2695, Waters Symmetry Shied RP C18 3  $\mu$ m column (3.5 x 50 mm), mobile phase was 70/30/1 (water/ acetonitrile/trifluoroacetic acid (TFA)), flow rate was 1.5 mL/min, isocratic mode, injection volume was 5  $\mu$ L and absorbance was set at 296 nm.

---

<sup>38</sup> US Pharmacopoeia & National Formulary- USP Monograph: Acetaminophen Tablets, USP [Online], <http://www.usp.org/> (accessed May 1, 2011).

The multi-component analysis experiment was performed using the following HPLC parameters: HP 1050 HPLC, Phenomenex Intersil ODS C18 5  $\mu\text{m}$  column (4.6 x 150 mm), mobile phase was 60/40/1 (methanol/ water/ trifluoroacetic acid (TFA)), flow rate was 1.0 mL/min, isocratic mode, injection volume was 25  $\mu\text{L}$  and absorbance was set at 280 nm.

### **2.1.6 ATR-IR analysis**

The ReactIR™ iC10 FTIR instrument is composed of a Mercury-Cadmium-Telluride (“MCT”) detector (liquid nitrogen cooled) and the FiberConduit™. When sample measurements must be made at high speed or when IR throughput is low, the highly sensitive mercury cadmium telluride (MCT) detector provides the ability to scan faster than a DLaTGS detector while maintaining a constant IR response. The FiberConduit™ is comprised of flexible IR transparent silver chloride/silver bromide optical fibers. The fiber optic probe interface (AgX 9.5 mm x 1.5 m Fiber (Silver Halide)) contains a diamond tip-DiComp ATR crystal. The resolution was set to 4 wavenumbers. The optical range used by the system is: 1900  $\text{cm}^{-1}$  to 650  $\text{cm}^{-1}$ . The gain adjustment was set to normal (1x) and the apodization method was set to Happ-Genzel. The system uses compressed air (house air, filtered and dehumidified) to purge the optics.

For the single component testing, data treatment was carried out using the following methodology: The data was first subjected to baseline correction. An absorption band at 1388  $\text{cm}^{-1}$  was selected for salicylic acid. The height was calculated using a baseline band correction set at 1370  $\text{cm}^{-1}$ . The ATR-IR system was configured to collect spectra every five minutes.

For *multi-tablet testing*, the data was first subjected to baseline correction. An absorption band at  $1388\text{ cm}^{-1}$  and baseline band at  $1370\text{ cm}^{-1}$  were selected to calculate the peak height for salicylic acid. An absorption band at  $1246\text{ cm}^{-1}$  and a baseline band of  $1276\text{ cm}^{-1}$  were selected to calculate the peak height for acetaminophen. The ATR-IR system was configured to collect spectra every five minutes.

For *multi-component testing*, the data was first subjected to baseline correction. An absorption band at  $1388\text{ cm}^{-1}$  and a two-point baseline set at  $1370\text{ cm}^{-1}$  and  $1414\text{ cm}^{-1}$  were selected to calculate the peak area for aspirin (acetylsalicylic acid). An absorption band at  $1246\text{ cm}^{-1}$  and a two-point baseline set at  $1217\text{ cm}^{-1}$  and  $1265\text{ cm}^{-1}$  were selected to calculate the peak area for acetaminophen. The ATR-IR system was configured to collect spectra every three minutes.

For all ATR-IR experiments, 256 scans were collected and co-added for each spectral point. On average, every spectral point, took about two-minutes to complete. For all testing, the calculated peak response was subjected to mathematical smoothing using the  $iC_{10}$  software. The data was compared to reference standards measurements collected prior to start of the linearity and dissolution experiments. Dissolution data was plotted vs. time and all dissolution experiments were allowed to equilibrate in the buffer for at least half an hour prior to the start of a dissolution experiment.



## **2.2 Results and discussion**

### **2.2.1 Single-component analysis**

#### **2.2.1.1 Linearity results for salicylic acid using pH 7.4 phosphate buffer**

Salicylic acid was thoroughly studied in pH 7.4 phosphate buffered solution as recommended by the USP. Since salicylic acid has a pKa of 2.97 it is almost completely ionized at physiologic pH 7.4. Thus, the ratio of salicylic acid: salicylate is approximately 1:25,000. During the method development phase, linear dilutions of salicylic acid reference standards were prepared and analyzed using ATR-IR spectroscopy. The linearity experiments served two purposes; 1) they determined whether IR spectroscopy provided a linear response to the different concentrations of salicylic acid, and, 2) whether IR spectroscopy can be used for very low concentration levels of salicylic acid. Initially, eight levels of salicylic acid standards were prepared. Based on the IR spectra obtained, salicylic acid has an IR frequency of interest at  $1388\text{ cm}^{-1}$  (Figure 2-1). The linearity experiments were further analyzed using linear regression. Based on the analysis, it was determined that salicylic acid had excellent linear correlation using IR spectroscopy with a 0.997 correlation coefficient ( $r^2$ ). Linear regression for salicylic acid was calculated using the IR absorption band at  $1388\text{ cm}^{-1}$  and subtracting the baseline absorption band at  $1370\text{ cm}^{-1}$ . A chart of the digitized data is attached in Appendix [A]. Since the IR system resolution was set to four, large data sets were obtained during the analysis. An example of the digitized data can be found in the appendix.

**Figure 2-1 Salicylic acid spectra at different concentrations in pH 7.4 phosphate buffered solution.**

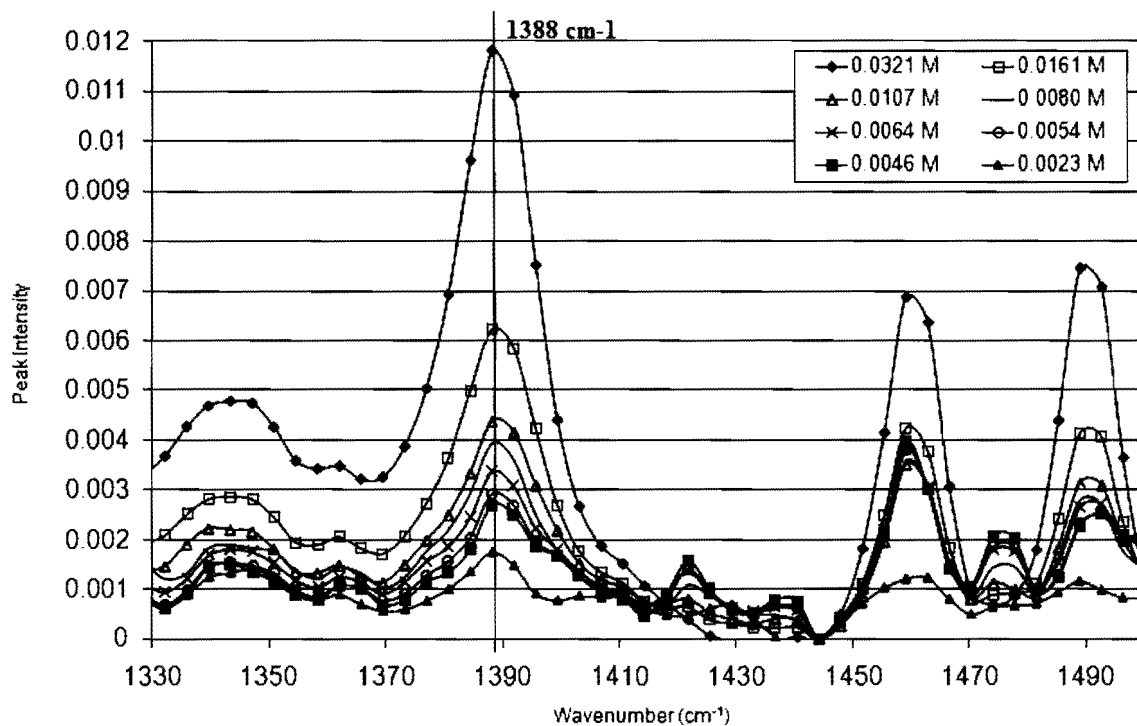


**Table 2-2 Method development summary for Salicylic Acid (Linearity and Dissolution results)**

Method development parameter	Typical Pharmaceutical Acceptance criteria	Results
Accuracy (mean) - Difference between IR and HPLC	Report value	2.1%
Linearity ( $n \geq 6$ ) - Correlation coefficient - Range(Linearity experiment)	$r \geq 0.990$ Specify range	0.997 0.016- 0.1130 mg/ml
Limit of detection (LOD)	Specify LOD	0.02 mg/ml
Limit of quantitation (LOQ)	Specify LOQ	0.08 mg/ml
Precision (%RSD)	Relative standard deviation ( $n \geq 6$ ), $\leq 2.0\%$	0.2%

### 2.2.2 Dissolution results for salicylic acid using pH 7.4 phosphate buffer

The next part of method development phase was to determine the accuracy of ATR-IR spectroscopy as a technique for measuring dissolution rates of a drug. This was determined by comparing the IR spectroscopy results with HPLC results. Although the USP methods typically recommend vessel volumes of 900 mL, the dissolution vessels were filled with 500 mL of pH 7.4 phosphate buffer in order to increase the signal-to-noise ratio. The purpose of this change was to detect very low concentrations (below 10%) of the active drug. Practically the laboratory is not interested in seeing 10% levels, but rather higher concentrations. Therefore, in order to test the limits of the system, the lower dissolution vessel volumes were used. Next, the paddle was lowered to the USP recommended position ( $25 \pm 2$  mm from the bottom of the vessel) and rotated at 100 rpm at ambient temperature. To minimize hydrodynamic effects, the ATR probe was inserted approximately 5 mm below the surface of the medium.<sup>39</sup> The first thirty-minutes were used to establish the spectral baseline, the shaft was momentarily stopped and one salicylic acid (300 mg) tablet was dropped into the vessel. Rotation was resumed and IR data were acquired every five minutes for a period of seven hours. During this time, aliquot samples were removed and stored in HPLC vials for subsequent analysis. As shown in Figure 2-2, the results from the IR and HPLC systems match extremely well and the relative accuracy is within  $\pm 2\%$ .

---

<sup>39</sup> Mauger J. W. Physicochemical and fluid mechanical principles applied to dissolution testing. *Dissolution Technologies*, 1996, 3, 7-11.

**Figure 2-2 Comparison of *in situ* ATR-IR and HPLC methods for dissolution of a salicylic acid tablet**

The dissolution plot below represents % dissolved of salicylic acid vs. time. This particular experiment was carried out over seven hours. The light blue diamond data points represent the ATR-IR results whereas the red squares represent the HPLC results. Moreover, as observed in the figure below, the IR data at approximately seven hours appears to be noisy. This is probably due to disturbance of the fiber optic probe during the HPLC sample collections at the seven-hour time points.

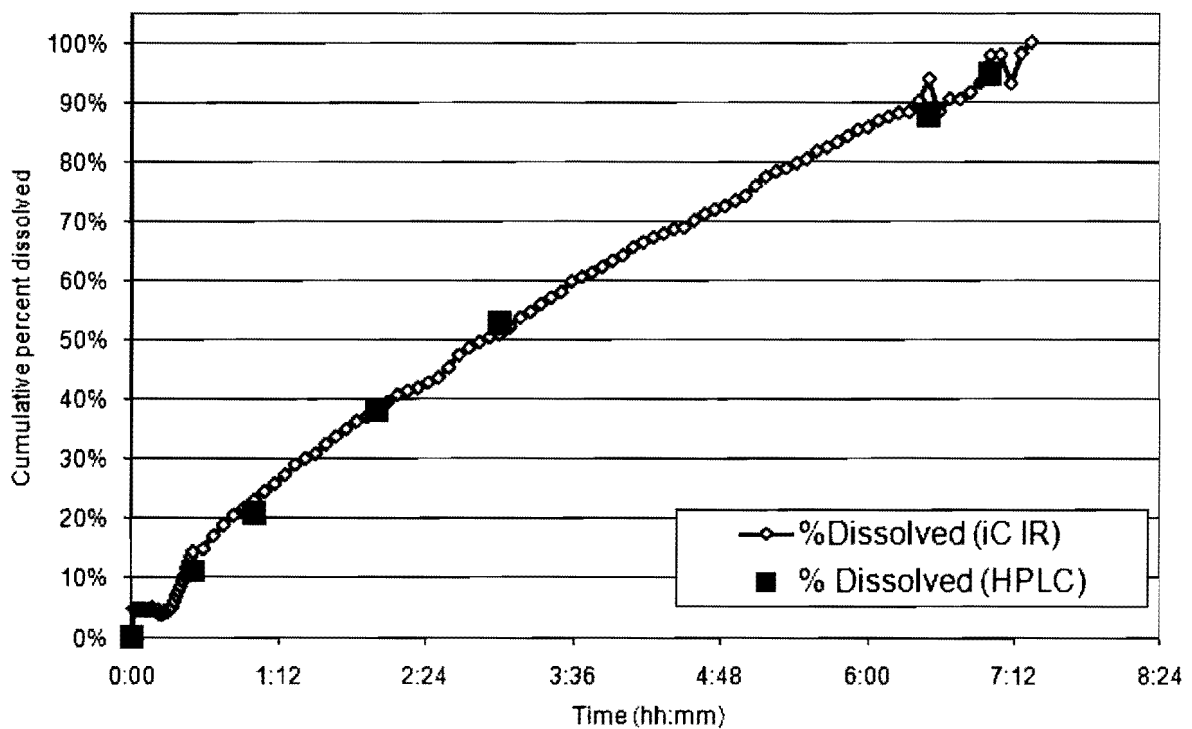


**Table 2-3      % Dissolved of salicylic acid: Absolute % dissolved difference between ATR-IR and HPLC results**

This data represents the dissolution results for salicylic acid from Figure 2-2. The ATR-IR data was compared to the HPLC data and the absolute difference between both methods was calculated. The average difference was also calculated.

<b>Time (h:mm)</b>	<b>Salicylic acid (HPLC) (% Dissolved)</b>	<b>Salicylic acid (ATR-IR) (% Dissolved)</b>	<b>Absolute Difference (%)</b>
0:00	0.0%	0.0%	0.0%
0:30	11.1%	14.4%	3.3%
1:00	20.9%	23.1%	2.2%
2:00	38.2%	38.0%	-0.1%
3:00	52.9%	50.9%	-2.0%
6:00	87.8%	93.8%	6.0%
7:00	94.8%	97.8%	3.0%
		<b>Average</b>	<b>2.1%</b>

### **2.2.3 Multi-tablet analysis**

#### **2.2.3.1 Linearity results for salicylic acid and acetaminophen in pH 5.8 phosphate buffer**

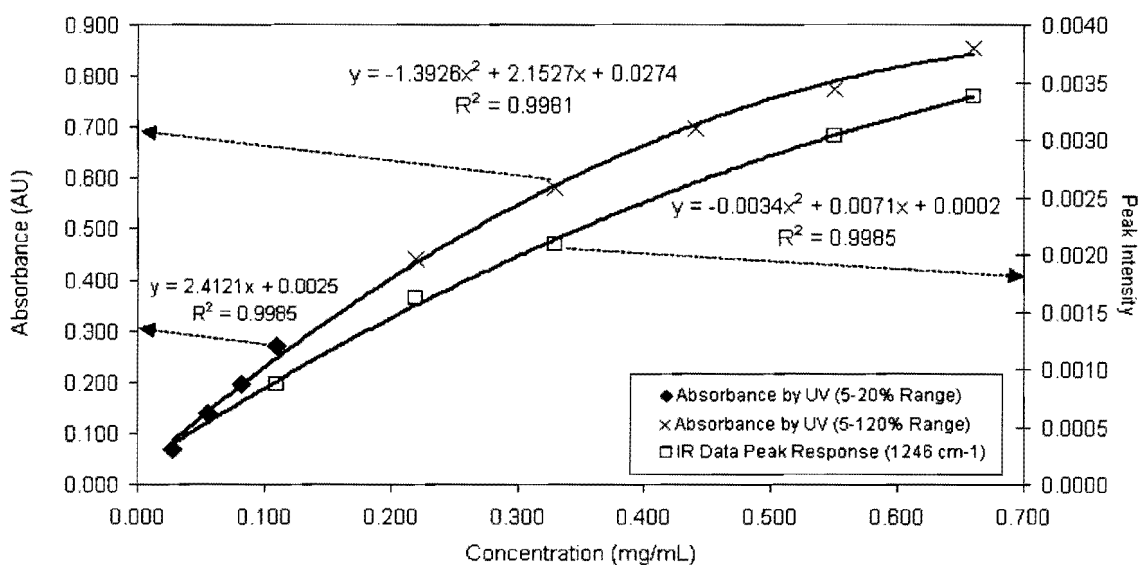
The USP monograph specifies pH 5.8 phosphate buffer as the medium of choice for acetaminophen. Thus, acetaminophen and salicylic acid were thoroughly studied in pH 5.8 phosphate buffer. As expected, regression analysis for salicylic acid indicated an excellent linear correlation ( $r^2 = 0.994$ ) of IR peak intensity vs. concentration. For acetaminophen, at low concentrations ( $\leq 0.11$  mg/ml, 0.7 mM), the relationship between absorbance and concentration is effectively linear ( $r^2 = 0.998$ ). However, to our surprise, non-linear behavior for both IR and UV-Vis methods was observed at higher concentrations. As shown in Figure 2-3, both methods can be modeled using second-order polynomial equations.<sup>40</sup>

---

<sup>40</sup> Dejaegher, B.; Bloomfield, M.S.; Smeyers-Verbeke, J.; Heyden, Y. Validation of a Fluorimetric Assay for 4-Aminophenol in Paracetamol Formulations. *Talanta* **2008**, *75*, 258-265.

**Figure 2-3 Calibration curves of acetaminophen standards at pH 5.8: UV/Vis absorbance at 296 nm and IR peak intensity at 1246 cm<sup>-1</sup>**

Acetaminophen in pH 5.8 buffer is linear at the lower concentrations. During the early stage of dissolution, the concentration (C) of the active drug is much lower than the saturation concentration (C<sub>s</sub>). However, as time progresses the solution becomes saturated at which point the drug will compete for solution space. Moreover, as more molecules of acetaminophen are in solution, more hydrogen bonding (between carbonyl and hydroxyl groups) will occur between the molecules potentially causing dimerization in solution.





### **2.2.3.2 Dissolution results for salicylic acid and acetaminophen in pH 5.8 phosphate buffer**

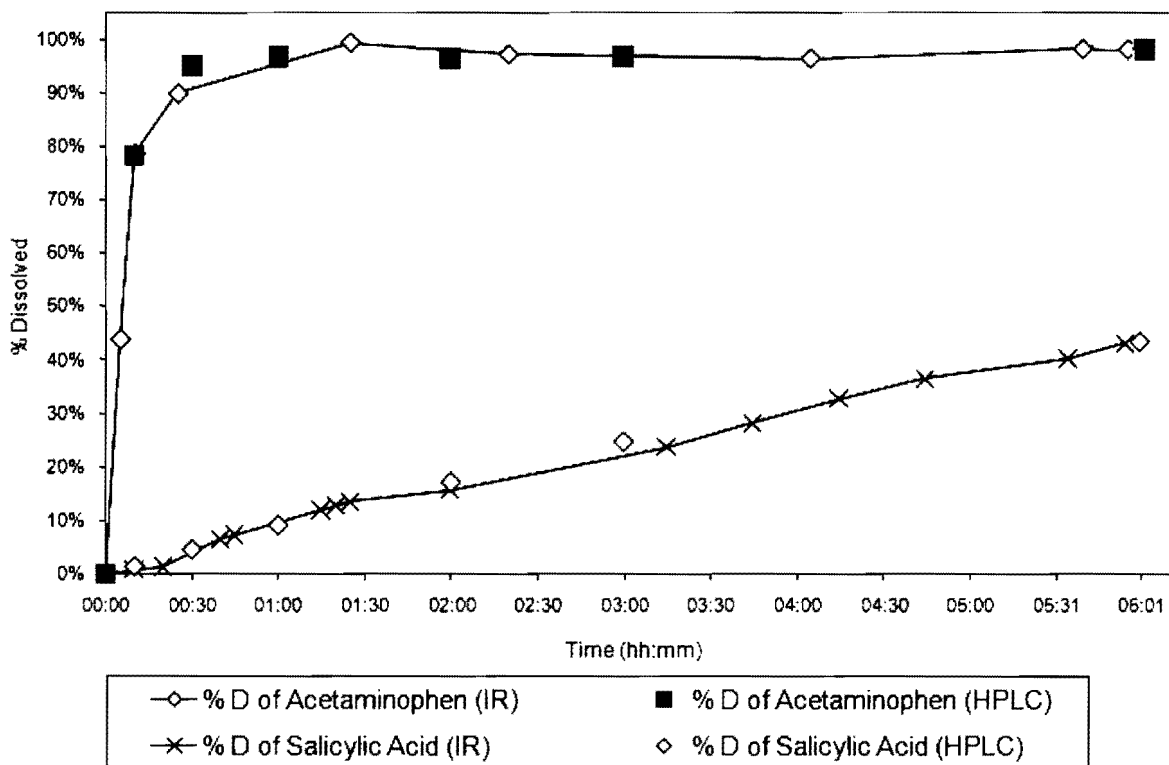
To demonstrate the ability of *in situ* ATR-IR to successfully monitor dissolution of two different tablets, the dissolution profile of salicylic acid and acetaminophen tablets was determined by simultaneously adding one tablet of each and monitoring the dissolution rate of both components over seven hours.

Although salicylic acid is not used clinically, it serves as an USP recommended standard for a slowly eroding tablet and acetaminophen serves as an example of a tablet that disintegrates. As shown in the figure below, the *in situ* ATR-IR method is clearly able to distinguish the dissolution of each component. For example, the acetaminophen tablet disintegrates and releases acetaminophen more rapidly than the salicylic acid tablet which slowly erodes over time. Thus, *in situ* ATR-IR method is successful in determining the dissolution profile of a two component system.

To compare the *in situ* ATR-IR method with HPLC and UV-Vis methods, aliquots were taken throughout the experiment and analyzed. The results from the *in situ* ATR-IR and HPLC systems are overlaid in Figure 2-4 and an excellent correlation is observed between the two methods. In addition, samples were analyzed using a UV/Vis instrument. Since both salicylic acid and acetaminophen absorb at approximately 296 nm (pH 5.8) it will not be ideal to monitor the dissolution of these two components using UV/Vis alone. Moreover, extensive mathematical equations will be required to solve simultaneous equations in order to differentiate the two active drugs.

**Figure 2-4 Simultaneous dissolution of acetaminophen and salicylic acid tablets: *in situ* ATR-IR vs. HPLC**

The dissolution plot below represents % dissolved of individual salicylic acid and acetaminophen tablets vs. time. Moreover, two separate tablets were inserted into a single vessel during the analysis. The dissolution was carried out at pH 5.8 phosphate buffer as suggested by the USP. This particular experiment was carried out over six hours. The red squares and yellow diamonds represent the HPLC data. As observed, the ATR-IR and HPLC results are very similar at the specified time-points shown below. Since acetaminophen tablets are designed to disintegrate rapidly, the drug release quickly as observed in the plot. Since salicylic acid is an eroding (slowly releasing) tablet, the drug releases slower as observed in the plot. In addition, the dissolution was carried out using an agitation speed of RPM.



## **2.2.4 Multi-component analysis**

### **2.2.4.1 Dissolution results for Excedrin® caplets (aspirin and acetaminophen) in pH 7.4 phosphate buffer**

To demonstrate the ability of *in situ* ATR-IR to successfully monitor multiple components within the same tablet, dissolution testing was carried out on Excedrin® caplets. The label claims for the Excedrin® caplet are acetylsalicylic acid (250 mg) and acetaminophen (250 mg) actives. The release profile was determined by simultaneously adding three Excedrin® caplets to a 500 mL vessel volume containing pH 7.4 phosphate buffer. Three caplets were necessary to ensure satisfactory signal to noise ratio. Refer to Figure 2-5 for ATR-IR spectra for Excedrin® caplets. The dissolution rates of both components were monitored over 1.5 hours. Based on the data, it was determined that acetylsalicylic acid and acetaminophen were fully released within 1.5 hours as shown in Figure 2-6. *In situ* ATR-IR method is clearly able to distinguish the dissolution the acetylsalicylic acid and acetaminophen components.

To compare the *in situ* ATR-IR method with HPLC, aliquots were taken throughout the experiment and analyzed. The results from the *in situ* ATR-IR and HPLC systems are overlaid in Figure 2-6 and an excellent correlation is observed between the two methods. Refer to Table 2-4 to Table 2-7 for statistical values. Overall, this set of experiments indicates the versatility of *in situ* ATR-IR for dissolution testing as it allows automated observation of a multi-component system without manual sampling and by successfully tracking the dissolution behavior of two of the major components.

**Figure 2-5 ATR-IR spectra of Excedrin® caplets at different time-points during dissolution in pH 7.4 phosphate buffered solution**

ATR-IR spectra for Excedrin® caplet (acetaminophen and acetylsalicylic acid) in pH 7.4 phosphate buffer solution. Acetaminophen was calculated using wavenumber  $1246\text{ cm}^{-1}$  and acetylsalicylic acid was calculated using  $1388\text{ cm}^{-1}$ .

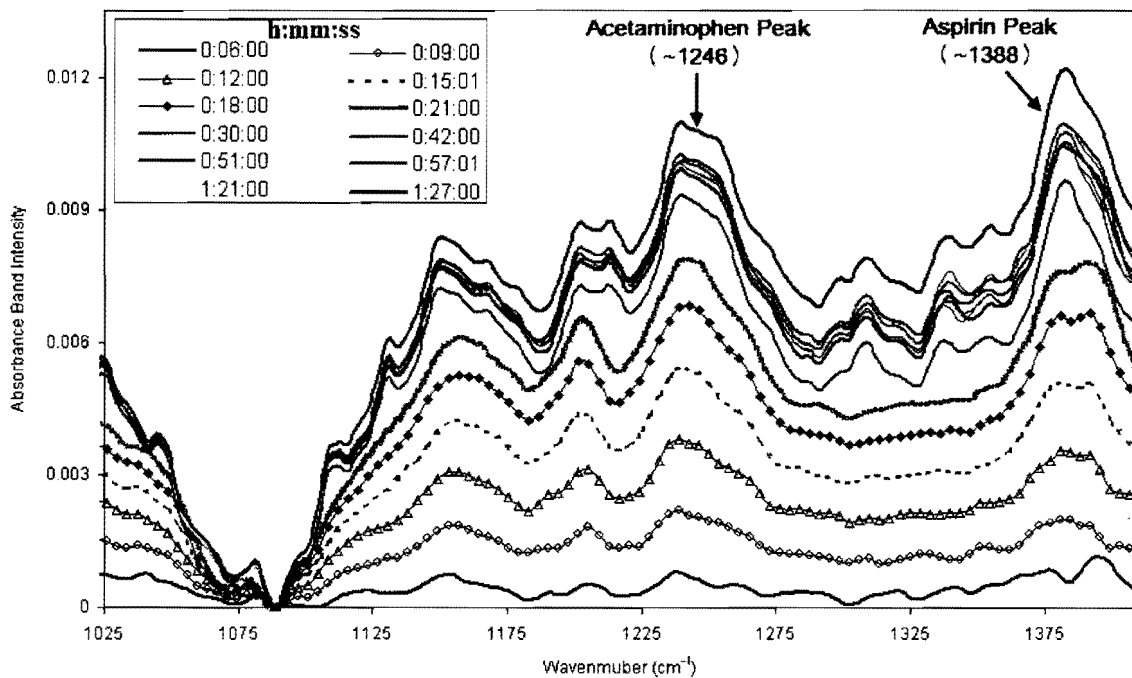


**Figure 2-6 Dissolution of acetylsalicylic acid and acetaminophen in Excedrin® caplets: *in situ* ATR-IR vs. HPLC**

The figure below represents a plot of Excedrin® (acetaminophen and acetylsalicylic acid % dissolved) vs. time. The blue squares and yellow triangles represent the HPLC data points. As observed, the two techniques (IR and HPLC) correlate very well. Refer to Table 2-4 for more details.

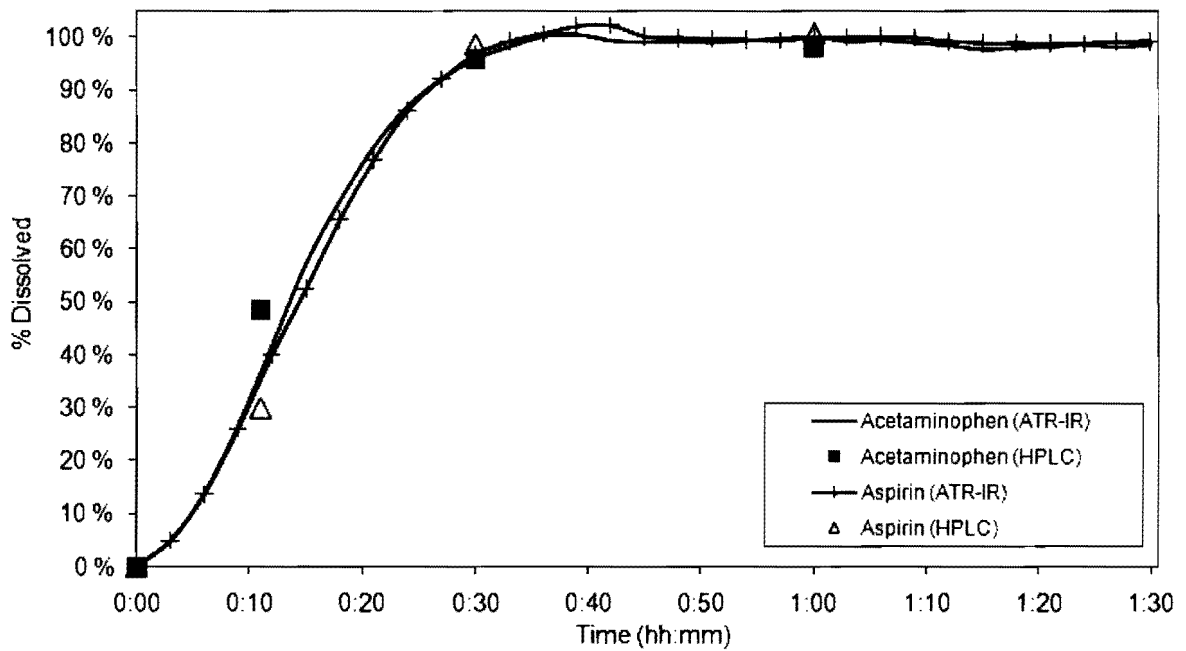


**Table 2-4 Dissolution of acetylsalicylic acid (aspirin) and acetaminophen in Excedrin® caplets: ATR-IR raw data**

Raw data results for the ATR-IR spectra of Excedrin® caplets.

Time (h:mm:ss)	Acetaminophen (ATR-IR) (% Dissolved)	Aspirin (ATR-IR) (% Dissolved)
0:00:00	0.0	0.0
0:03:00	4.8	4.9
0:05:59	13.7	13.6
0:08:59	26.5	25.9
0:11:59	41.6	39.8
0:15:00	57.3	52.5
0:17:59	69.0	65.6
0:20:59	79.2	76.7
0:23:59	86.8	86.1
0:27:00	92.1	92.0
0:29:59	95.8	96.8
0:32:59	98.2	99.2
0:35:59	100.1	100.6
0:38:59	100.4	102.1
0:41:59	99.3	102.2
0:44:59	99.0	100.2
0:48:00	99.2	99.9
0:50:59	98.9	99.7
0:53:59	99.3	99.5
0:57:00	99.6	99.3
0:59:59	100.0	100.0
1:02:59	99.2	100.0
1:06:00	99.3	100.1
1:08:59	98.9	99.9
1:12:00	98.4	99.2
1:14:59	97.6	98.9
1:17:59	97.9	98.9
1:20:59	98.1	98.8
1:24:00	98.6	98.8
1:26:59	98.0	99.2
1:30:00	98.6	99.2

**Table 2-5 Dissolution of acetylsalicylic acid (aspirin) and acetaminophen in Excedrin® caplets: HPLC raw data**

Raw HPLC data results for Excedrin® caplets.

Time (h:mm:ss)	Acetaminophen (HPLC) (% Dissolved)	Aspirin (HPLC) (% Dissolved)
0:00:00	0.0	0.0
0:11:00	48.4	29.9
0:30:00	95.7	98.6
1:00:00	98.0	100.7

**Table 2-6 % Dissolved of acetaminophen: Difference between ATR-IR and HPLC results**

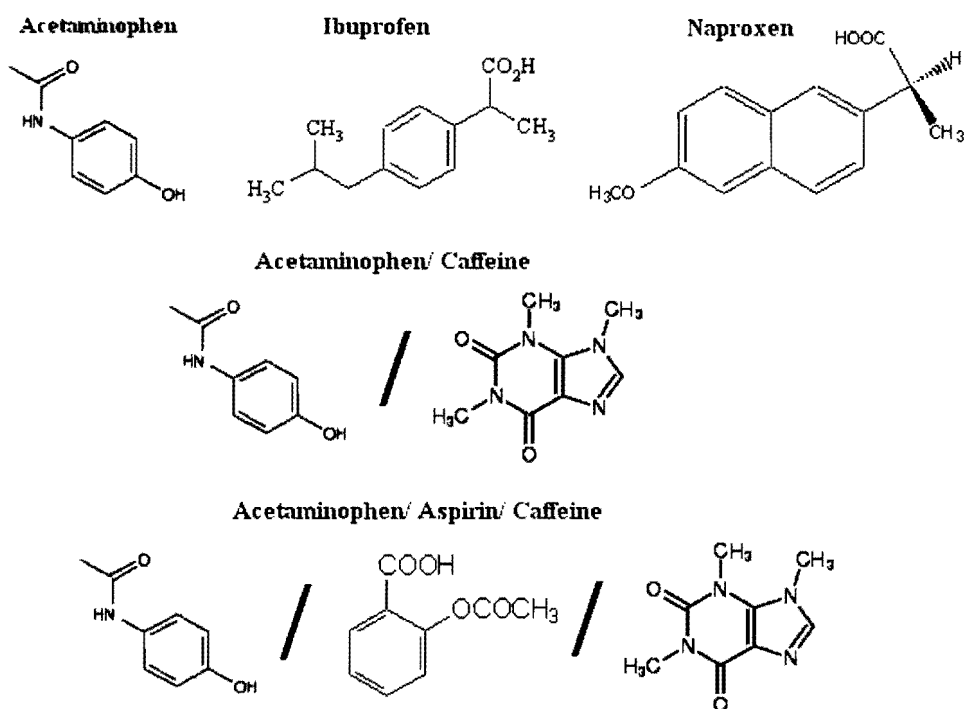
Time (h:mm:ss)	Acetaminophen (HPLC) (% Dissolved)	Acetaminophen (ATR-IR) (% Dissolved)	Absolute Difference
0:00:00	0.0	0.0	0.0
0:11:00	48.4	41.6	6.8
0:30:00	95.7	95.8	-0.1
1:00:00	98.0	100.0	-2.0

**Table 2-7 % Dissolved acetylsalicylic acid (aspirin) analysis: Difference between ATR-IR and HPLC results**

Time (h:mm:ss)	Aspirin (HPLC) (% Dissolved)	Aspirin (ATR-IR) (% Dissolved)	Absolute Difference
0:00:00	0.0	0.0	0.0
0:11:00	29.9	39.8	-9.9
0:30:00	98.6	96.8	1.8
1:00:00	100.7	100.0	0.7

**Figure 2-7 Compounds studied/of interest for future work (Chem. Draw)**

This figure represents some of the compounds studied during the research (i.e. acetaminophen, aspirin). Also, other compounds and combinations of these compounds will be studied during future research. These potential compounds include ibuprofen, naproxen and caffeine.



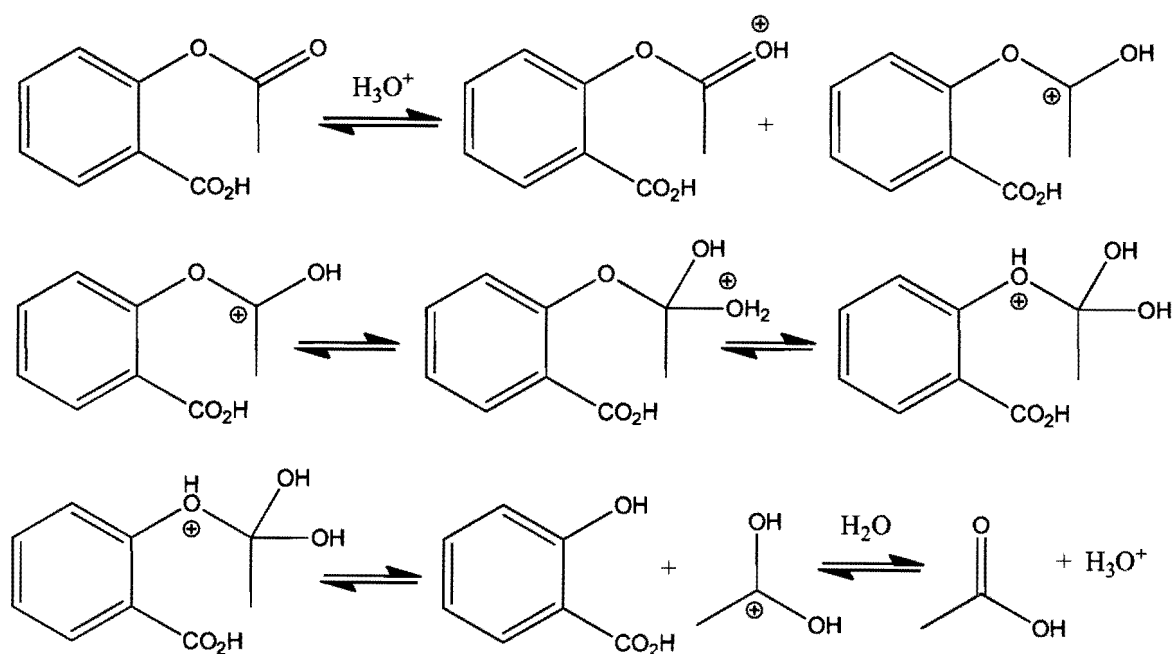


### 2.3 Chapter summary

*In situ* infrared spectroscopy was found to be a viable alternative for measuring dissolution profiles of pharmaceutical tablets. The IR system was found to be impressive in its capability of measuring very low concentrations. The limit of detection was found to be 0.02 mg/ml per IUPAC calculations. The IR system was able to distinguish separate components of a multiple component system without requiring manual sampling. This versatility is demonstrated by observing the simultaneous dissolution of acetaminophen and salicylic acid tablets. In contrast, UV-Vis spectroscopy may require mathematical corrections to resolve the two active drugs. Furthermore, HPLC must be used which requires laborious manual sampling or purchase of a complicated automated instrument setup of dissolution with HPLC analysis. The *in situ* ATR-IR method has been validated by comparing dissolution profiles using UV-Vis and HPLC methods. In addition, an accuracy of  $\pm 2\%$  between IR and HPLC for the salicylic acid results was established. With the current configuration of the IR instrument, this analysis is limited by the sensitivity and wavelength range of the *in situ* fiber optic probe. However, since this chapter successfully demonstrates the versatility of this novel application of ATR-IR spectroscopy, it is clear that the method has excellent potential to be improved by modification of the IR instrument and selection of more sensitive probes.

### 3 Kinetics of drug hydrolysis of common over-the-counter (OTC) drugs via ATR-IR spectroscopy

This chapter focuses on describing the hydrolysis of acetylsalicylic acid (aspirin) under acidic conditions. The hydrolysis of aspirin was tested and monitored using ATR-IR spectroscopy. In the presence of an acidic medium, acetylsalicylic acid undergoes hydrolysis<sup>41</sup> to form salicylic acid by the following acid-catalyzed mechanism:

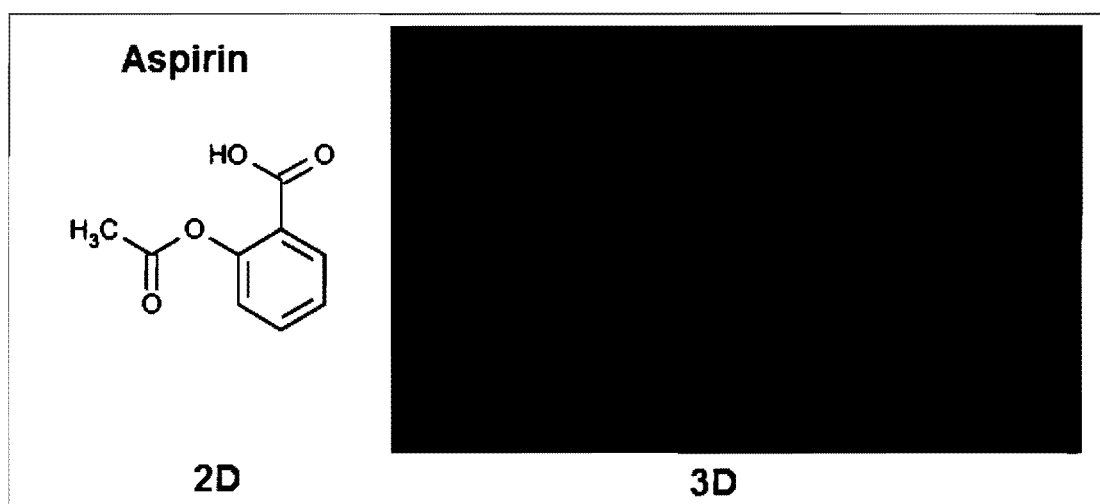


<sup>41</sup> Choudhury, S.; Mitra, A.K. Kinetics of aspirin hydrolysis and stabilization in the presence of 2-hydroxypropyl- $\beta$ -cyclodextrin. *Pharmaceutical Research* **1993**, 10 (1), 156-159.

### 3.1 Background and history of Aspirin

Aspirin is unique in its history and has many important roles in drug therapy. Aspirin is known to decrease pain. It fights the pain and inflammation by blocking the action of an enzyme called cyclooxygenase which inhibits the formation of prostaglandins.<sup>42</sup> Prostaglandins are chemicals that signal an injury and trigger pain. Moreover, aspirin is mostly known for its ability to reduce strokes. Since aspirin inhibits the formation prostaglandins this results in the inhibition of blood clots which could cause a heart attack or stroke.

**Figure 3-1 Structures of acetylsalicylic acid (aspirin)**

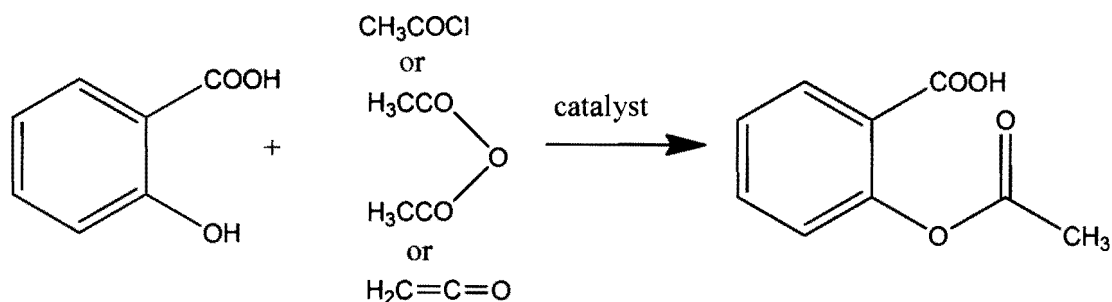


---

<sup>42</sup>Ito, Seiji; Okuda, Emiko; Minami, Toshiaki. Central and peripheral roles of prostaglandins in pain and their interactions with novel neuropeptides nociceptin and nocistatin. *Neuroscience Research* **2001**, 41(4), 299-332.

The first synthesis of aspirin is credited to Gerhardt<sup>43</sup> in 1853. Gerhardt was investigating mixed organic acid anhydrides. Felix Hoffman (1868-1946) used acetic anhydride<sup>44</sup> for aspirin's preparation. Felix Hoffmann synthesized aspirin in the laboratories of Farbenfabriken Bayer, Elberfeld, Germany in 1897.<sup>45</sup> Legend has it that Hoffman wanted to help his sick father who was suffering from rheumatism and was no longer able to tolerate sodium salicylate, then widely used for his father's arthritis disease. Salicylic acid, however, has several bad flaws. Its bad taste, stomach irritation and other side effects spurred researchers to look for other derivatives. The intent was to keep salicylic's efficacy without the disadvantages it posed. Acetylation of the hydroxyl group was one of the logical modifications. This logical thinking eventually led to the synthesis and discovery of aspirin. Refer to Figure 3-2 below for one of the synthesis pathways that were investigated back in the late 1800's.

**Figure 3-2**      **Synthesis of aspirin-late 1800's (Chem. Draw)**



<sup>43</sup> C. Gerhardt, *Annalen der Chemie*, 67, 149(1853)

<sup>44</sup> F. Hoffmann, U.S. Patent C44077 of February 27, 1900.

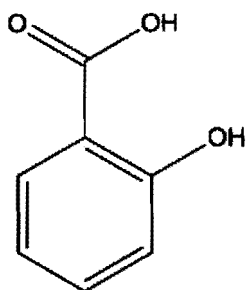
<sup>45</sup> *Analytical Profiles of Drug Substances*, 8 Aspirin, Klaus Florey, (1979).

## **3.2 Experimental section**

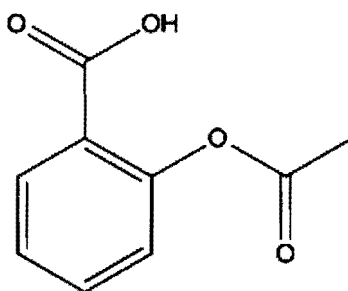
### **3.2.1 Chemical and materials**

Acetylsalicylic acid (aspirin) reference material (batch no. 016K0131) was purchased from Sigma-Aldrich. This same material was used “as is” for the powdered aspirin. Salicylic acid reference material (batch no. 04708HE) was purchased from Sigma-Aldrich. Acetylsalicylic acid 325 mg tablets (Bayer batch no. 219050N) were purchased from a local pharmacy. Methanol, acetone and acetonitrile (HPLC grades) were purchased from Pharmaco-Aaper. Sodium chloride crystals (batch no. J39602), used to prepare the Simulated Gastric Fluid (SGF) reagent, was purchased from Mallinckrodt Chemicals. Conc. hydrochloric acid (batch no. H44032), used to prepare the SGF reagent, was purchased from J.T. Baker. All solutions were prepared using water treated by a Milli-Q Millipore purification system. All purified water aliquots have resistivity of not less than 18 M $\Omega$ -cm<sup>-1</sup>.

**Figure 3-3**      **Chemical structures studied (Chem. Draw)**



**Salicylic Acid**



**Acetylsalicylic acid  
(aspirin)**

### 3.2.2 Instrumentation

Samples were tested using Mettler Toledo's iC10 FT-IR system using a fiber optic probe equipped with a 1 mm diamond coated ATR probe. The IR system was operated by Mettler Toledo's iC IR version 3.0 or 4.0 software. The pH determinations were carried out using a Symphony pH meter (model no. SB70P). All dissolution experiments were tested in Mettler Toledo EasyMax 102 apparatus using iC Control 4.1 software. All analytical weight measurements were carried out using Mettler Toledo's DeltaRange and AG204 DeltaRange scale.

### 3.2.3 Buffered solutions

The Simulated Gastric Fluid ("SGF"), pH 1.2, was prepared with sodium chloride and aqueous hydrochloric acid in accordance with the USP.<sup>46</sup> The detailed procedure for preparing this test solution is shown below

#### Hydrochloric Acid Solution (0.2M):

The volumes shown in the table are for 200 mL of buffer solution. Note: Where water is specified for solution or dilution of test substances in pH determinations, use carbon dioxide-free water.

- Sodium Hydroxide (0.2 M) - Dissolve 4.0 g of sodium hydroxide in water to make 100 mL.
- Potassium Chloride (0.2 M) - Dissolve 14.91 g of potassium chloride (KCl) in water, and dilute with water to 1000 mL.

---

<sup>46</sup> US Pharmacopoeia & National Formulary- Gastric Fluid, Simulated, USP [Online], <http://www.usp.org/> (accessed May 1, 2011).

**Table 3-1 Hydrochloric acid buffer preparations as per United States Pharmacopeia (USP)**

<b>Composition of Standard Buffer Solutions</b>											
<i>Hydrochloric Acid Buffer</i>											
Place 50 mL of the potassium chloride solution in a 200-mL volumetric flask, add the specified volume of the hydrochloric acid solution, then add water to volume.											
pH	1.2	1.3	1.4	1.5	1.6	1.7	1.8	1.9	2.0	2.1	2.2
0.2 M HCl, mL	85.0	67.2	53.2	41.4	32.4	26.0	20.4	16.2	13.0	10.2	7.8

### 3.2.4 Hydrolysis Experiments

#### HYDROLYSIS USING ASPIRIN TABLETS:

Aspirin tablets: 325 mg acetylsalicylic acid tablets were tested in pH 1.2 simulated gastric fluid solutions. Dissolutions were conducted using vessel volumes of 100 mL and at 37 °C. All dissolutions were conducted using an agitation speed of 100 rpm. The dissolution run times were set for 1.5 hours.

#### HYDROLYSIS USING ASPIRIN POWDER:

Aspirin powder: acetylsalicylic acid powder samples were tested in pH 1.2 simulated gastric fluid solutions. Dissolutions were conducted using vessel volumes of 100 mL and at 37 °C. All dissolutions were conducted using an agitation speed of 100 rpm. The dissolution run times were set for 1.5 hours.

### 3.2.5 ATR-IR analysis

The ReactIR™ iC10 FTIR instrument is composed of an MCT detector (liquid nitrogen cooled) and the FiberConduit™. The FiberConduit™ is comprised of flexible IR transparent silver chloride/silver bromide optical fibers. The fiber optic probe interface (AgX 9.5 mm x 1.5 m Fiber (Silver Halide)) contains a diamond tip-DiComp ATR crystal. The resolution was



set to 8 wavenumbers. The optical range used by the system is:  $1900\text{ cm}^{-1}$  to  $650\text{ cm}^{-1}$ . The gain adjustment was set to normal (1x) and the apodization method was set to Happ-Genzel.<sup>47</sup> The system uses compressed air (house air, filtered and dehumidified) to purge the optics.

#### HYDROLYSIS USING ASPIRIN TABLETS:

For the hydrolysis of aspirin tablet experiments, data treatment was carried out using the following methodology: The data were first subjected to baseline correction. An absorption band at  $1202\text{ cm}^{-1}$  ( $1202\text{-}1198\text{ cm}^{-1}$ ) was selected for **acetylsalicylic acid**. The peak area was calculated using a two-point baseline correction set at  $1180\text{ cm}^{-1}$  and  $1203\text{ cm}^{-1}$ . The ATR-IR system was configured to collect spectra every two minutes.

For this experiment, data processing is critical to obtain well-resolved spectra. Here is how the data is processed. First, the peak of interest was identified ( $1202\text{ cm}^{-1}$ ) and the area was calculated using a two-point baseline correction. Next, a trend analysis was performed using the iCIR software on this peak. This provided a plot of absorbance vs. time. This plot was subjected to smoothing using a 25 point smoothing parameter. After smoothing, and while still in the trend analysis, the baseline correct routine was performed. Then, the data were exported to Excel. Further data processing in Excel involved the subtraction of solvent spectra from reaction spectra. To perform this, a 30 min set of spectra at the beginning of the experiment, before aspirin pill was added, was selected. These spectra were subtracted from the spectra taken after the pill was dropped to give the final set of data. Within the final set of data, the area of the  $1202\text{ cm}^{-1}$  peak was calculated at each time point. Then plot of area vs.

---

<sup>47</sup> Application Note: Effect of resolution to vapor phase spectrum of HCl in the Infrared Spectroscopy, Shimadzu Co., [http://www2.shimadzu.com/applications/fir/App1\\_FTIR\\_HCl-vapor-phase\\_06D\\_en.pdf](http://www2.shimadzu.com/applications/fir/App1_FTIR_HCl-vapor-phase_06D_en.pdf), accessed 25 May 2011.

time were performed to give rate information. In addition, using a calibration curve, peak areas were converted to concentration to provide concentration vs. time plots.

An absorption band at  $1086\text{ cm}^{-1}$  ( $1080\text{-}1090\text{ cm}^{-1}$ ) was selected for **salicylic acid**. The peak area was calculated using a two-point baseline correction set at  $1078\text{ cm}^{-1}$  and  $1101\text{ cm}^{-1}$ . The ATR-IR system was configured to collect spectra every two minutes.

Preparation of salicylic acid standards: 325 mg of standard salicylic acid was added to a 100 mL volumetric flask and 50 mL of SGF solution was added and the flask was sonicated for 1 min to ensure all solids were dissolved. Finally, the solution was diluted to 100 mL using SGF.

Preparation of acetylsalicylic acid standards (in this case, there are competing concerns about the lower solubility of the compound and the need to limit the amount of hydrolysis of the compound): To decrease time, the IR was set-up and background spectra were taken prior to preparing the standard solution. Acetylsalicylic acid (325 mg) was added to a 100 mL volumetric followed by 75 mL of SGF. The flask was sonicated for 10 – 15 to effect complete dissolution of the solids, diluted to 100 mL with SGF.

#### HYDROLYSIS USING ASPIRIN POWDER:

For the hydrolysis of aspirin powder experiments, data treatment was carried out using the procedure described above. An absorption band at  $1202\text{ cm}^{-1}$  ( $1202\text{-}1198\text{ cm}^{-1}$ ) was selected for **acetylsalicylic acid**. The peak area was calculated using a two-point baseline correction set at  $1180\text{ cm}^{-1}$  and  $1203\text{ cm}^{-1}$ . The ATR-IR system was configured to collect spectra every two minutes.

An absorption band at  $1086\text{ cm}^{-1}$  ( $1080\text{-}1090\text{ cm}^{-1}$ ) was selected for **salicylic acid**. The peak area was calculated using a two-point baseline correction set at  $1078\text{ cm}^{-1}$  and  $1101\text{ cm}^{-1}$ . The ATR-IR system was configured to collect spectra every two minutes.

For all ATR-IR experiments, 256 scans were collected and co-added for each spectral point. On average, every spectral point, took about two-minutes to complete. For all testing, the calculated peak response was subjected to mathematical smoothing using the  $iC_{10}$  software. The data were compared to reference standards measurements collected prior to start of the linearity and dissolution experiments.

Preparation of salicylic acid standards: 325 mg of standard salicylic acid was added to a 100 mL volumetric flask and 50 mL of SGF solution was added and the flask was sonicated for 1 min to ensure all solids were dissolved. Finally, the solution was diluted to 100 mL using SGF.

Preparation of acetylsalicylic acid standards (in this case, there are competing concerns about the lower solubility of the compound and the need to limit the amount of hydrolysis of the compound): To decrease the preparation time, the IR was set-up and background spectra were taken prior to preparing the standard solution. Acetylsalicylic acid (325 mg) was added to a 100 mL volumetric followed by 75 mL of SGF. The flask was sonicated for 10 – 15 to effect complete dissolution of the solids, diluted to 100 mL with SGF.

All dissolution experiments were allowed to equilibrate in the buffer for at least half an hour prior to the start of a dissolution experiment. Dissolution data were collected and plots of percent (%) dissolved vs. time were made.

### **3.3 Results and discussion**

#### **3.3.1 Hydrolysis of aspirin to salicylic acid in test tubes**

Prior to starting the hydrolysis experiments, a qualitative measurement was investigated for determining the presence of salicylic acid in solution. As discussed earlier, acetylsalicylic acid hydrolyzes to salicylic acid in the presence of an acidic medium. Ferric chloride was found to be a good qualitative test for salicylic acid. Ferric chloride, or iron (III) chloride, will not react with aspirin. It will, however, react with salicylic acid, which is used to synthesize aspirin and is also the hydrolysis product of aspirin. Moreover, the formation of an iron-phenol complex will occur.<sup>48</sup> Thus, adding an aqueous ferric chloride solution to a sample of aspirin is a good way to see if there is any salicylic acid present and a purple color is an indication of salicylic acid. A sample of pure aspirin should not exhibit any color change. The ferric chloride color test is shown in Figure 3-4.

---

<sup>48</sup> Cha, K.; Park, K. Determination of iron (III) with salicylic acid by fluorescence quenching method. *Talanta* **1998**, 46(6), 1567-1571.

Figure 3-4 Ferric chloride color test- control samples

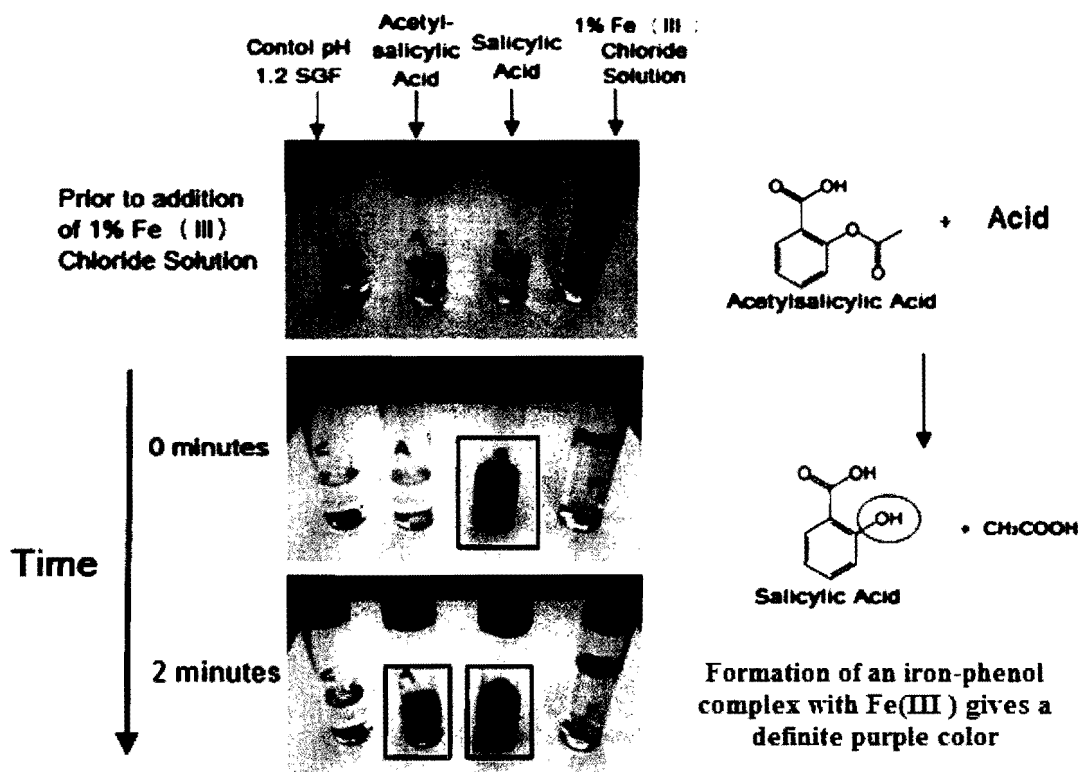


**Table 3-2 Ferric chloride color test concentrations**

Experiment number	Weight of Aspirin (mg)	Weight of Salicylic Acid (mg)
1	32.1	33.4
2	33.9	33.7
3	31.7	35.1
Average weight (mg)	32.6	34.1
Volume of flask(s) (ml)	10.0	10.0
Average Concentration (mg/ml)	3.3	3.4

**Table 3-3 Ferric chloride color test observations [added 2mg /ml Fe (III) solution]**

Time (min)	CONTROL Sample (SGF)	Acetylsalicylic acid Sample	Salicylic Acid Sample
0 min	Clear (no color change)	Clear (no color change)	Dark purple
1 min	Clear (no color change)	Clear (no color change)	Dark purple
2 min	Clear (no color change)	Light purple	Dark purple
5 min	Clear (no color change)	Dark purple	Dark purple

### **3.3.2 Hydrolysis of aspirin to salicylic acid using aspirin tablet as the starting ingredient**

The hydrolysis of acetylsalicylic acid (aspirin) tablets was carried out in pH 1.2 SGF solutions. The solutions were preheated to body temperature, 37 °C, and the ATR-IR fiber optic probe collected baseline spectra (blank medium) for the first 30 minutes. A single 325 mg Bayer aspirin tablet was dropped into the vessel containing 100 mL of pH 1.2 solution.

Standard spectra of pure acetylsalicylic acid (aspirin) and salicylic acid were collected prior to running the dissolutions. These standards were used to identify the unique peaks of interests for these active drugs and for calculating absorbance intensities to concentration. As shown in Figure 3-5, aspirin has a unique band at 1202  $\text{cm}^{-1}$  while salicylic acid has one at 1086  $\text{cm}^{-1}$ . Dissolution plots for aspirin and salicylic acid hydrosylate were made. Refer to Figure 3-6 which plots the concentration of acetylsalicylic acid vs. time and salicylic acid hydrosylate vs. time. This plot shows the formation and elimination of acetylsalicylic acid. Moreover, the acetylsalicylic acid hydrolyzed completely to form salicylic acid as shown in the plot. The presence of salicylic acid is detected by the IR system and plotted on a secondary axis as shown in Figure 3-6. In addition, the ferric chloride color test was used to visually inspect the presence or absence of salicylic acid. The ferric chloride solution was added to the aspirin tablet dissolution vessel after sixty minutes. The solution within the vessel quickly turned to a purple color as shown in Figure 3-7.

**Figure 3-5 Waterfall plot of aspirin tablet dissolution**

This is a waterfall plot for the dissolution of 325 mg aspirin tablet in SGF. As seen in the figure, there are two peaks of interest; one at  $\sim 1086\text{ cm}^{-1}$  and one at  $\sim 1205\text{ cm}^{-1}$ . These represent salicylic acid and aspirin respectively. The purple color in the figure represents higher intensities while the blue green represent lower intensities or concentrations. As seen in the figure aspirin increases with time and then disappears while salicylic acid increases with time.

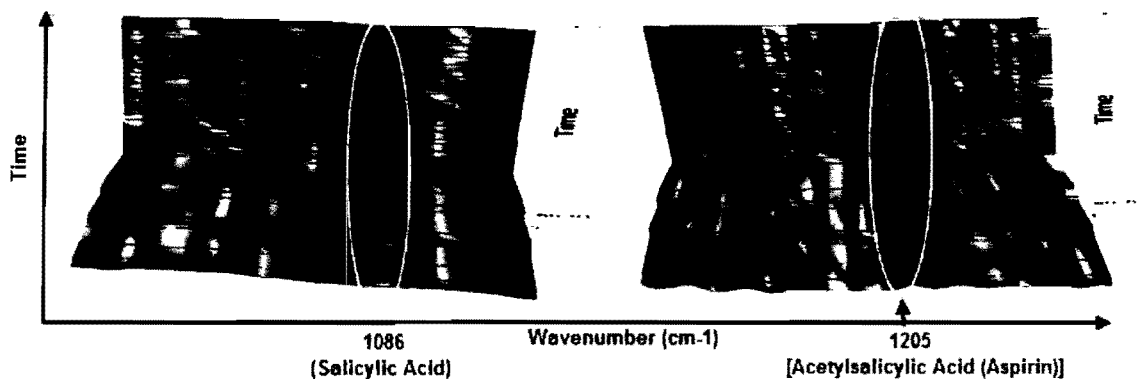




**Figure 3-6 Hydrolysis of Aspirin Tablets (325 mg) in pH 1.2 SGF Solution (n=2)**

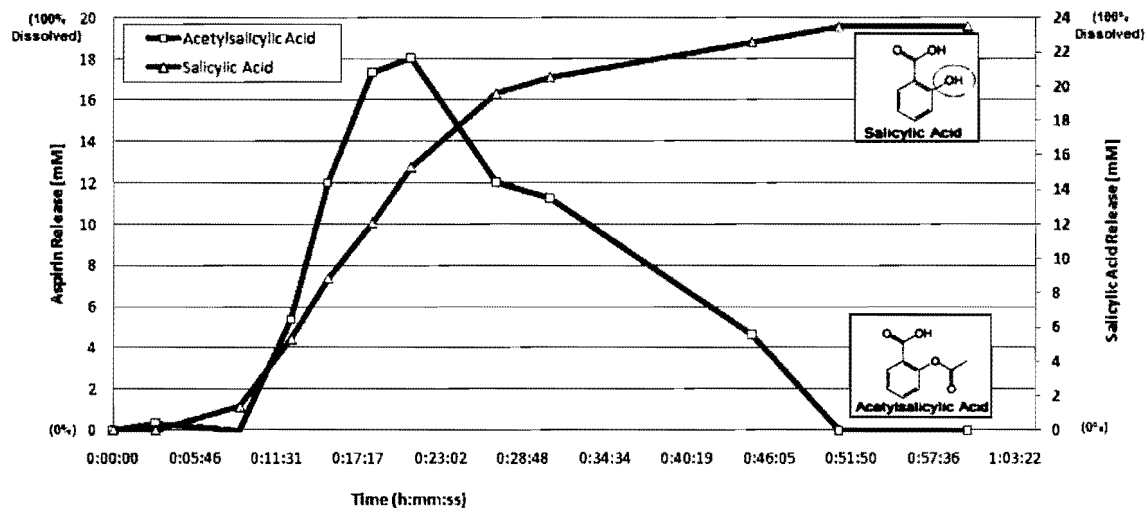
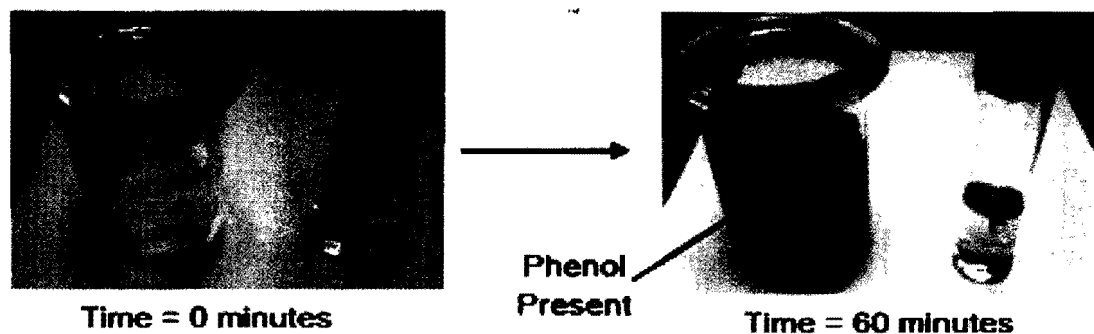


**Figure 3-7 Ferric chloride color test for salicylic acid (tablet dissolution)**

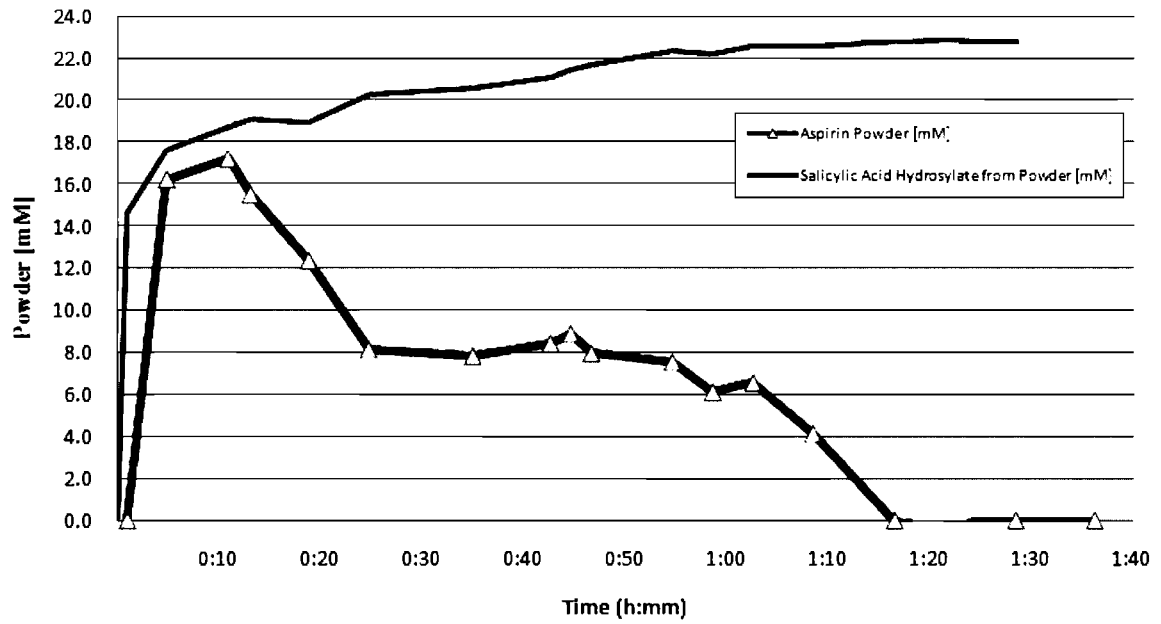
**Dissolution Vessel Ferric Chloride Test Results**



### **3.3.3 Hydrolysis of aspirin to salicylic acid using aspirin powder as the starting ingredient**

It was equally important to understand the rate of hydrolysis of aspirin in powder form. Since the hydrolysis of aspirin in a tablet depends on the dissolution of aspirin into solution first, the rate of hydrolysis of pure aspirin powder should be relatively quicker because all particles are immediately exposed to the dissolving medium. In fact, the rate limiting step in this case would be the dissolution of the particles into the acidic medium. As a result, the hydrolysis of aspirin to salicylic acid was monitored and measured using pure aspirin powder. Known amounts, equivalent to the amount found in a tablet, were placed in the dissolution vessels containing an acid solution (pH 1.2 SGF) and the dissolution profiles were collected using ATR-IR spectroscopy. Figure 3-8 shows the dissolution profiles of aspirin and salicylic acid using aspirin powder. In addition, the figure clearly shows the formation and then elimination of acetylsalicylic acid in solution (black line) and the simultaneous formation of salicylic acid hydrolylate in solution (red line).

**Figure 3-8 Hydrolysis of acetylsalicylic acid powder to salicylic acid hydrosylate in pH 1.2 solution**



### **3.3.4 Hydrolysis data: comparison between tablet and powder formulations**

Figure 3-9, compares the IR dissolution profiles of the salicylic acid component in powder and tablet form. As expected the rate of dissolution and hence hydrolysis of salicylic acid, is faster in the powder form. The tablet formulation has to undergo wetting, disintegration and deaggregation which take time. Similarly, Figure 3-10, compares the IR dissolution profiles of the aspirin component in powder and tablet form. As expected the rate of dissolution of aspirin, is faster in the powder form. For the tablets, in each case, there is an initial mechanical lag associate with the physical breakdown of the tablet. However, in the case of the experiments with the powders, there no mechanical lag and dissolution occurs immediately. However, with powdered acetylsalicylic acid, there is an interesting bimodal behavior. Initially, an immediate fast dissolution is observed and a secondary process is also observed at a slower rate as the dissolution occurs. Refer to Figure 3-8. The initial rapid dissolution likely occurs from particles that are well wetted in the initial exposure to the dissolution medium. However, aggregation of the powder was also observed suggesting that some of the acetylsalicylic acid particles were not wetted. The dissolution of these aggregates is associated with the slower dissolution process. In addition, the aspirin powder was used “as is” from the reagent container, therefore, the powder was inhomogeneous consisting of differ particle sizes with small and large crystal. It is likely that the larger particles and crystals contribute to the secondary dissolution process. However, that this process is not observed with salicylic acid (see Figure 3-9) is reasonable, first, because salicylic acid is more hydrophilic than acetylsalicylic acid, and, second, because salicylic acid dissolves at a faster rate, leaving less time for aggregation to occur.

To develop an overall understanding of the dissolution/hydrolysis processes that occur with aspirin, a composite plot was prepared (Figure 3-11). In this plot, the dissolutions of aspirin powder and tablet and the hydrolysis of aspirin powder and tablet to form the salicylic acid hydrolylate are shown. The solid blue-line (aspirin powder) and the dotted red-line (aspirin tablet) compare the IR dissolution profiles of the aspirin component in powder and tablet form respectively. As expected, the rate of dissolution of aspirin is faster in the powder form. For the tablets, in each case, there is an initial mechanical lag associated with the physical breakdown of the tablet. However, in the case of the experiments with the powders, there is no mechanical lag and dissolution occurs immediately. This plot also compares the release profiles of the salicylic acid hydrolylate in tablet (dotted green-line) and powder formulation (solid black line). Again, for the tablet, there is an initial mechanical lag associated with the physical breakdown of the tablet. Also, the hydrolysis of aspirin in the powder formulation appears to be quite rapid. Moreover, the plot shows this phenomenon occurring prior to the dissolution of the powder aspirin. Currently, the dissolution profiles were run at 100 rpm with a collection rate of two-minutes. A higher agitation speed and faster acquisition time (i.e. every 1 minute) should synchronize the dissolution of the aspirin and then the release of the salicylic acid hydrolylate in the powder formulation.

**Figure 3-9** Release profile of Salicylic Acid ("SA") during hydrolysis in SGF (pH1.2): powder vs. tablet

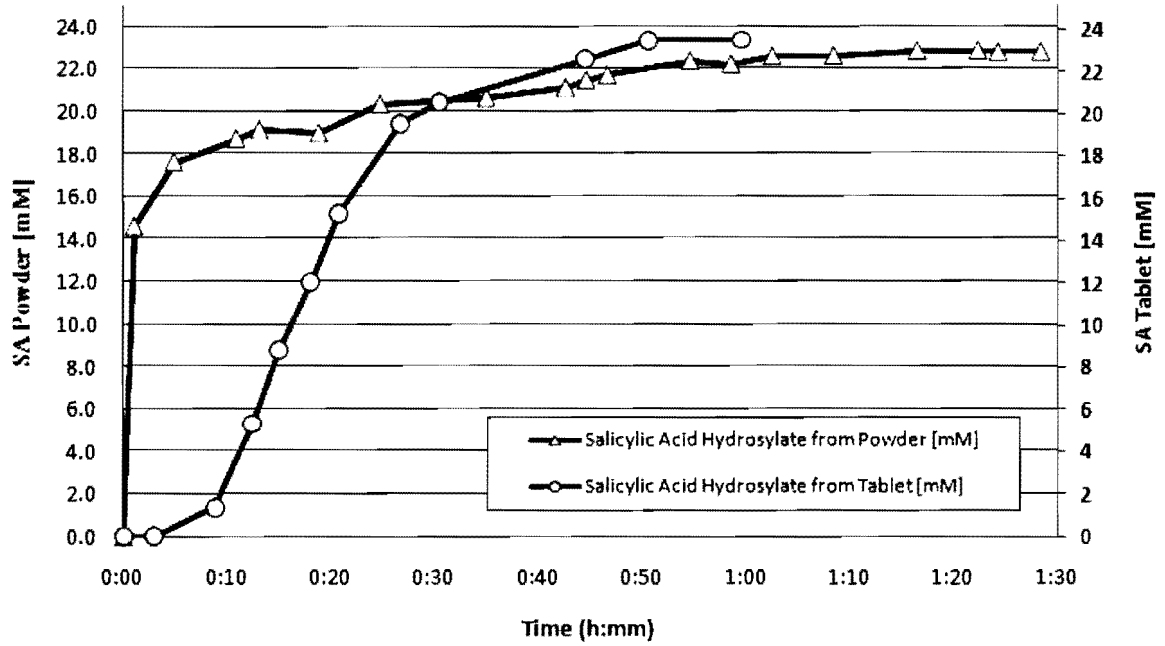
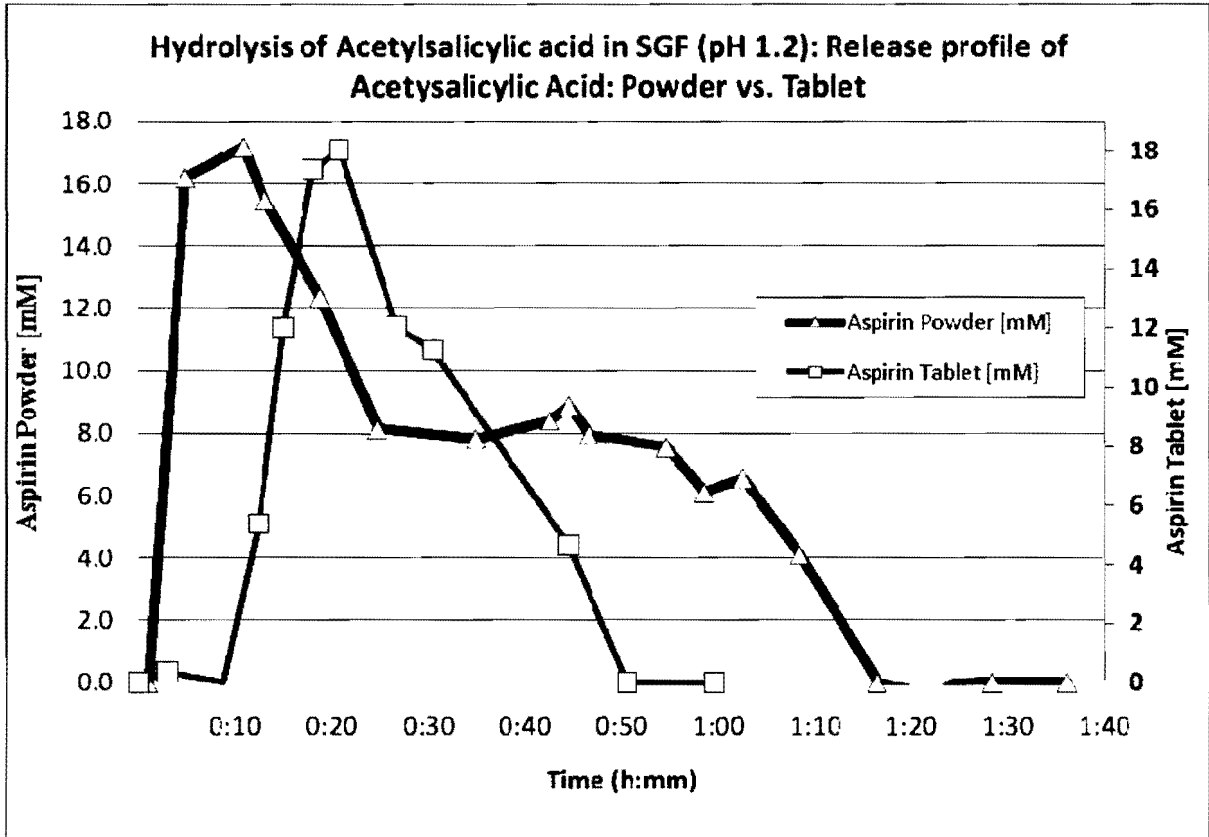
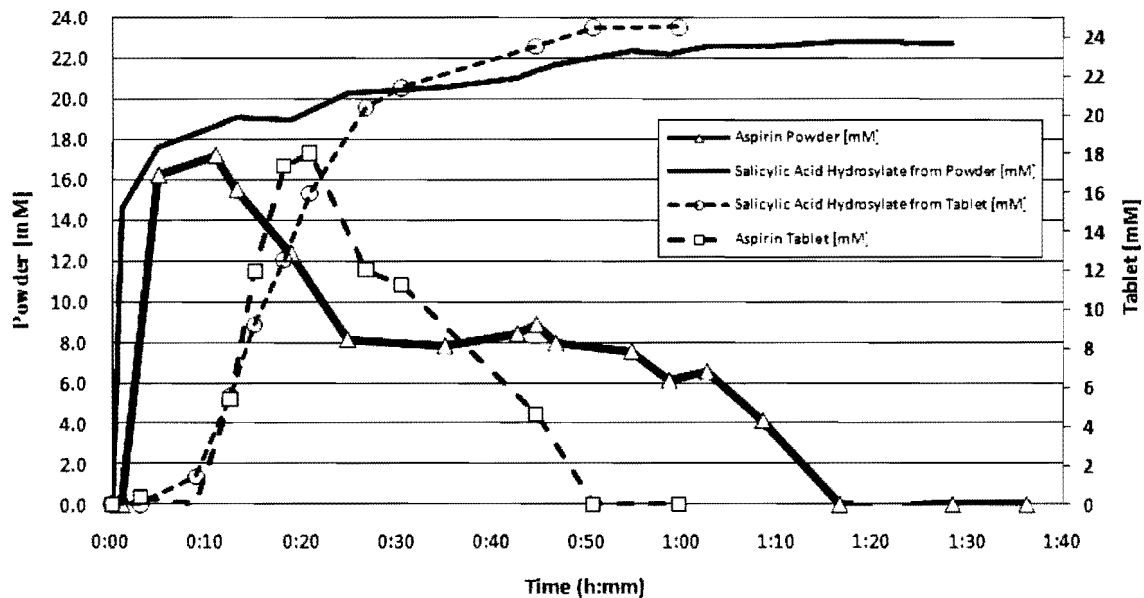


Figure 3-10 Release profile of acetylsalicylic acid (aspirin) during hydrolysis: powder vs. tablet



**Figure 3-11 Release profile of acetylsalicylic acid (aspirin) and salicylic acid hydrosylate during hydrolysis: powder vs. tablet**





### 3.3.5 Kinetic rates observed during hydrolysis experimentation

The kinetic rates were also determined for the experiments discussed earlier. The rates were determined using the slopes of the dissolution plots. The rates were compared to literature research<sup>49</sup> and were found to be equivalent within experimental error. In fact, the literature data shows the rate of hydrolysis of aspirin under acid medium varies from  $0.91 \text{ min}^{-1}$  to  $1.74 \text{ min}^{-1}$  depending on the pH and temperature of the solution. Refer to Table 3-4 for details. According to Habib and co-workers the hydrolysis rate of aspirin was found to be  $0.91 \text{ min}^{-1}$  at pH 1.0 and  $30^\circ\text{C}$ . Choudhury and co-workers reported the hydrolysis rate as  $1.74 \text{ min}^{-1}$  at pH 1.3 and  $40^\circ\text{C}$ . If both literature studies are taken into account and a linear plot is constructed with rate vs. pH/temp, the expected rate of hydrolysis at conditions similar to this research should be  $1.46 \text{ min}^{-1}$ . Furthermore, in this study, the hydrolysis of aspirin to salicylic acid, using OTC aspirin tablets in pH 1.2 SGF and at  $37^\circ\text{C}$ , was found to be  $1.03 \text{ min}^{-1}$ . The hydrolysis of aspirin powder to salicylic acid was found to be  $1.23 \text{ min}^{-1}$ .

---

<sup>49</sup> a) Habib, M.J.; Rogers, J.A. Kinetics of hydrolysis and stabilization of acetylsalicylic acid in liposome formulations. *International Journal of Pharmaceutics* **1998**, 44, 235-241. b) Choudhury, S.; Mitra, A.K. Kinetics of aspirin hydrolysis and stabilization in the presence of 2-hydroxypropyl- $\beta$ -cyclodextrin. *Pharmaceutical Research* **1993**, 10 (1), 156-159.

**Table 3-4 Kinetic rates for hydrolysis of aspirin in acidic medium**

Description	Kinetics Rate (1/min <sup>-1</sup> )
At pH 1.0 and 30 °C (acetylsalicylic acid= 7.5 mM) Ref	--
Rate of Hydrolysis	0.91
At pH 1.3 and 40 °C (acetylsalicylic acid= 5.55 mM) Ref	--
Rate of Hydrolysis	1.74
At pH 1.2 and 37 °C (acetylsalicylic acid= 18 mM) (this work)	--
Rate of Dissolution (Tablet)	1.62
Rate of Hydrolysis (Tablet)	1.03
Rate of Dissolution (Powder)	1.59
Rate of Hydrolysis (Powder)	1.23

The rates of the reactions were determined from the dissolution plots. Refer to Figure 3-10. In order to calculate the rates using the plot, the following procedure was implemented. First, a plot of % dissolved vs. time is obtained. Next, a straight line is drawn over the area of the dissolution curve where dissolution starts to occur (middle area in this case). Furthermore, the slope of the curve is obtained and from this the rate of hydrolysis is reported. Refer to Figure 3-12 and Figure 3-13.

Figure 3-12 Typical calculation plot of rate from dissolution

Below is a schematic diagram illustrating how to calculate the rate.

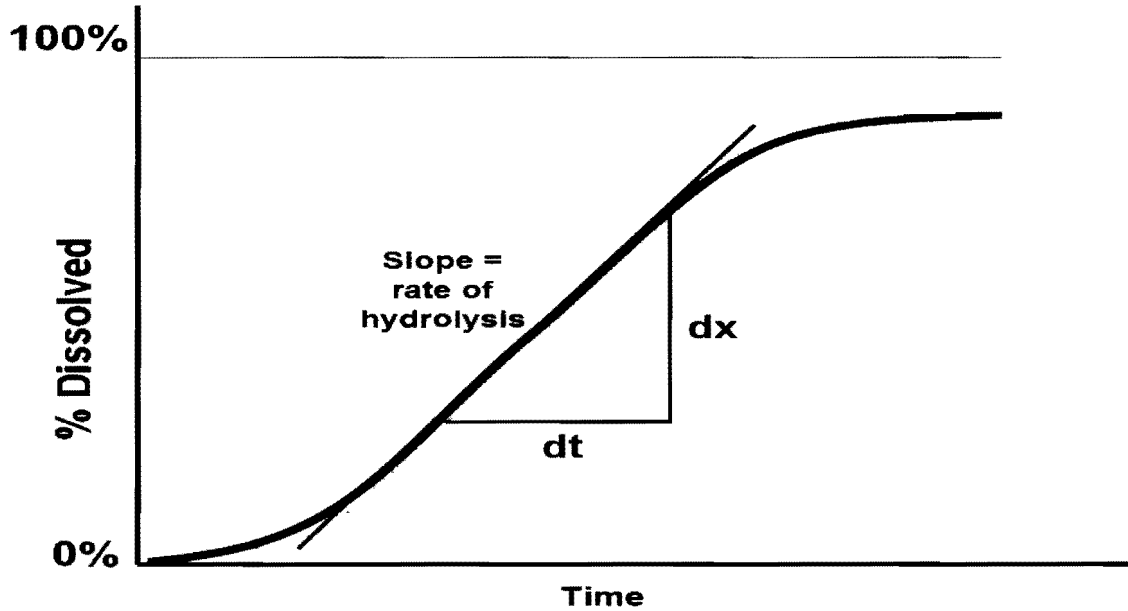
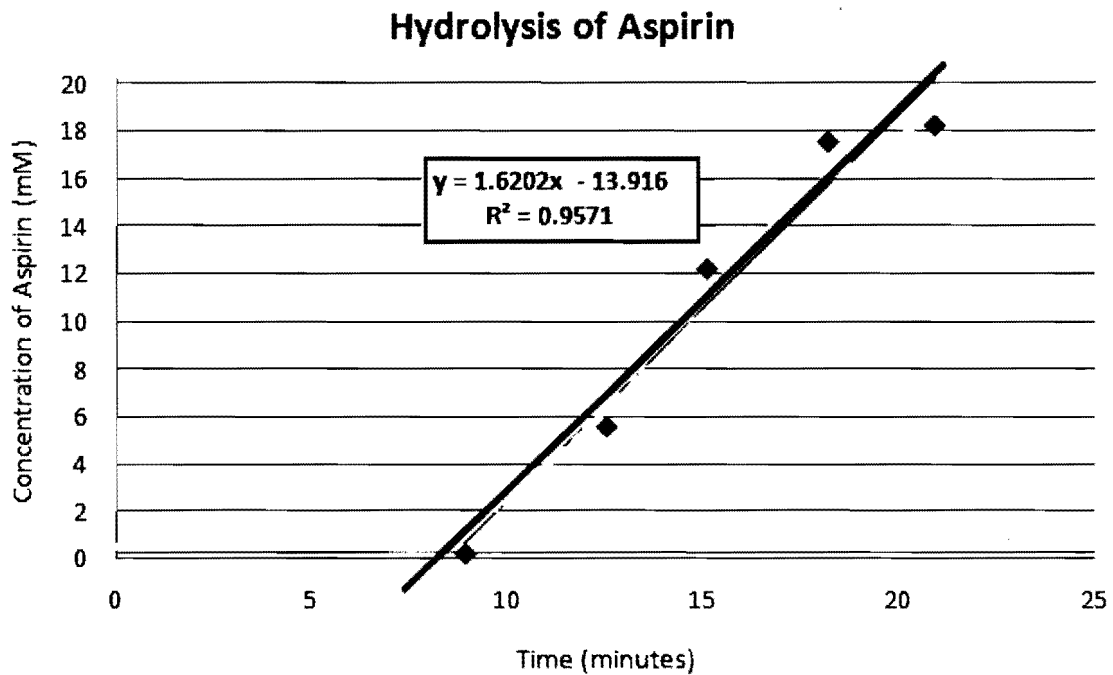


Figure 3-13 Rate of dissolution for Aspirin (based on slope of dissolution plot)



### 3.4 Chapter summary

In this chapter, it was demonstrated that *in-situ* infrared spectroscopy is a viable technique for detecting and measuring the hydrolysis of acetylsalicylic acid (aspirin) in acidic media. The IR system was found to be impressive in its capability of measuring very low concentrations and was able to distinguish separate components of a multiple component hydrolysis system without requiring manual sampling. This versatility is demonstrated by observing the simultaneous dissolution and then conversion of the acetylsalicylic acid API to salicylic acid. In the tablet formulation, the rate of dissolution was found to be  $1.62 \text{ min}^{-1}$  based on the initial slope of the dissolution profile. Moreover, the hydrolysis rate was found to be  $1.03 \text{ min}^{-1}$  based on the salicylic acid formation and dissolution profiles. In the powder formulation, the rate of dissolution was  $1.59 \text{ min}^{-1}$ . The rate of hydrolysis was found to be  $1.23 \text{ min}^{-1}$ . As expected, this rate is slightly higher since tablets require an initial period of disintegration and deaggregation. Moreover, the rate of hydrolysis of the powder formulation is closer to Choudhury's finding. In the tablet experiment, the rate of hydrolysis of aspirin does not exactly match the rate of hydrolysis from the powder experiment. This could be explained by several reasons. First, there is competing dissolution within the vessel. The tablet has to undergo disintegration and dissolution prior to hydrolysis occurring. Second, the stirring rate was too slow. In the powder formulation, by the time the active drugs reaches the fiber optic probe, the hydrolysis has already begun. This is especially important in the powder form where there is not competing dissolution of tablet. Refer to Figure 3-9. The salicylic acid hydrosylate was observed before the acetylsalicylic acid from the powder. Third, the IR

system was allowed to collect spectra every two minutes. This should be enhanced to collect every one minute in order to detect the hydrolysis quicker.

This research was possible because of the versatility of ATR-IR system. Specifically, the unique fingerprint region of the IR spectra gave detailed information about the release profile of the drug. Conventional methods, namely, *in-situ* UV-Vis, would only show the release profile of one component. However, peak deconvolution software can be used to analyze aspirin hydrolysis. Moreover, the hydrolysis and transformation of the drug from one form to another may be missed with conventional techniques. ATR-IR captures those minor details and displays them in the fingerprint region, as shown earlier in the results. The unique feature of this system is that it is able to detect several forms of the same drug. In other words, it was able to detect the formation and elimination of a pharmaceutical drug (aspirin) while detecting the formation of the hydrolyte of the aspirin (salicylic acid) in real-time. In addition, this system could be used to study other potential transformations. One example might be the dimerization of acetaminophen as mentioned earlier. The novelty with this particular system is its capability to see drug transformations in solutions while conducting the experiment *in-situ*. Since this chapter successfully demonstrates the versatility of this novel application of ATR-IR spectroscopy, indicating that that the method has excellent potential for detailed studies of the dissolution and hydrolysis kinetics of pro-drug formulations and drugs which hydrolyze under acidic conditions simulating stomach conditions.

## **4 Instrument Development Proposal: "Solv-IR" as an *In-Situ* ATR-IR Instrument for Solvation Chemistry**

This chapter focuses on describing the design and potential application of the "Solv-IR" system. The Solv-IR system is a new system that combines dissolution technology with attenuated total reflectance-infrared spectroscopy (ATR-IR). A Major Research Instrumentation (MRI) grant was recently submitted with the National Science Foundation for funding of this project. The details, described below, give an overview of the new system as well describe the specific components of the proposed new system.

### **4.1 Background**

Solvation, also sometimes called dissolution, is the process of attraction and association of molecules of a solvent with molecules or ions of a solute. As ions dissolve in a solvent they spread out and become surrounded by solvent molecules. By an IUPAC definition, solvation is an interaction of a solute with the solvent, which leads to stabilization of the solute species in the solution.<sup>50</sup> Solvation is also a kinetic process with a thermodynamic conclusion.<sup>51</sup> Most instrumentation used to investigate solvation focuses on the thermodynamic conclusion, i.e., the structure and concentration of the solvated species at equilibrium. Dynamic study of solvation either requires manual sampling or *in situ* UV-Vis detection which (in spite of excellent curve fitting software) has limited capability for multi-component analysis and for species that chemically transform. The goal is to construct a new instrument that allows

---

<sup>50</sup> IUPAC, Compendium of Chemical Terminology, 2nd ed. (the "Gold Book") (1997). Online corrected version: (2006-) "solvation".

<sup>51</sup> Anslyn, E. V.; Dougherty, D. A. Chapter 3: Solutions and Non-Covalent Binding Forces. *Modern Physical Organic Chemistry*; University Science, California, 2006.

dynamic measurement of solvation of a chemical substance or chemical mixture with *in situ* infrared detection. Because of the large number of vibration modes available for many molecules, infrared spectroscopy is much more selective than UV-Vis. In addition, characteristics of the IR band can provide information about the mechanism of dissolution including hydrogen bonding interactions and aggregation of solute molecules.<sup>52</sup> As discussed earlier, infrared spectroscopy using attenuated total reflectance (ATR) probes is quantitative, thus, providing precise measurement of solute concentrations. The proposed name for the instrument is Solv-IR which indicates that it uses infrared technology for investigation of solution chemistry. The target instrument will have several attractive features: a)  $10^{-6}$  M sensitivity, b) chemically robust; c) conventional IR spectral range; d) precise control of reaction vessel temperature; e) integrated stirring controls; g) n=6 solvation vessels to provide appropriate statistics; f) software for instrument control, data acquisition and processing. The Solv-IR will prove to be useful in the following scientific applications:

- Solvation of single component species such as homogeneous catalysts<sup>53</sup> and substances with different crystalline morphologies.<sup>54</sup>
- Crystallization studies (the reverse of solvation!).<sup>55</sup>

---

<sup>52</sup> The Chemical Physics of Solvation, Part B, Spectroscopy of Solvation, R. R. Dogonadze, E. Kálmán, A. A. Kornyshev, J. Ulstrup, Eds., Elsevier, The Netherlands, 1986. See: Chapter 1: "Spectroscopic approaches to the study of ionic solvation," G. Kabisch, E. Kálmán; Chapter 2: "Interactions in and structures of ionic solutions and polyelectrolytes, Infrared Results," G. Zundel, J. Fritsch; Chapter 3: "Infrared Spectroscopic results on solvate structures in crystals," G. Zundel, J. Fritsch.

<sup>53</sup> Studies of catalyst dissolution, a) Sun, Y.K.; Le Blond, C. R.; Wang, J.; Blackmond, D. G.; Laquidara, J.; Sowa, J. R. Observation of a [RuCl<sub>2</sub>((S)-(-)-tol-binap)]<sub>2</sub>•N(C<sub>2</sub>H<sub>5</sub>)<sub>3</sub>-Catalyzed Isomerization-Hydrogenation Network, *Journal American Chemical Society* **1995**, 117, 12647. b) Shaw, J.; Chen, Y.S.; Fulton, J.; Linehan, J.; Gutowska, A.; Bitterwolf, T. Structural evolution of a recoverable rhodium hydrogenation catalyst. *Journal of Organometallic Chemistry* **2008**, 693, 2111-2118.

<sup>54</sup> a) Acquah, C.; Karunanithi, A. T.; Cagnetta, M.; Achenie, S. L. Linear models for prediction of ibuprofen crystal morphology based on hydrogen bonding propensities. *Sub Fluid Phase Equilibria* **2009**, 277(1), 73-80.

- Studies of chemical and mechanical parameters that effect solvation including temperature, agitation, solvent-type, pH, shape and hardness of the solid.<sup>56</sup>
- \*Studies of tablet formulations including chemical effects of co-ingredients.<sup>57</sup>
- \*Monitoring of multi-component and controlled release formulations.<sup>58</sup>
- \*Solvation rates for components that chemically transform on the solvation time scale.<sup>59</sup>
- \*Environmental chemistry for study of dispersants (emulsifier, surfactants) for treating chemical (e.g., petroleum) spills and other anthropomorphic events.<sup>60</sup>
- Kinetics of micelle formation.<sup>61</sup>

The above examples represent key applications of IR spectroscopy in the chemistry of solution; however, there are many more examples.<sup>62</sup> Preliminary results have been obtained

---

b) Chieng, N; Rades, T.; Aaltonen, J. An overview of recent studies on the analysis of pharmaceutical polymorphs. *Journal of Pharmaceutical and Biomedical Analysis*, In Press (2011).

<sup>55</sup> Halasz, I.; Biljan, I.; Novak, P.; Meštrović, E.; Plavec, J.; Mali, G.; Smrečki, V.; Vančik, H. Cross-dimerization of nitrosobenzenes in solution and in solid state. *Journal of Molecular Structure* **2009**, 918(1-3).

<sup>56</sup> Vitha, M.; Carr, P. W. The chemical interpretation and practice of linear solvation energy relationships in chromatography. *Journal of Chromatography A* **2006**, 1126(1-2), 143-194.

<sup>57</sup> a) Van der Weerd, J.; Chan, K. L. A.; Kazarian, S. G. An innovative design of compaction cell for in situ FT-IR imaging of tablet dissolution. *Vibrational Spectroscopy* **2004**, 35(1-2), 9-13. b) Chan, K.L.A.; Elkhider, N.; Kazarian, S.G. Spectroscopic Imaging of Compacted Pharmaceutical Tablets. *Chemical Engineering Research and Design* **2005**, 83(11), 1303-1310. c) Dressman, J. J.; Kramer, J. K., Eds. *Pharmaceutical Dissolution Testing*; Taylor and Francis: Florida, 2005. d) Hanson, R; Gray, V. *Handbook of Dissolution Testing*, 3rd ed., *Dissolution Technologies*: Delaware, 2004.

<sup>58</sup> Van der Weerd, J.; Kazarian, S.G.; Combined approach of FTIR imaging and conventional dissolution tests applied to drug release. *Controlled Release* **2004**, **98**, 295-305.

<sup>59</sup> Kokot, Z.; Burda, K. Simultaneous determination of salicylic acid and acetylsalicylic acid in aspirin delayed-release tablet formulations by second-derivative UV spectrophotometry. *Journal of Pharmaceutical and Biomedical Analysis* **1998**, **18**, 871-875.

<sup>60</sup> a) Fingas, M. Oil Spill Dispersants: A Technical Summary. *Oil Spill Science and Technology* **2011**, 435-582. b) Brandvik, J; Daling, S. Optimising oil spill dispersants as a function of oil type and weathering degree: a multivariate approach using partial least squares (PLS). *Chemometrics and Intelligent Laboratory Systems* **1998**, 42(1-2), 73-91. c) Regan, F.; Meaney, M.; Vos, J.G.; Maccraith, B.D.; Walsh, J.E. Determination of Pesticides in water using ATR-FTIR spectroscopy on PVC/chloroparaffin coatings. *Analytical Chimica Acta* **1996**, 334, 85-92.

<sup>61</sup> Ceraulo, L.; Dormond, E.; Mele, A.; Turco Liveri, V. FT-IR and nuclear overhauser enhancement study of the state of urea confined in AOT-reversed micelles. *Colloids and Surfaces A: Physicochemical and Engineering Aspects* **2003**, 218(1-3), 255-264.



for the above examples with an asterisk (\*) using a single probe/vessel prototype.<sup>63</sup> However, all of the above examples are important to chemists and the Solv-IR instrument will provide fundamental and practical insight into these processes.

## 4.2 Broader impacts from the proposed activities

The activities described in this project have several characteristics that are likely to have a broad impact on our nation's scientific infrastructure and perhaps provide economic opportunities. Thus, the *broader impacts from the proposed activities* are described here.

- First, there is substantial evidence that the proposed Solv-IR will be commercially viable. Investigation of solvation chemistry of single compounds or mixtures ensures that compounds are accurately delivered or dispersed at desired concentration and time. In the US alone there are at least nine companies that sell solvation units (basic: Hanson, Varian, Sotax, Logan, Distek; robotic: Zymark; UV-Vis monitoring: Pion, C-Technologies, Leap Technologies) and retail prices range from \$20 K for basic units, \$100 K for UV-Vis equipped units and \$250 K for robotically controlled units. The total market capital of this industry is estimated to be \$500 M USD.
- Second, the Solv-IR is a potential driver to a field of research that is hungry for more information about the chemistry that is occurring inside the reaction vessel.

---

<sup>62</sup> J. Workman Jr. Review of Near-Infrared and Infrared Spectroscopy. *The Handbook of Organic Compounds*; Academic Press: California, 2001; pp 79-129.

<sup>63</sup> Kassis, A.; Bhawtankar, V.M.; Sowa, J.R. Attenuated total reflection infrared spectroscopy (ATR-IR) as an in situ technique for dissolution studies. *Journal of Pharmaceutical and Biomedical Analysis* 2010, 53, 269-273.

### 4.3 Limit of detection (LOD) and limit of quantitation (LOQ) data

Before the instrument design is discussed, an overview of limit of detection (LOD) and limit of quantitation (LOQ) will be made.<sup>64</sup> The LOD and LOQ levels were calculated for the existing ATR-IR system coupled with different types of fiber optic probes. Three types of fiber optic probes were tested: DiComp probe, Flow-Cell probe and K4 probe.<sup>65</sup> Differences between these probes will be discussed below.

As per the IUPAC, The limit of detection, expressed as a concentration or quantity, is derived from the smallest measure that can be detected with reasonable certainty for a given analytical procedure. The limit of detection is the lowest concentration of an analyte that the analytical process can reliably detect.<sup>66</sup> The LOD level is calculated from the average of the blank, standard deviation of the blank and a confidence factor.<sup>67</sup> The limit of quantification refers to the smallest concentration or the mass which can be quantitatively analyzed with reasonable reliability by a given procedure. There are several techniques available to calculate detection limits. The limit of detection is estimated as three times the standard deviation of the blank and the limit of quantitation is estimated as ten times the standard deviation of the blank. Of the three fiber optic probes mentioned earlier, the DiComp probe is the most useful to dissolution chemistry. The DiComp probe is diamond coated to protect the Zn-Se ATR crystal from attack by acidic medium. Since a lot of the dissolutions are carried out in acidic medium (pH 1-3), the ATR crystal needs the extra coating to ensure longevity of the probe. Based on

---

<sup>64</sup> Venkatasami, G.; Sowa, J.R. A Rapid, Acetonitrile-Free, HPLC Method for Determination of Melamine in Infant Formula. *Analytica Chimica Acta* **2010**, *665*, 227–230.

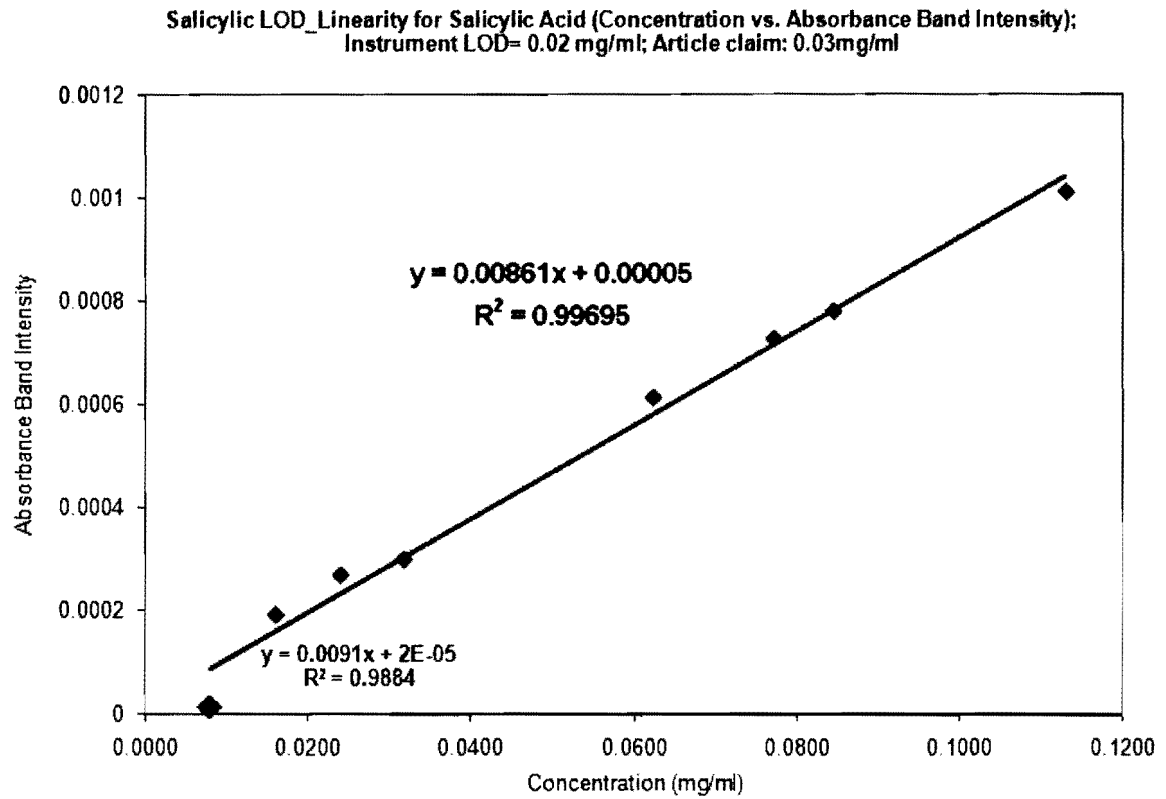
<sup>65</sup> Fiber optic probe specification obtained from: <http://us.mt.com/us/en/home.html#> (accessed May 1, 2011).

<sup>66</sup> IUPAC, Compendium of Chemical Terminology, 2nd ed. (the "Gold Book") (1997)

<sup>67</sup> MacDougall, D.C.; Warren B. Guidelines for Data Acquisition and Data Quality Evaluation in Environmental Chemistry. *Analytical Chemistry* **1980**, *52*, 2242–49.

the research it was determined that the LOD and LOQ levels for the DiComp probe were found to be  $1.7 \times 10^{-4}$  M and  $5.7 \times 10^{-4}$  M, respectively. This implies that the LOD level is 0.02 mg/ml. Refer to Figure 4-1. Thus, the optics of the ATR-IR system will need to be enhanced in future research in order to achieve a lower limit of detection level. The goal is to increase the sensitivity so that the system is able to detect one mg of an active drug in a 500 ml vessel volume or 0.002 mg/ml. The ratio of placebo to active will play an important role in the sensitivity and will need to be considered during the analysis.

Figure 4-1 Limit of detection of ATR-IR system

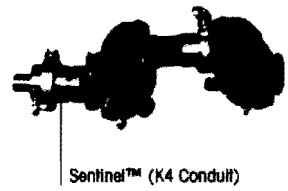
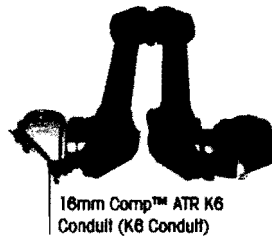
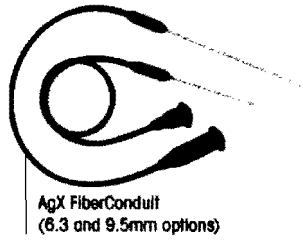


**Figure 4-2 Fiber optic probes specifications (ref 65)**



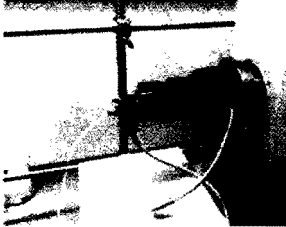
Available Probe Options

Probe model (Conduit)	AgX Fiber - 6.3mm	AgX Fiber - 9.5mm	AgX Fiber - 9.5mm	Comp™ ATR (K6 Conduit)	Sentinel™ (K4 Conduit)
Probe diameter	6.3mm	9.5mm	9.5mm	16mm	25.4mm
Probe length	254mm and 406mm	254mm and 406mm	254mm and 406mm	176mm, 299mm, 362mm	28.6mm (other lengths as special)
Probe sensor	Diamond	Diamond	Silicon	Diamond, Silicon	Diamond, Silicon
Fiber length	1.5m and 2m	1.5m and 2m	1.5m	N/A	N/A
Temperature range	-40°C - 120°C	-40°C - 120°C	-40°C - 120°C	-80°C to 200°C (300°C as special)	-80°C to 200°C (300°C as special)
Maximum pressure	34bar (500psi)	34bar (500psi)	34bar (500psi)	7bar, 100bar (350bar as special)	7bar, 100bar (350bar as special)
Measurement range	1950cm <sup>-1</sup> - 850cm <sup>-1</sup>	1950cm <sup>-1</sup> - 850cm <sup>-1</sup>	2900cm <sup>-1</sup> - 850cm <sup>-1</sup>	4000cm <sup>-1</sup> - 850cm <sup>-1</sup> *	4000cm <sup>-1</sup> - 850cm <sup>-1</sup> *

\*Diamond absorbs between 2300cm<sup>-1</sup> - 1950cm<sup>-1</sup>



**Figure 4-3**      **Calculated LOD and LOQ values**

Description	LOD and LOQ Results for iC10 IR System Probes		
IR Probe	K4 Probe	Di Comp Probe	Flow Cell
<b>S/N</b>	2	13	23
<b>LOD (mM)</b>	0.63 mM	0.17 mM	0.10 mM
<b>LOQ (mM)</b>	2.11 mM	0.57 mM	0.33 mM
<b>Probe Picture</b>	 <p data-bbox="597 831 753 852">Sentry™ (K4 Conduit)</p>	 <p data-bbox="857 819 1026 856">AgX FiberConduit (8.3 and 9.5mm options)</p>	

**Figure 4-4 LOD/LOQ Sample Calculation Sheet- DiComp Probe Results-1**

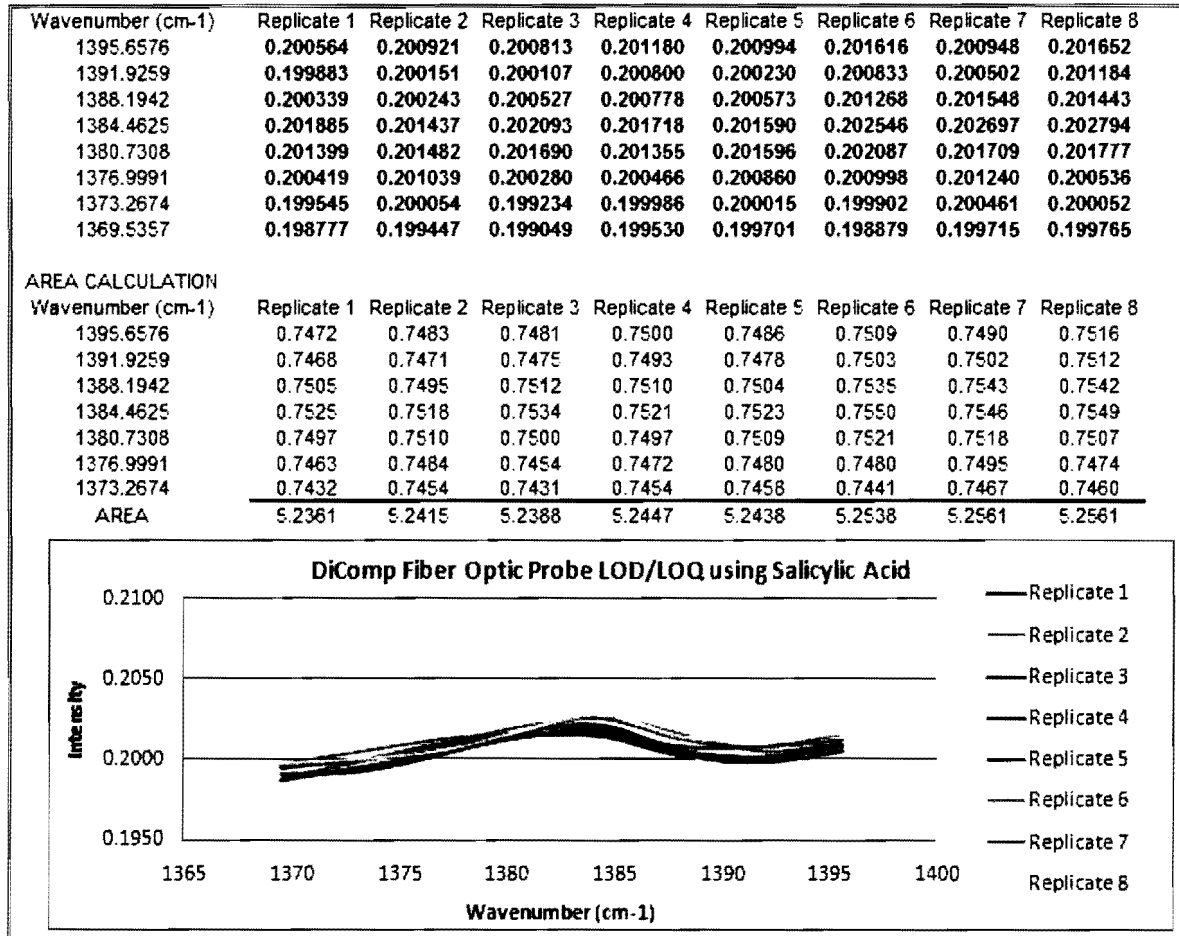


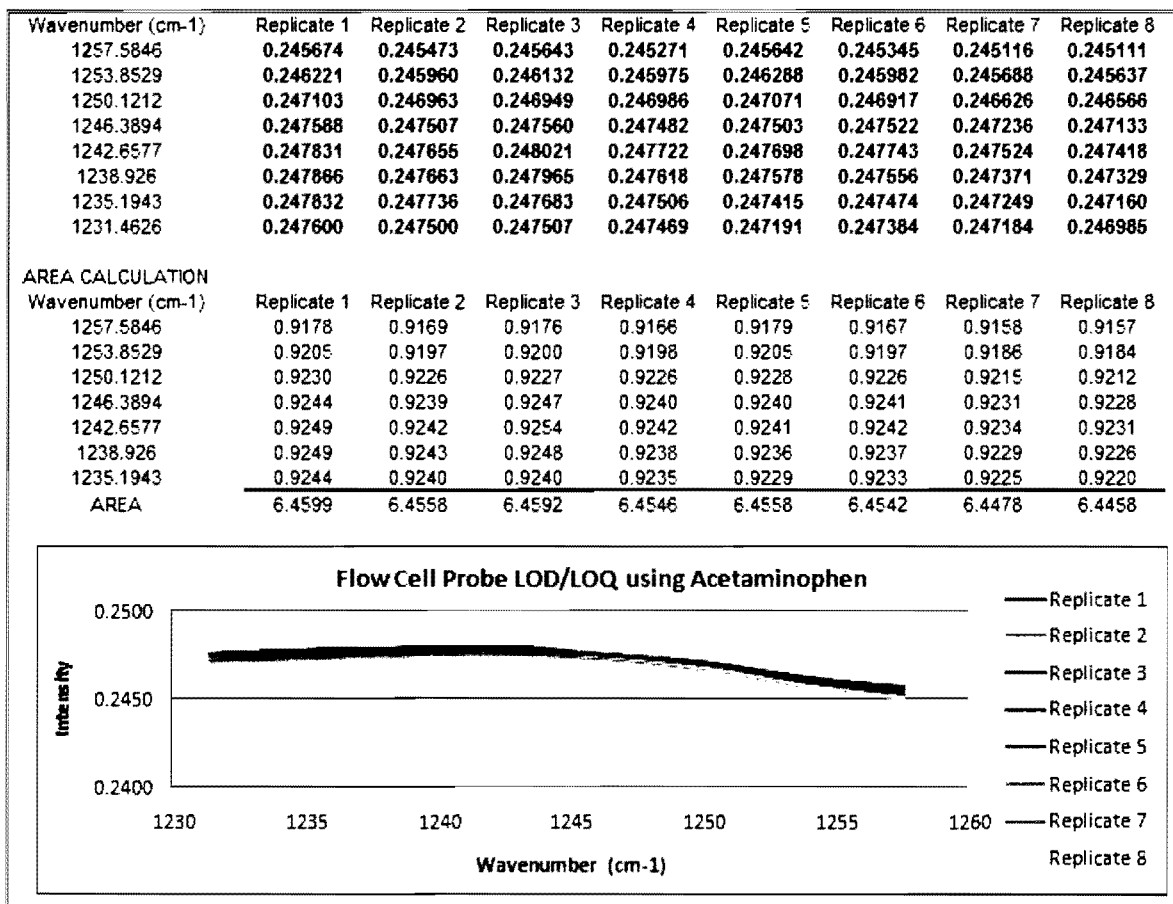
**Table 4-1 LOD/LOQ Sample Calculation Sheet- DiComp Probe Result-2**

Title: LOD/LOQ Calculations

Row Number	Column A	Column B
1	Analyte	Salicylic Acid
2	Method	LOD/LOQ
3	Date	Nov. 27. 2010
4	Instrument	iC10 Di Comp Probe
5	Spike	0.01594
6	Units	mg/mL
7	Replicate 1	5.23610
8	Replicate 2	5.2415
9	Replicate 3	5.2388
10	Replicate 4	5.2447
11	Replicate 5	5.2438
12	Replicate 6	5.2538
13	Replicate 7	5.2561
14	Replicate 8	5.2561
15	Mean	5.2464
16	Std. Dev	0.0079
17	LOD	0.02 mg/mL
18	LOQ	0.08 mg/mL



**Figure 4-5 LOD/LOQ Sample Calculation Sheet- Flow Cell Probe Results-1**



#### 4.4 Instrument design

The proposed instrument is illustrated in Figure 4-7. It has ten overall features which are grouped into the following units: I) Optical Path which includes the source, fiber optic cables, ATR crystal, and detector, II) Six Solvation Vessels including the overhead stirrers, reaction vessels and temperature control, and, III) Instrumentation Control and data acquisition/processing software. The choice of six solvation vessels comes from a statistical requirement that is frequently found encountered in complicated experiments where agreement of  $n=6$  experiments is considered to provide a statistically robust analysis.<sup>68</sup> Although chemists are frequently satisfied with one reproducible yield or agreement of three measurements of a rate constant, applied applications of chemistry frequently require more rigorous statistics.

Some regulatory agencies require statistical agreement of six simultaneous solvation studies. Thus, to make the instrument more statistically rigorous and competitive with related instruments on the market, it is important that we use  $n=6$  reaction vessels. Also note that a circular arrangement of the solvation vessels is proposed as this design is takes up less space relative to a linear or block arrangement.

We will assemble our new instrument from commercially available components. Thus, our main role will be to select the most appropriate components, to make sure that they properly communicate and have reliable computer software for instrument control data acquisition and processing. Our target specifications are:

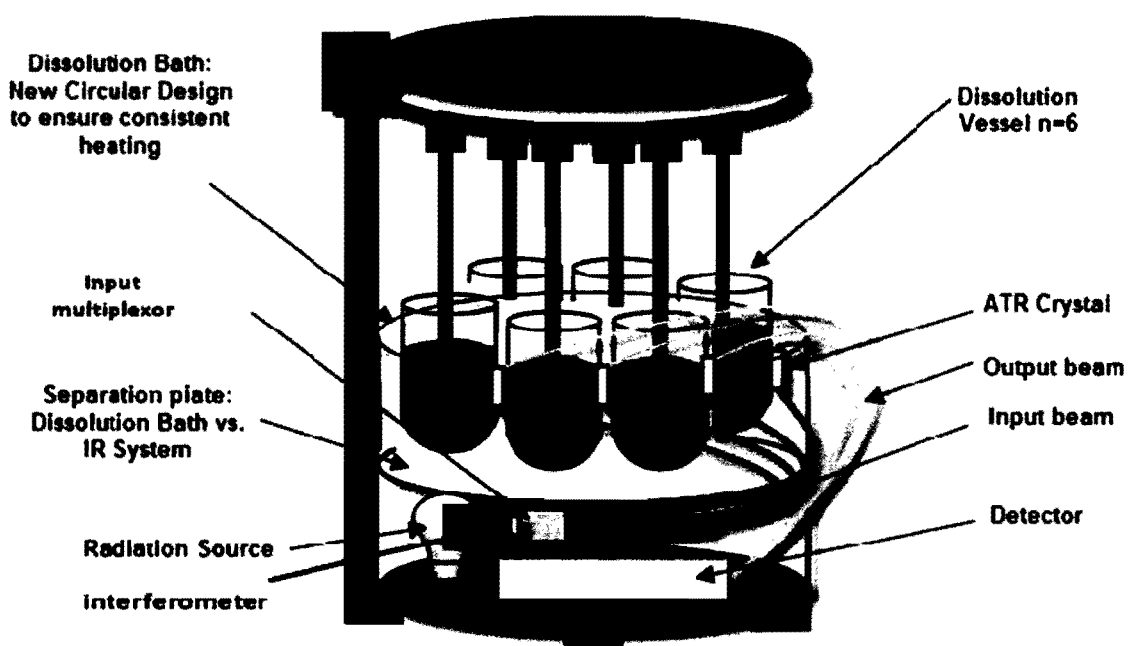
---

<sup>68</sup> a) Wilson, E. B. *An Introduction to Scientific Research*; Dover Press: New Jersey, 1991. b) Dumont, M. L.; Berry, M. R.; Nickerson, B. Probability of passing dissolution acceptance criteria for an immediate release tablet. *Journal of Pharmaceutical and Biomedical Analysis* **2007**, 44(1), 79-84.

- 1) Sensitivity (as defined as limit of detection, where signal: noise ratio = 3:1)  $< 10^{-6}$  M.
- 2) Sample time  $< 1$  min per solvation vessel.
- 3) Wavelength range:  $4000 - 500 \text{ cm}^{-1}$ .
- 4) Temperature control  $< \pm 0.5^\circ \text{ C}$  and range  $-20$  to  $100^\circ \text{ C}$ .
- 5) Chemical stability: aqueous solvent conditions (pH 1 – 12), common organic solvents and tested for safe use of volatile organic solvents such as diethyl ether when used in a fume hood.
- 6) Although this is a scientific proposal, we desire that the instrument will be marketable, thus, we will aim for a retail cost of \$200 K.

**Figure 4-6**      **Diagram of proposed Solv-IR Instrument**

A diagram of the proposed instrument is shown below.



## **4.5 System components**

### **4.5.1 Radiation source**

This is an encased source for IR radiation consisting of an IR element and Zn-Se lens. A suitable unit is available from Oriel, Apex Infrared Source, Model 66471 (7" H x 12" W x 10" D).

### **4.5.2 Interferometer**

This is necessary to modify the source IR light to a broad range of frequencies. Interferometers provide for rapid acquisition and signal averaging. Potential vendors include BrukerOptics. However, an interesting alternative for initial investigations will be to salvage components from a surplus IR (we have two units in disrepair in our department with interferometers).

### **4.5.3 Two Six-device Multiplexors**

These devices channel the light from the source so that the maximum amount of light passes through each vessel and then directs the absorbed light to the detector. They are sequential devices such that input/output light spends a defined amount of time at each vessel.

### **4.5.4 Six ATR Probes**

Each probe consists of an input fiber optic cable, an ATR crystal and an output fiber optic cable. The cables are chalcogenide fibers that perform well in the mid-IR range and are sufficiently flexible so they can be arranged within the instrument and connected to the ATR

crystal. Potential suppliers are also RoMack Corp. and Hellma Scientific. The ATR crystal is a Zn-Se crystal will provide the desired spectral window (4000 – 500  $\text{cm}^{-1}$ ); however, since Zn-Se is sensitive to acids and easily abraded, we will identify a suitable coating. So far, the best choice is a diamond coated Zn-Se crystal which provides excellent chemical stability. The narrower spectral range 1900 – 600  $\text{cm}^{-1}$  is a satisfactory compromise because the “fingerprint” region frequently provides an excellent array of absorption bands. Pike Technologies provides an excellent selection of ATR and coated ATR crystals.

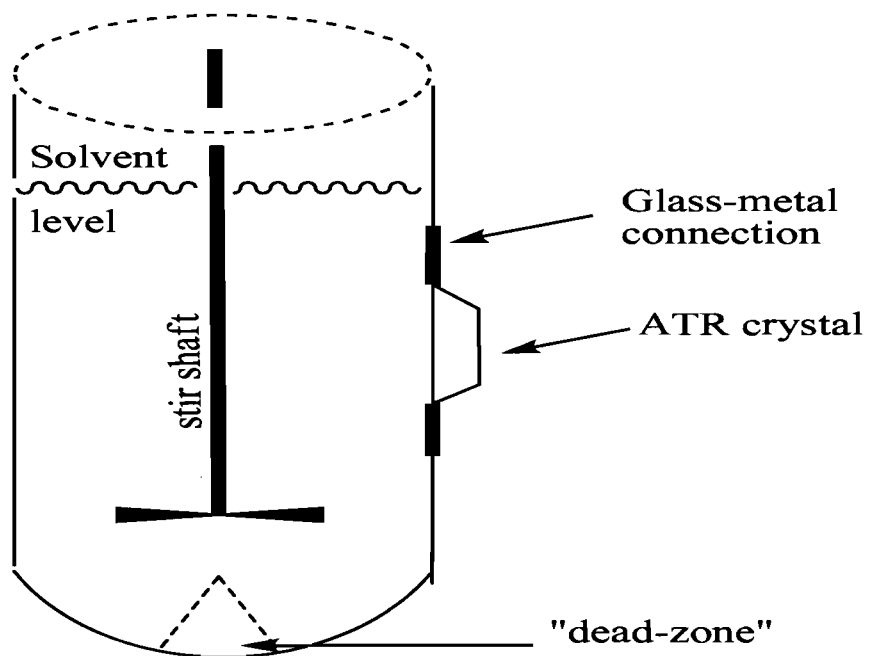
#### **4.5.5 Detector**

The goal is to obtain a single detector sensitive to  $10^{-6}$  M. Currently, the most sensitive detectors are liquid nitrogen-cooled HgCdTe (MCT) detectors. However, if technology advances, we hope to incorporate a sensitive ambient temperature detector such as Peltier-stabilized DTGS (deuterated triglycine sulfate) detector. Commercial vendors include BrukerOptics.

#### **4.5.6 Six Solvation Vessels**

Preliminary work can be performed on glass 1 L vessels that we have in stock. We will need to hire a glass blower (ChemGlass, Vineland, NJ) to modify each vessel with a rectangular fitting capable of holding rhombohedral ATR crystal as shown in Figure 4-7.

**Figure 4-7** Sketch of ATR crystal embedded in the side wall of the 1 L glass vessel. The area directly under the stir shaft is known to have poor mixing and as indicated by the term "dead zone".



Alternatively, polyethylene and fluoropolymer vessels are available which will be easier to modify especially in prototypes. Quality Lab Accessories (QLA) provides an excellent catalog of glass and polymer vessels, caps and stir shafts. Controlled overhead stirring is performed by a simple gear assembly (Figure 4-8).

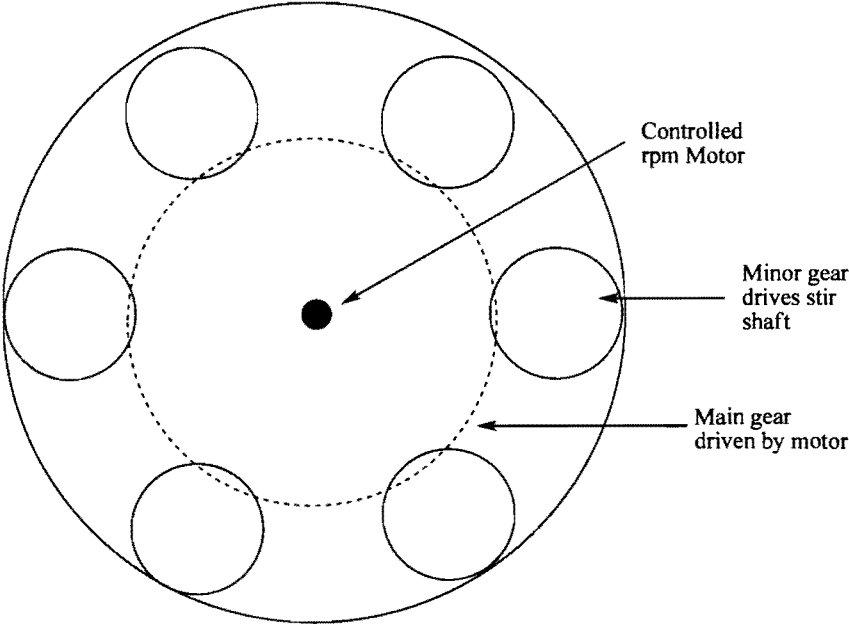
Temperature control will be provided by assembling a water bath around the solvation vessels. However an ideal alternative is provide a thermally-conductive jacket around each vessel with which temperature is controlled (for example, see Distek's Evolution 6100 Bathless apparatus.<sup>69</sup>

---

<sup>69</sup> Evolution 6100 – Distek Bathless Dissolution Testing Equipment, Distek Home Page [Online], [http://www.distekinc.com/products/dissolution\\_evolution\\_6100.htm](http://www.distekinc.com/products/dissolution_evolution_6100.htm) (accessed on January 26, 2011).



**Figure 4-8** Top plate of constant rpm stirring assembly showing motor, main gear and minor gears which drive the stir shafts in each vessel



#### **4.6 Instrument Control/ Acquisition/ Processing.**

Software packages to perform these operations have been well-designed by a number of vendors we will seek an opportunity to license their software and hire a consultant to modify the software package.

#### **4.7 Anticipated technical difficulties**

- i. It may be difficult to match items from different vendors. Solution: try to use one or two primary vendors. For example, BrukerOptics has MATRIX and TENSOR IR spectrophotometers which allow multiple ATR probe attachments. If either of these meet sensitivity requirements, then it would be best to build the Solv-IR from one of these units. A quote for the MATRIX-MF instrument including spectrophotometer, ATR-probes and software has been obtained to support this approach.
- ii. It may be difficult to achieve sensitivity within a reasonable time frame if all six vessels are to be measured with one spectrophotometer. Solution: assemble an apparatus with two or three spectrophotometers.
- iii. It may be difficult to achieve sensitivity with a vessels are to be measured with one spectrophotometer. Solution: assemble an apparatus with two or three spectrophotometers.

#### **4.8 Chapter summary**

The preliminary studies in Chapters 2 and 3 indicate great potential for use of the Solv-IR instrument in pharmaceutical chemistry, especially to study dissolution of pharmaceutical formulations. Chapter 5 will address a potential application of this instrument in the study of the chemistry behind oil spills.

This instrument development proposal aims to construct a new type of instrument that will allow the study of solvation of solutes in aqueous and organic systems. The main feature of the instrument design is the use of infrared (IR) spectroscopy to study this dynamic behavior. Traditionally, IR is not considered to be a quantitative technique. However, using ATR crystals ensures that the technique is most certainly quantitative. Also, IR is traditionally not considered to be a sensitive method, however, our preliminary results indicate detection limits of  $10^{-4}$  M. Employing better optics and detection will improve sensitivity to our target value of  $10^{-6}$  M. The instrument has an additional feature which may seem strange to most chemists as it will have six reaction vessels. This feature is important for statistical reasons and for marketing reasons. Solvation is a chemically and mechanically complex process. To ensure accurate studies of the solvation process, it is important to have a large array of data such that statistically significant interpretations can be made. In addition, competing instruments that use UV-Vis technology have six reaction vessels so they conform to certain regulatory requirements.

We propose to assemble the instrument using commercially available components. We will build to spectroscopic part of the instrument starting with this unit. In addition, we feel that we work with their data acquisition software to incorporate instrument control and data processing. Finally, we will construct the reaction vessels, stirring function and thermal control and integrate this unit with the spectroscopy unit to have a fully functioning integrated Solv-IR instrument.

Students working on this project will obtain valuable experience on working with electrical, optical and mechanical parts and tools which is quite rare for a chemistry student. However,

since this is all focused on discovering new ways to study the fundamental and practical aspects of solvation chemistry, this will be an exciting and worthwhile challenge. While assembling the instrument students will be able to investigate chemical phenomenon in a way that has been previously inaccessible.

## **5 Analysis of the BP Gulf oil spill by Attenuated Total Reflection-Infrared Spectroscopy and Dissolution**

This chapter focuses on describing the scientific research that was conducted on the recent BP oil spill in the Gulf of Mexico. Moreover, this research was accomplished using the React-IR/dissolution system. Although the BP oil spill occurred outside of New Orleans, Seton Hall University employed its faculty members, students and research facilities toward understanding this environmental disaster.

A general background on the BP oil spill will be provided to gain more understanding of the subject matter, which will be useful when discussing the results later in the chapter. The BP oil spill (also referred to as the Deepwater Horizon oil spill, Gulf of Mexico oil spill or Macondo blowout), is the largest accidental marine oil spill in the history of the industry. The Deepwater Horizon was a nine-year drilling unit that was floating in the Gulf of Mexico. Refer to Figure 5-1 for a photo of Deepwater Horizon before the accident occurred. The spill occurred on April 20, 2010 due to an explosion of the Deepwater Horizon. This led to a loss of 4.9 million barrels of crude oil to the ocean. As a result, the spill caused extensive damage to the fishing and tourism industries around the Gulf of Mexico.

**Figure 5-1** Photo of oil rig similar to Deepwater Horizon<sup>70</sup>



---

<sup>70</sup> Photo obtained from Lauren Michael Ridley during her NOAA trip to Gulf (obtained July 2011).

## PETROLEUM AND CRUDE OIL

Both crude oil and natural gas are mostly made up of hydrocarbons. The lighter hydrocarbons which include methane, ethane, propane and butane occur as gases, while the heavier hydrocarbons (i.e., pentane and higher) occur in the form of liquids or solids. The hydrocarbons in crude oil are mostly alkanes, cycloalkanes and several aromatic hydrocarbons. Moreover, other organic compounds contain nitrogen, oxygen and sulfur, and trace amounts of metals such as iron, nickel, copper and vanadium.

### 5.1 Research with React-IR

As part of the multidisciplinary project to understand the effect of the oil spill, the React-IR system coupled to a dissolution system was used to study the dispersion effect of dispersants on crude oil. Dispersants were used to break up the Deepwater Horizon oil spill before it reached the shore. The dispersants are designed to break down the crude oil into tiny drops, which can be mechanically dispersed or consumed by bacteria. The aim is to lessen the impact of giant plumes of crude oil washing onto oyster beds and birds' nests and on the sandy beaches. The dispersants or chemicals used in the BP oil spill could also do more damage than good in the long run. The dispersants are toxic in nature and could have devastating effects on future generations of marine life. The financial cost of using these dispersants could run into the millions. Some of the chemicals used in commercial dispersants<sup>71</sup> are shown in Table 5-1. This information was obtained from the EPA website.

---

<sup>71</sup> Environmental Protection Agency Home Page. <http://www.epa.gov/bpspill/dispersants-qanda.html#list> (accessed May 1, 2011).

Specifically, the system was used to study dispersion of oil in the presence of dishwashing soaps as preliminary models for commercial dispersants. From these preliminary experiments, the research was able to measure the effect of dispersants on petroleum oil. In addition, these preliminary experiments were able to determine the feasibility of the technique in order to move forward with the project at a larger scale. This would include purchasing commercial dispersants. Furthermore, Dawn® dishwashing soap was used because of its powerful claim to clean wildlife affected by oil spills. Dawn® specifically uses anionic surfactants, such as alkyl dimethyl amine oxide, to break down oil samples. These surfactants reduce the surface tension of water and can weaken the barrier that automatically forms between oil and water, allowing them to unnaturally mix.



**Table 5-1 Chemicals used in commercial dispersants (COREXIT 9500 and 9527)**

CAS Registry Number	Chemical Name
57-55-6	1,2-Propanediol
111-76-2	Ethanol, 2-butoxy-*
577-11-7	Butanedioic acid, 2-sulfo-, 1,4-bis(2-ethylhexyl) ester, sodium salt (1:1)
1338-43-8	Sorbitan, mono-(9Z)-9-octadecenoate
9005-65-6	Sorbitan, mono-(9Z)-9-octadecenoate, poly(oxy-1,2-ethanediyl) derivs.
9005-70-3	Sorbitan, tri-(9Z)-9-octadecenoate, poly(oxy-1,2-ethanediyl) derivs
29911-28-2	2-Propanol, 1-(2-butoxy-1-methylethoxy)-
64742-47-8	Distillates (petroleum), hydrotreated light

\*This ingredient is present in 9527 but is eliminated in 9500.

## **5.2 Experimental section**

### **5.2.1 Chemical and materials**

Crude oil samples were collected by Dr. John Sowa and University of New Orleans scientists from a location near the city of Venice, Louisiana. Refer to the figures below showing the locations where the oil samples were collected. The University of New Orleans faculty collected samples from the Gulf of Mexico. The location of the samples collected was determined by GPS at the following location: 28° 53.412'N, 89° 08.780'W. Methanol, acetone and acetonitrile (HPLC grades) were purchased from Pharmaco-Aaper. Dawn® Antibacterial and Ultra Joy® (lemon scent) dishwashing detergent soaps were used as the dispersants for this research. All solutions were prepared using water treated by a Milli-Q Millipore purification system. All purified water aliquots have resistivity of not less than 18 MOhm-cm<sup>-1</sup>.

**Figure 5-2**      **Aerial view:<sup>72</sup> location of BP Gulf oil samples**



---

<sup>72</sup> Google Maps: <http://maps.google.com/maps?hl=en&tab=wl> (accessed May 1, 2011).

**Figure 5-3** Zoom view: location of BP Gulf oil samples [Both samples were collected near the UNO site]

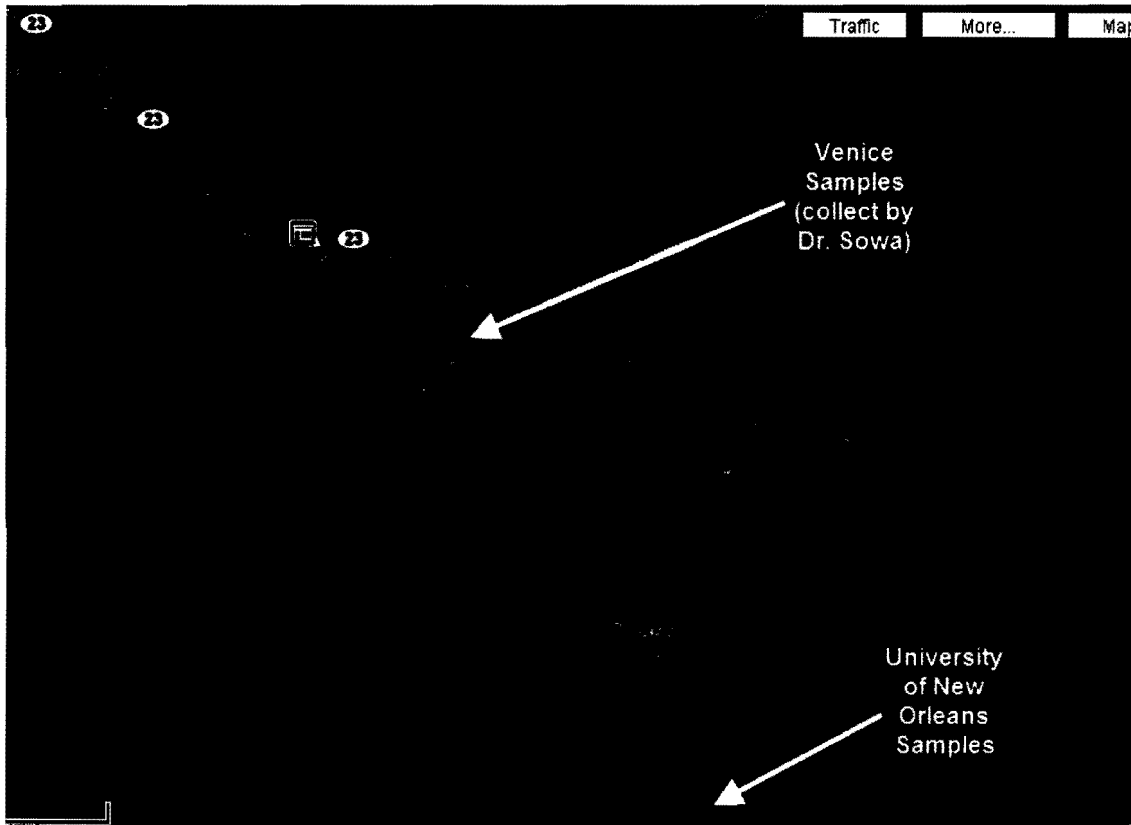
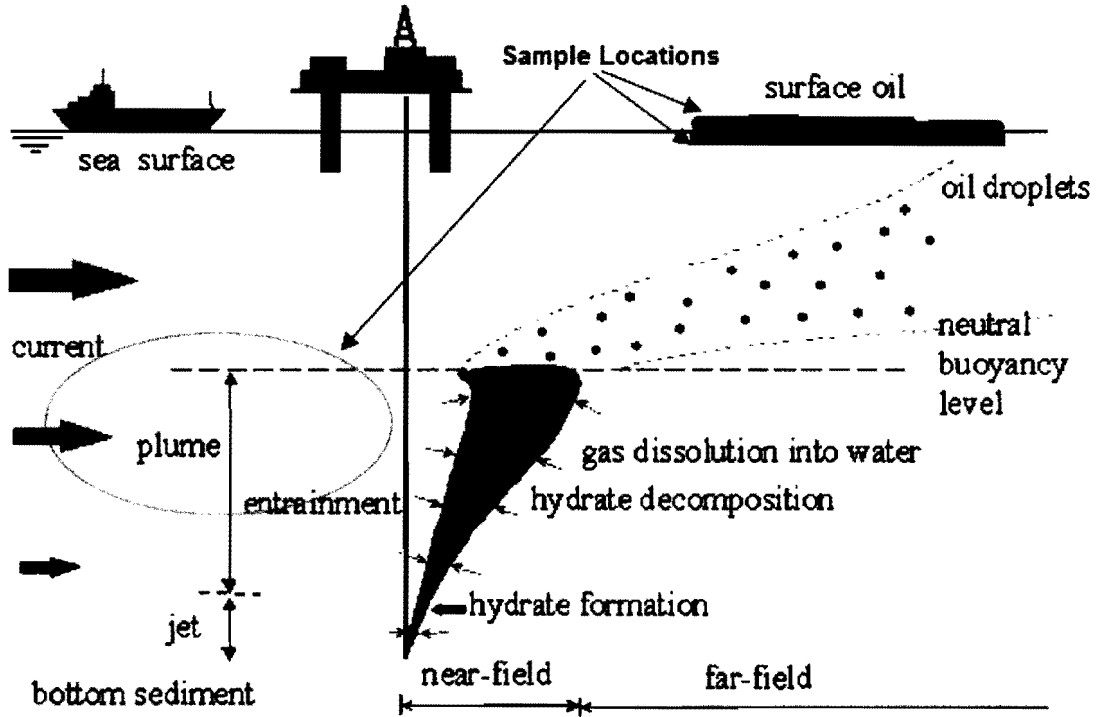


Figure 5-4 Ocean depth diagram<sup>73</sup> showing location of BP Gulf oil samples (reproduced and modified from Ref 73)



<sup>73</sup> Figure obtained from <http://www.crrc.unh.edu/final/Yapa2003final/figure1.jpg> (accessed May, 2011).

### **5.2.2 Instrumentation**

Samples were tested using Mettler Toledo's iC10 FT-IR system using a fiber optic probe equipped with a 1 mm diamond coated ATR probe. The IR system was operated by Mettler Toledo's iC IR version 3.0 or 4.0 software. All dissolution experiments were tested using a Vankel Dissolution Bath (model no. 700). All UV/Visible testing was carried out using HP 8453 spectrophotometer. All analytical weight measurements were carried out using Mettler Toledo's DeltaRange and AG204 DeltaRange.

**Figure 5-5 Instrument photo: ATR-IR and dissolution apparatus**



**Table 5-2      Experimental details and sample information**

<b>No.</b>	<b>Parameter</b>	<b>Setting</b>
1	Vessel volume	900 mL
2	Medium	Distilled water
3	Agitation speed	100 rpm
4	Temperature	25 °C
5	Dawn®/ Joy® Dishwashing detergents	0.2% solutions
6	Dissolution bath	VanKel VK700
7	ATR-IR	Mettler Toledo iC10

### **5.2.3 Dispersant stock solution**

A 0.2% solution of Dawn® dishwashing solution was made up (0.2 mL was added to approximately 120 mL of distilled water). A 0.2% solution of Joy dishwashing solution was made up (2 mL into 1000 mL of distilled water).

#### **5.2.3.1 Dawn® ingredients:**

Water, Sodium Lauryl Sulfate, Sodium Pareth-23, Sulfate C-12-14-16, Dimethyl Amine Oxide, SD Alcohol, Undeceth-9, Propylene Glycol, Cyclohexandiamine, Polyacetate, Protease, Fragrance, FD&C blue, no phosphate.

#### **5.2.3.2 Joy ingredients:**

Water , Sodium Lauryl Sulfate , Sodium Pareth-23 , C12-14-16 Dimethyl Amine Oxide , SD Alcohol 40-B , Undeceth-9 , PPG-26 , Sodium Chloride , Cyclohexanediamine , Polyacetate , Fragrance , FD&C Yellow #5 , D&C Red No. 33

### **5.2.4 Crude oil sample preparation**

The dispersion experiments were carried out by adding different amounts of Dawn® dishwashing detergent in vessels containing 900 mL of distilled water and five (5) grams of semi-solid oil sample. Photographs of the oil dispersion studies were collected at different time points throughout the runs. The dispersion experiments were carried out over two hours.



### **5.2.5 ATR-IR analysis**

The ReactIR™ iC10 FTIR instrument is composed of an MCT detector (liquid nitrogen cooled) and the FiberConduit™. The FiberConduit™ is comprised of flexible IR transparent silver chloride/silver bromide optical fibers. The fiber optic probe interface (AgX 9.5 mm x 1.5 m Fiber (Silver Halide)) contains a diamond tip-DiComp ATR crystal. The resolution was set to 8 wavenumbers. The optical range used by the system is: 1900  $\text{cm}^{-1}$  to 650  $\text{cm}^{-1}$ . The gain adjustment was set to normal (1x) and the apodization method was set to Happ-Genzel. The system uses compressed air (house air, filtered and de-humified) to purge the optics.

## **5.3 Results**

The experiments in this chapter demonstrate how ATR-IR may be used in the study of treatments of oil spills. During the BP oil spill, the use of dispersants at the well-head and on the ocean surface was extremely controversial. Thus, this research was interested in finding ways to evaluate this treatment process. Although the commercial dispersants were not used in this research, dishwashing soaps were used as preliminary models. The results show that it takes considerable time for the oil to be broken down by the dishwashing soaps. Controlled dissolution experiments were carried out in an attempt to simulate the dispersion of oil as it occurred during the oil spill. The dissolution experiments were tested over the course of several hours and were held under elevated agitation conditions and at 25°C. These parameters were used in order to simulate the conditions of the ocean water in the Gulf of Mexico. In all of the dispersion experiments a known amount of crude oil was added to the dissolution vessel. Dispersants were then added and the experiments were monitored over several hours. During this time several photos were taken to compare and record the size of

the crude oil samples. Moreover, the ATR-IR probe was placed in the vessel as a way to monitor the release of oil within the vessel as a consequence of dispersant in solution.

### **5.3.1 Standards and expected absorption values**

Standard spectra of crude petroleum oil were obtained during this phase of the research. Crude oil is expected to have prominent IR bands at  $1375\text{ cm}^{-1}$  (due to methyl groups) and  $1465\text{ cm}^{-1}$  (due to methylene groups). Refer to Table 5-3. Also, blank ocean solutions were tested to confirm there was no interference at these two FTIR bands. As shown in Figure 5-6 below, the crude oil samples obtained by Dr. Sowa and the faculty of University of New Orleans show prominent peaks at  $1375$  and  $1465\text{ cm}^{-1}$ . Moreover, ocean samples obtained from regions under the surface oil did not show these two bands.

**Table 5-3 Expected FT-IR stretching values for crude oil and sulfonated soaps**

Functional group	Absorption ( $\text{cm}^{-1}$ )	Description
$\text{CH}_2$	$1465 \text{ cm}^{-1}$	Methylene groups have a characteristic bending
$\text{CH}_3$	$1375 \text{ cm}^{-1}$	Methyl groups have a characteristic bending
$\text{SO}_2$	$1150\text{-}1165 \text{ cm}^{-1}$	Symmetric stretch
	$1342\text{-}1352 \text{ cm}^{-1}$	Asymmetric stretch



**Figure 5-7**      **Baseline corrected: ATR-IR scans of BP oil and Ocean Water samples**

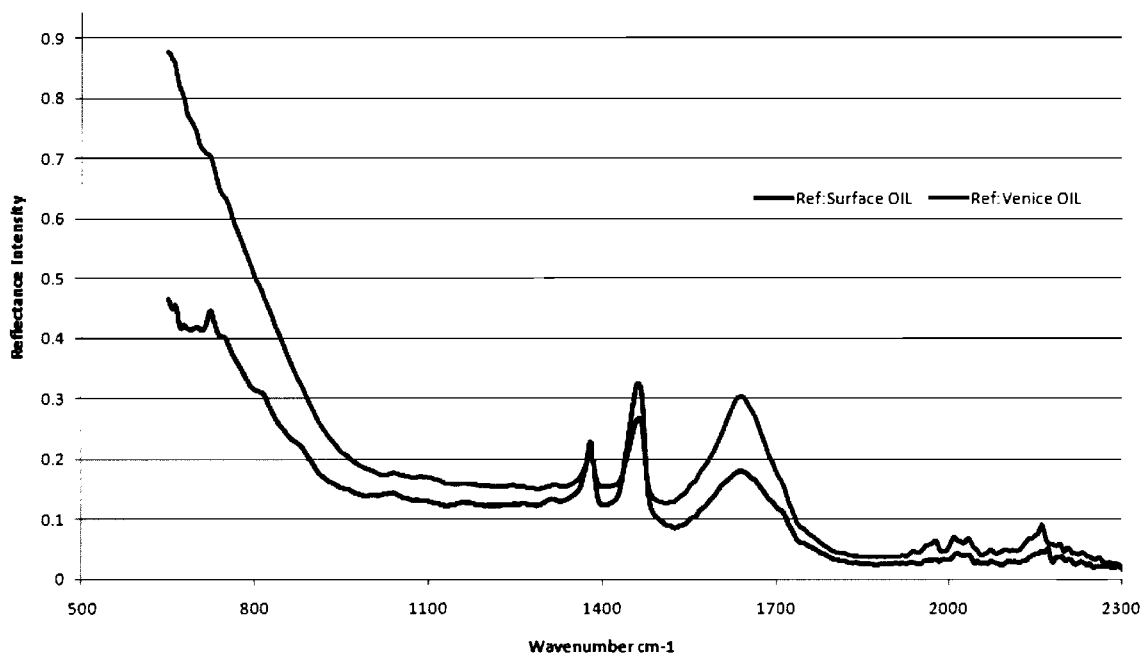
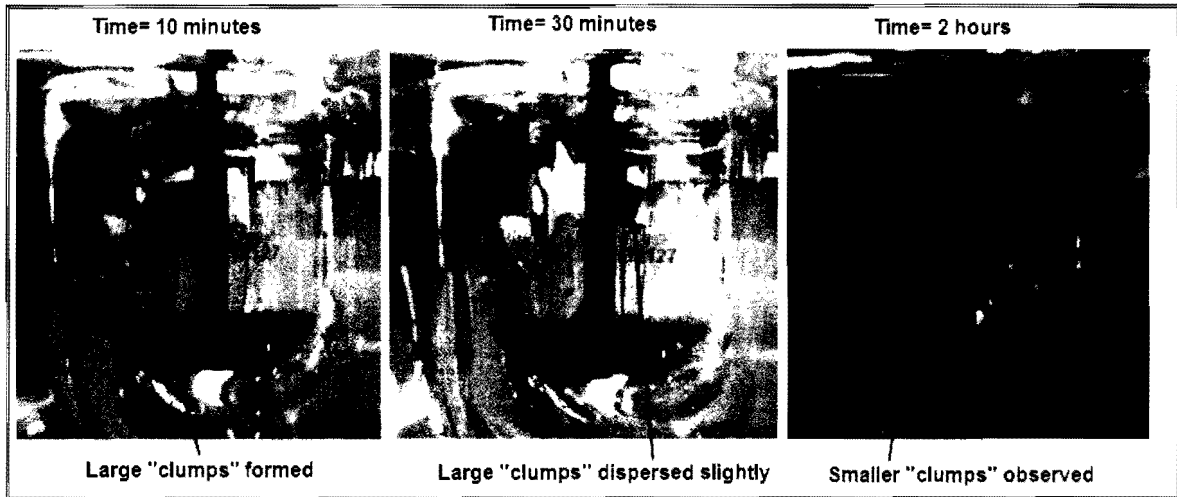


**Figure 5-8** Photo of vessels at different time points during the dispersion experiments



### **5.3.2 Venice oil samples dispersed using Joy soap**

During the first phase of experimentation, Joy was used to simulate dispersant. Approximately 50 mL of the Joy stock dispersive solutions were added to different vessels containing 900 mL of distilled water and five (5) grams of crude oil collected near Venice, Louisiana. The final dispersant concentrations, compared to the concentration of commercial dispersants used in the ocean, are expected to be higher. The temperature was held constant at 25°C. The agitation speed was set to 100 rpm. Unfortunately, the Joy dispersant solution contained interference peaks at  $1465\text{cm}^{-1}$  as shown in Figure 5-9 due to the presence of  $\text{SO}_2$  groups in the soap.

**Figure 5-9 ATR-IR scans of Venice oil and 50 mL of Joy soap**

This figure displays ATR-IR spectra of a solution containing distilled water, Joy dispersant solution and crude oil collected from Venice, LA. As seen in the figure, there are several peaks observed between  $1000\text{ cm}^{-1}$  and  $1500\text{ cm}^{-1}$ . These peaks, moreover, increase with time. As discussed earlier, the peaks at  $1375\text{ cm}^{-1}$  and  $1465\text{ cm}^{-1}$  are indicative of crude oil. These peaks represent the methyl and methylene groups respectively. The other peaks at  $1050\text{ cm}^{-1}$ ,  $1205\text{ cm}^{-1}$  and  $1254\text{ cm}^{-1}$  were found in the blank solution and were attributed to the phosphates in Joy.

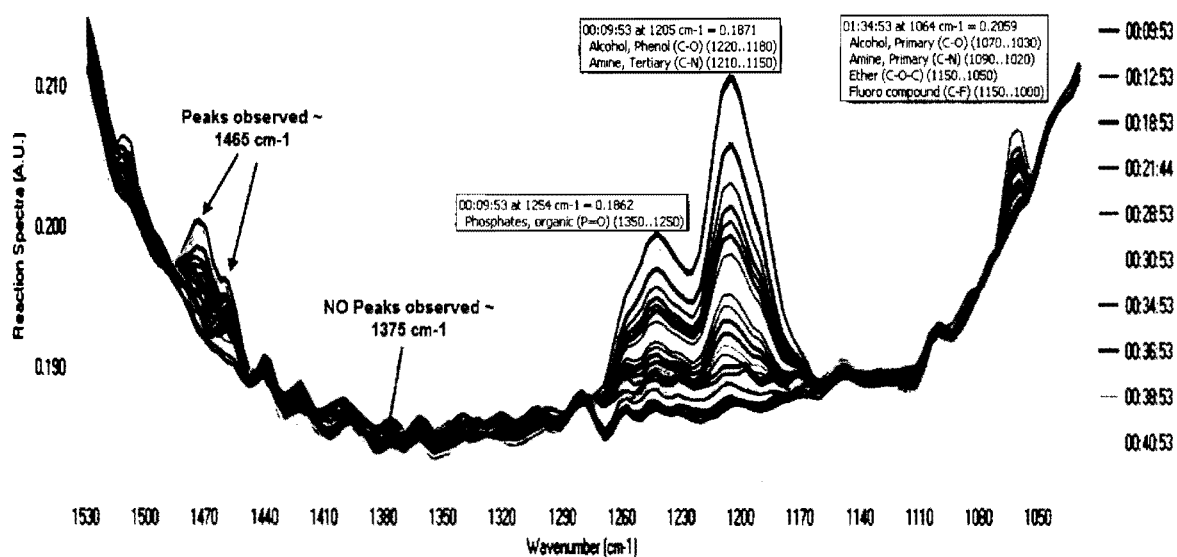
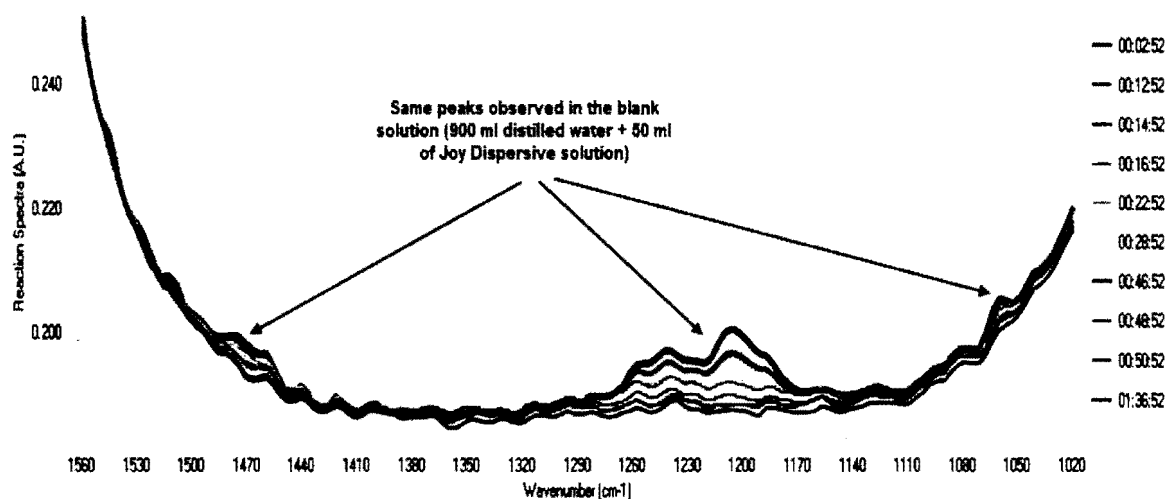




**Figure 5-10 ATR-IR scans of 50 mL of Joy soap only (Blank solution)**

This figure displays ATR-IR spectra of a solution containing distilled water and Joy dispersant solution but no crude oil. As seen in the figure, there are several peaks observed between  $1000\text{ cm}^{-1}$  and  $1500\text{ cm}^{-1}$ . These peaks, moreover, increase with time. The peaks observed at  $1050\text{ cm}^{-1}$ ,  $1205\text{ cm}^{-1}$  and  $1254\text{ cm}^{-1}$ , were attributed to the phosphates in Joy.



### 5.3.3 Venice oil samples dispersed using Dawn® soap

Dawn® dishwashing solution was used during the second phase of the research. Approximately 50 mL of stock dispersive solutions were added to vessels containing 900 mL of distilled water and 5 grams of Venice oil. The final dispersant concentrations, compared to the concentration of commercial dispersants used in the ocean, were expected to be higher. This preliminary model, although not an exact model of the commercial setting, was considered a worst case scenario. It was considered worst case because of the higher concentration of dispersant used in the controlled 900 ml volume setting. The temperature was held constant at 25 °C. The agitation speed was set to 100 rpm. Dawn® dispersant solutions did not give interference peaks at  $1465\text{cm}^{-1}$  or extra sulfonate peaks at  $\sim 1200\text{cm}^{-1}$ . Therefore, Dawn® dishwashing detergent soap was ultimately used to simulate the properties of the dispersant.

**Figure 5-11 ATR-IR scans of Venice oil and 50 mL of Dawn® soap**

This figure displays ATR-IR spectra of a solution containing distilled water, Dawn® dispersant solution and crude oil collected from Venice, LA. As seen in the figure, there are several peaks observed between  $1140\text{ cm}^{-1}$  and  $1520\text{ cm}^{-1}$ . These peaks, moreover, increase with time. As discussed earlier, the peaks at  $1375\text{ cm}^{-1}$  and  $1465\text{ cm}^{-1}$  are indicative of crude oil. These peaks represent the methyl and methylene groups respectively.

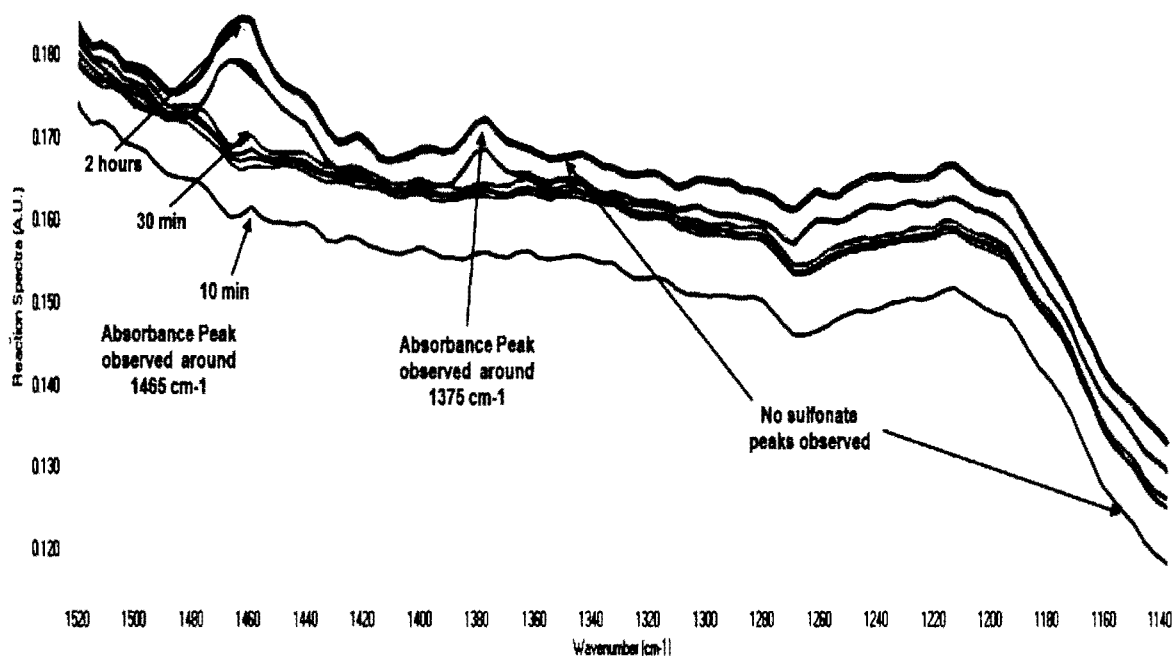
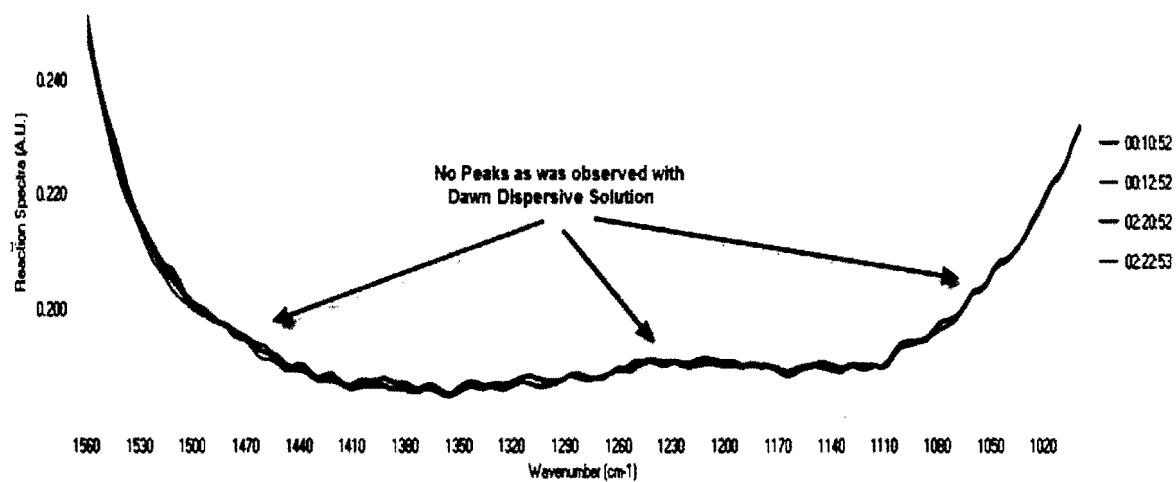


**Figure 5-12** ATR-IR scans of 50 mL of Dawn® soap only (Blank solution)

This figure displays ATR-IR spectra of a solution containing distilled water and Dawn® dispersant solution but no crude oil.



### 5.3.3.1 Percent (%) dispersant used

An example of the percent of dispersants used during the research is shown in Table 5-4, Table 5-5 and Table 5-6. First, the ratio of Dawn® sample to the vessel volume is displayed in Table 5-4. This is represented as (A). Next, the ratio of oil to the vessel volume is displayed. This is represented by (B). Last, the ratio of (A) to (B) is shown in Table 5-6, which represents the percent dispersant calculated.

**Table 5-4 Amount of Dawn® in solution**

Description	Amount
Amount of Dawn® sample in solution*	0.0017
Total Volume of Dawn® Solution Added (mL)	54
Total Volume in Vessel (mL)	954
Ratio of Dawn® sample vs. Volume in Vessel (A)	0.0001

\* Approximately 0.2 ml of Dawn® Solution was added to approximately 120 ml of distilled water

**Table 5-5 Amount of BP oil in solution**

Description	Amount
Amount of Oil (Venice Samples) added (grams)	5
Total Volume in Vessel (mL)	954
Ratio of Oil Sample vs. Volume in Vessel (B)	0.0052

**Table 5-6 % Dispersant calculated**

Description	Amount
Ratio of Dawn® sample vs. Volume in Vessel (A)	0.0001
Ratio of Oil Sample vs. Volume in Vessel (B)	0.0052
% Dispersant calculated (A / B)	1.8%

Common dishwashing detergent was found to have little affect on the dispersion of crude oil. As discussed earlier, dissolution experiments configured with IR spectroscopy were carried out whereby aliquots of crude oil were subjected to different brands of dishwashing detergent in order to measure and determine dispersion effect. Moreover, the dissolution experiments were carried out under controlled conditions in an attempt to simulate the Gulf waters. Also, the type of dispersant used played a major role. As shown in the figures earlier, Joy and Dawn® dishwashing detergents were used during this phase of the research. The Joy blanks solutions (did not contain crude oil), however, showed interference peaks at 1170-1270  $\text{cm}^{-1}$  and 1465  $\text{cm}^{-1}$ . These bands were associated to the sulfonate functional groups and methylene groups respectively. Dawn® blank solutions, however, did not give interference peaks at 1465 $\text{cm}^{-1}$  or extra sulfonate peaks at  $\sim 1200 \text{ cm}^{-1}$ . Therefore, Dawn® dishwashing detergent soap was ultimately used to simulate the properties of the dispersant. The dispersion results clearly show that dispersion of crude oil took at least 30 minutes and up to 2 hours.

#### **5.3.4 Analysis by UV-Vis Spectroscopy**

In addition, the BP Oil samples were tested by UV/Vis spectroscopy. The objective of this part of the research was to determine the amount of porphyrins, if any, in crude oil.<sup>74</sup> Porphyrins are structurally similar to both chlorophyll and hemoglobin molecules and are destroyed by oxygen and heat. Porphyrins are heterocyclic macromolecules composed of four modified pyrrole subunits interconnected at their *alpha* carbon via methine bridges. These molecules are aromatic and highly conjugated systems. Porphyrins have very intense

absorption bands in the visible region. Porphyrins can also contribute to the formation of stable oil-in-water emulsions<sup>75</sup> which will aid in the dispersion process. Chlorophyll, for example, contains several intense absorbance maximums in the region between 453 nm and 665 nm. Refer to Figure 5-13 for a UV/Vis spectrum<sup>76</sup> of chlorophyll a and b. Also, refer to Figure 5-14 and Figure 5-15 for chemical structures of chlorophyll a and b.

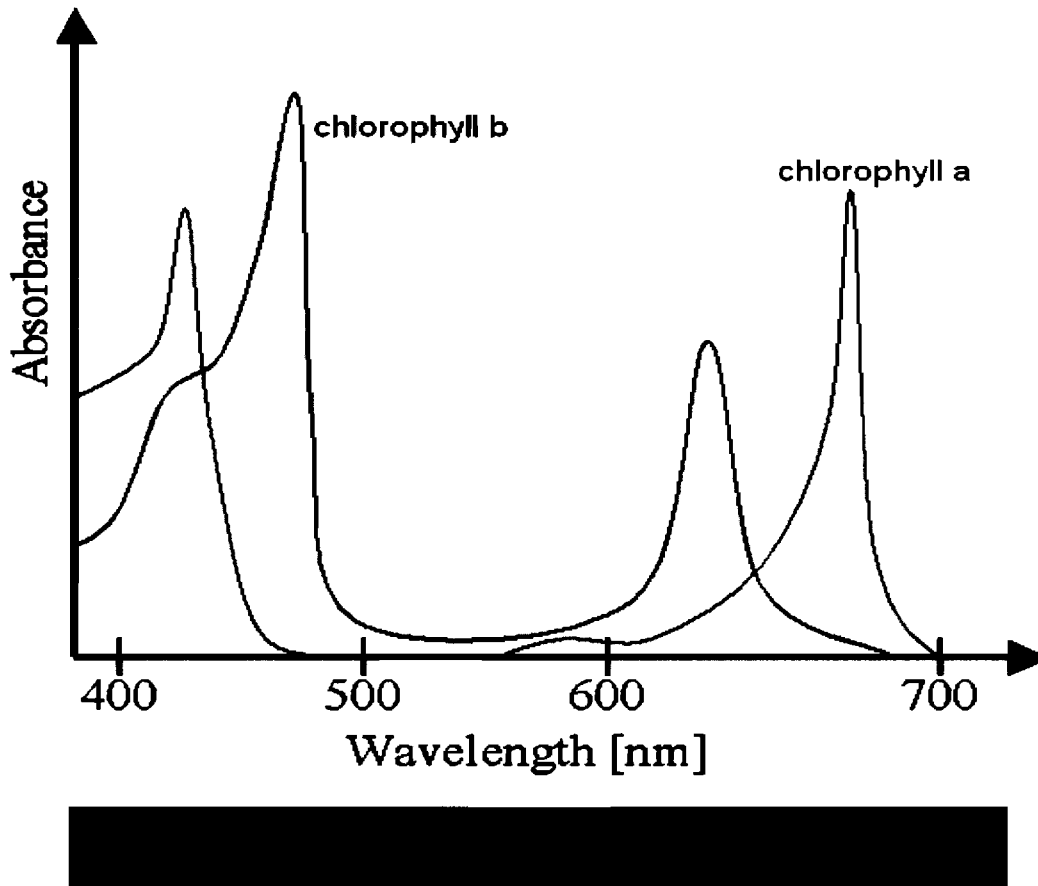
---

<sup>74</sup> Hsu, C. S.; Drinkwater, D., "Gas Chromatography – Mass Spectrometry in the Petroleum Industry", in *Current Practice of Gas Chromatography – Mass Spectrometry*, W. M. A. Niessen, Ed., Chromatographic Science Series, Vol 86, Dekker: New York, 2001, Chapter 3, pp. 55 – 94.

<sup>75</sup> Lee, Richard. Agents which promote and stabilize water-in-oil emulsions. *Spill Science and Technology Bulletin* **1999**, 5(2), 117-126.

<sup>76</sup> Figure obtained from Wikipedia [Online]. [http://en.wikipedia.org/wiki/File:Chlorophyll\\_ab\\_spectra2.PNG](http://en.wikipedia.org/wiki/File:Chlorophyll_ab_spectra2.PNG) (accessed May 1, 2011).

Figure 5-13 Visible spectra of chlorophyll a and b<sup>77</sup>



<sup>77</sup> Figure obtained from [http://en.wikipedia.org/wiki/File:Chlorophyll\\_ab\\_spectra2.PNG](http://en.wikipedia.org/wiki/File:Chlorophyll_ab_spectra2.PNG) (accessed May, 2011).



**Figure 5-14** Chemical structure of chlorophyll a (Chem. Draw)

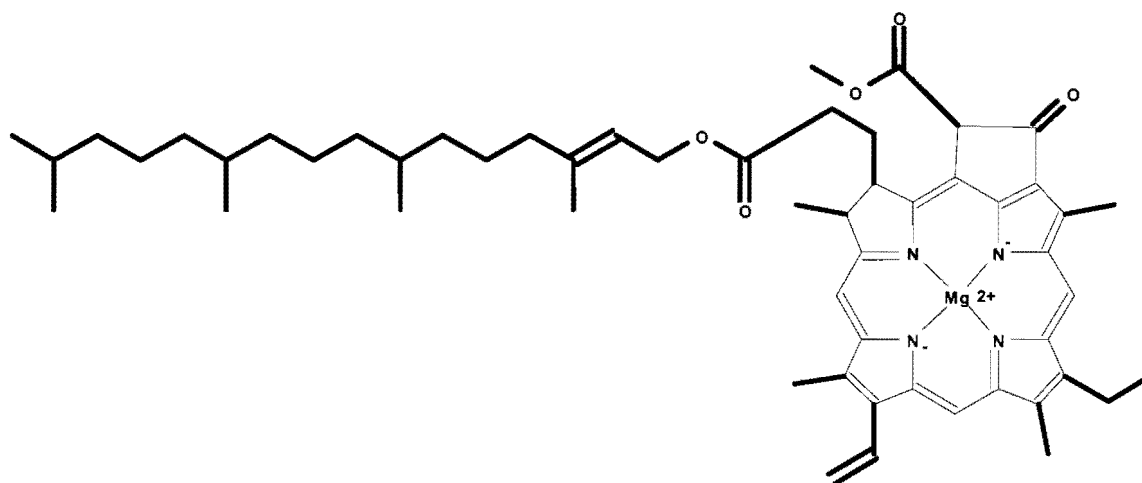


**Figure 5-15** Chemical structure of chlorophyll b (Chem. Draw)

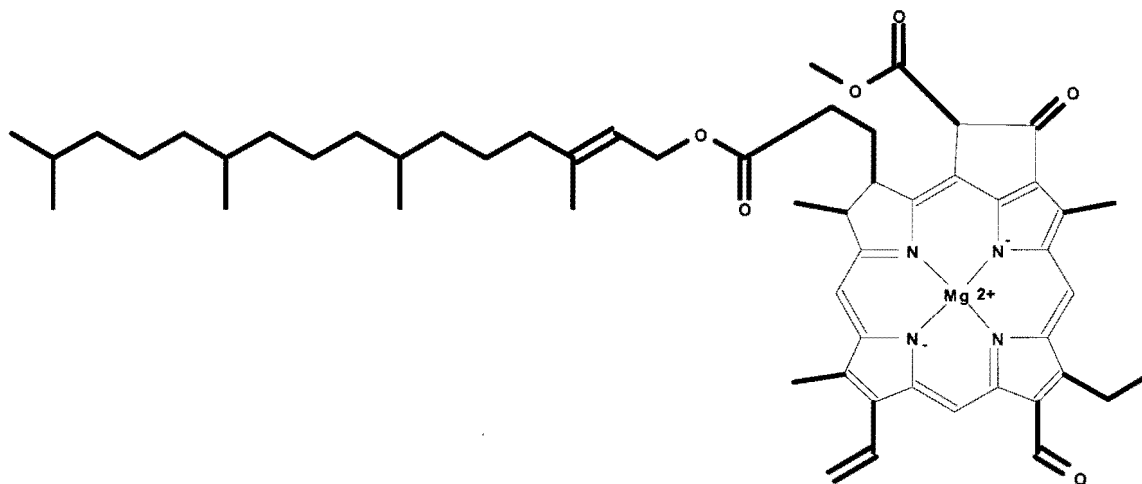
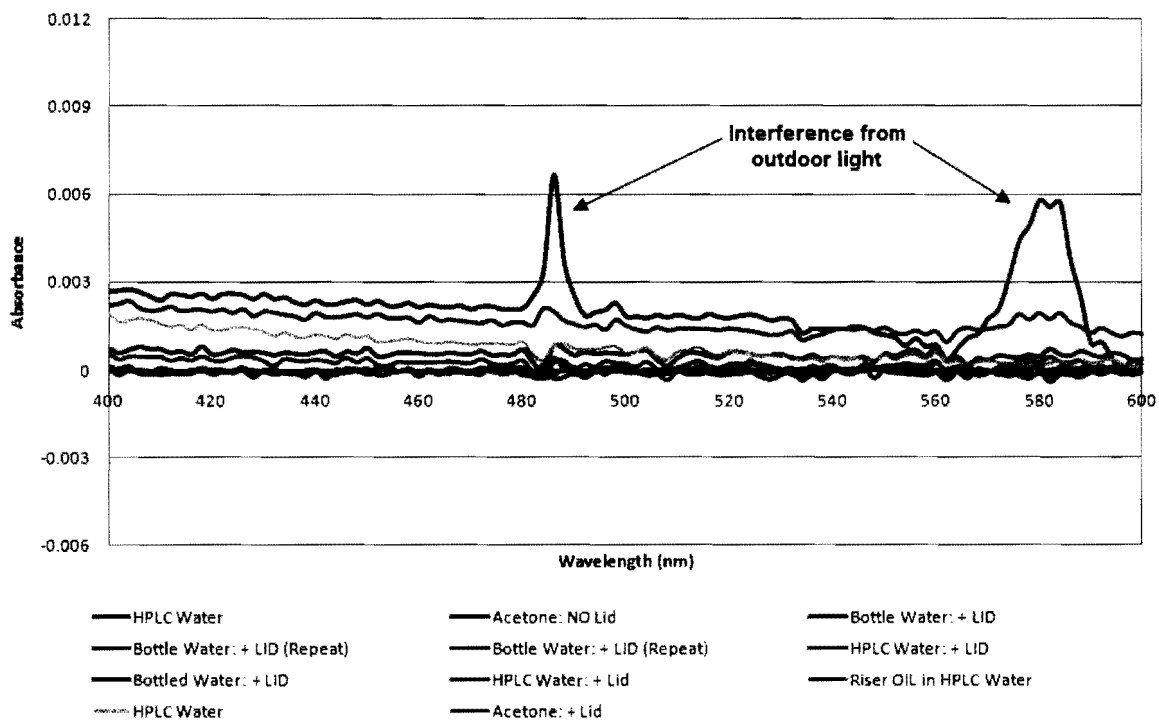


**Figure 5-16 UV/Vis spectra of BP oil samples in different solvents: 1 mm cell: spectrophotometer fully covered from outside lighting**

No porphyrin peaks were observed for the oil samples collected. The only absorbance peaks that were detected were associated to interference from the trees and outside light. Refer to the figure below.



## 5.4 Chapter summary

ATR-IR has been used to simulate the effects of dispersants used to treat a petroleum spill. In response to concerns about the use of dispersants to fight the petroleum spill in the Gulf of Mexico this past summer, we used ATR-IR to investigate how dispersants work. Sample of the BP oil were exposed to 2 wt % of commercial dishwashing soap. The studies indicate that the hydrocarbon components ( $\text{CH}_2$  bend at  $1466\text{ cm}^{-1}$  and  $\text{CH}_3$  rock at  $1345\text{ cm}^{-1}$ ) of the petroleum can be detected in the presence of the soap. However, it took more than 30 min for it to take effect. This is probably due to time and concentration factors to allow micelles to form. Moreover, this is a creative application of the React-IR concept to study the dynamic behavior of dispersants. Millions of dollars were spent on dispersants to alleviate and eliminate the spread of the BP oil to the natural coast lines. The dispersion experiments demonstrated that even in a controlled and accelerated laboratory environment, it still took several hours for the oil samples to be dispersed. Thus, one begs to question the effectiveness, if any, of the dispersants on the uncontrolled oil spill in the Gulf of Mexico.

Efforts to observe the presence of chlorophyll molecules that are potentially present in the crude oil by UV-Vis spectroscopy were unsuccessful. At this time, the status of this investigation is inconclusive as the presence of these molecules in crude oil is well documented. It is possible that concentrations were below detection limits or the chlorophyll derivatives were insufficiently soluble. Although inconclusive, these investigations provide a foundation for future studies.

## 6 Research conclusions

Dissolution studies are critical tests for measuring the performance of a drug product. In this dissertation, a new technique, *in situ* attenuated total reflection-infrared spectroscopy (ATR-IR), has been developed to monitor dissolutions of pharmaceutical drug formulations. Two over-the-counter (OTC) active drugs (acetaminophen and acetylsalicylic acid) and one calibrator tablet (salicylic acid) were tested during the research. Moreover, both single component and multi-component drug formulations were tested and the individual components were identified by IR spectroscopy. For example, individual components of acetaminophen and acetylsalicylic acid in a caffeine-free formulation of Excedrin® tablets were easily distinguished. The ATR-IR system was found to have very good sensitivity and can analyze samples as low as 0.03 mg/mL ( $2 \times 10^{-4}$  M).

In addition, the IR system was able to distinguish separate components of a multiple component system without requiring manual sampling. This versatility was also demonstrated by observing the simultaneous dissolution of acetaminophen and salicylic acid tablets. In contrast, UV-Vis spectroscopy may require mathematical corrections to resolve the two active drugs. Furthermore, HPLC must be used which requires laborious manual sampling or purchase of a complicated automated instrument setup of dissolution configured with HPLC analysis. The *in situ* ATR-IR method has been validated by comparing dissolution profiles using UV-Vis and HPLC methods. In addition, an accuracy of  $\pm 2$  % between IR and HPLC for the salicylic acid results was established. With the current configuration of the IR instrument, this analysis is limited by the sensitivity and wavelength range of the *in situ* fiber

optic probe. However, since this chapter successfully demonstrates the versatility of this novel application of ATR-IR spectroscopy, it is clear that the method has excellent potential to be improved by modification of the IR instrument and selection of more sensitive probes.

Next, the system has the capability of monitoring drug transformations during dissolution. For instance, the hydrolysis of aspirin to salicylic acid was studied using this technique. The instrument was able to monitor the simultaneous formation and elimination of aspirin while at the same time monitor the formation of salicylic acid in solution. This research was possible because of the versatility of ATR-IR system. Specifically, the unique fingerprint region of the IR spectra gave detailed information about the release profile of the drug. Conventional methods, namely, *in-situ* UV-Vis, would only show the release profile of one component. However, peak deconvolution software can be used to analyze aspirin hydrolysis. Moreover, the hydrolysis and transformation of the drug from one form to another may be missed with conventional techniques. ATR-IR captures those minor details and displays them in the fingerprint region, as shown earlier in the results. The unique feature of this system is that it is able to detect several forms of the same drug. In other words, it was able to detect the formation and elimination of a pharmaceutical drug (aspirin) while detecting the formation of the hydrolylate of the aspirin (salicylic acid) in real-time. In addition, this system could be used to study other potential transformations. One example might be the dimerization of acetaminophen as mentioned earlier. The novelty with this particular system is its capability to see drug transformations in solutions while conducting the experiment *in-situ*.

Also, this system was used to support the research related to the BP oil spill. The ATR-IR system coupled with dissolution was able evaluate the effect of dishwashing soaps in the

dispersion of crude oil and the results call into question the efficacy of application of dispersants in certain situations.

Lastly, a new instrument design was proposed and discussed in this thesis. The proposed system, also known as the Solv-IR, would be built at Seton Hall University. An MRI NSF grant was recently filed for this proposal. The proposal to develop this instrument aims construct a new type of detection technique that will allow the study of solvation of solutes in aqueous and organic systems.<sup>78 79 80</sup> The proposed unit has great potential for use in studies of dissolution of drugs and monitoring competing reactions such as hydrolysis of pro-drugs in pharmaceutical development, formulation and quality assurance. The proposed instrument also has application in environmental chemistry, especially to study of the fundamental chemistry and remediation of anthropomorphic events.<sup>81 82 83</sup>

---

<sup>78</sup> Chen, Zeng-Ping; Morris, Julian; Borissova, Antonia; Khan, Shahid; Mahmud, Tariq; Penchev, Rado; Roberts, Kevin. On-line monitoring of batch cooling crystallization of organic compounds using ATR-FTIR spectroscopy coupled with an advanced calibration method. *Chemometrics and Intelligent Laboratory Systems* **2009**, 96, 49-58.

<sup>79</sup> Wartewig, Siegfried; Neubert, Reinhard. Pharmaceutical applications of Mid-IR and Raman spectroscopy. *Advanced Drug Delivery Reviews* **2005**, 57, 1144-1170.

<sup>80</sup> Kubicki, J.D.; Schroeter, L.M.; Itoh, M.J.; Nguyem, B.N.; Apitz, S.E. Attenuated total reflectance Fourier-transform infrared spectroscopy of carboxylic acids adsorbed onto mineral surfaces. *Geochimica et Cosmochimica Acta* **1999**, 63(18), 2709-2725.

<sup>81</sup> Mas, Silvia; Juan, Anna de; Tauler, Roma; Olivieri, Alejandro; Escandar, Graciela. Application of chemometric methods to environmental analysis of organic pollutants: A review. *Talanta* **2010**, 80, 1052-1067.

<sup>82</sup> Varela, R.F.; Rodriguez, D.S.; Carracedo, M.P.; Andrade, J.M.; Fernandez, E; Muniategui, S.; Prada, D. Screening the origin and weathering of oil slicks by attenuated total reflectance mid-IR spectrometry. *Talanta* **2005**, 68 116-125.

<sup>83</sup> Varela, R.F.; Carracedo, M.P.; Rivera, P.F.; Andrade, J.M., Muniategui, S.; Prada, D. Monitoring photooxidation of the Prestige's oil spill by attenuated total reflectance infrared spectroscopy. *Talanta* **2006**, 69, 409-417.

## 7 Appendix [A]: *In situ* ATR-IR Spectroscopy and Dissolution Data

The chart below is an example of the digitized data that is obtained for the calibration of salicylic acid using ATR-IR. The data corresponds to Figure 2-1 in Chapter 2.

Salicylic Acid Linearity Raw Data

	L	M	N	O	P	Q	R	S
1	Wavenumber (cm-1)	Std-1	Std-2	Std-3	Std-4	Std-5	Std-6	Std-7
2	1899.4378	0.001186	0.000446	0.000116	0.000126	0.000327	0.000332	-0.00013
3	1895.7061	0.000956	0.000368	2.97E-05	6.36E-05	-0.0001	-2.8E-05	-0.00048
4	1891.9744	0.001085	0.000601	0.000275	5.67E-05	-3.7E-05	-0.00021	-0.00061
5	1888.2427	0.00135	0.000766	0.000266	0.000206	-8.9E-05	-0.0001	-0.00035
6	1884.511	0.001409	0.000702	0.000398	8.74E-06	-0.00021	0.000126	6.02E-05
7	1880.7793	0.001273	0.000655	0.000511	7.17E-06	-0.00016	0.000112	0.000106
8	1877.0476	0.001176	0.000475	0.000361	0.000187	3.85E-05	-9.1E-05	0.000104
9	1873.3159	0.000934	0.000146	-3.1E-05	-0.00017	5.28E-05	-0.00037	5.46E-05
10	1869.5842	0.000714	0.00013	-0.00018	-0.00025	-0.00018	-0.00035	-0.00013
11	1865.8525	0.000853	0.000385	0.000114	0.000137	-8.6E-05	-7E-05	-0.00018
12	1862.1208	0.000974	0.000557	0.00033	0.000109	7.95E-05	-9.2E-05	-0.00014
13	1858.3891	0.001009	0.000404	0.000217	-0.00014	-6.7E-05	-0.00033	-0.00025
14	1854.6574	0.001254	0.000447	0.000337	0.000101	0.000163	-9.8E-05	-0.00016
15	1850.9256	0.001315	0.000639	0.00059	0.000189	0.000494	0.00038	0.000282
16	1847.1939	0.000906	0.000532	0.000408	0.000194	0.00038	0.000376	0.000391
17	1843.4622	0.000585	0.000351	6.54E-05	0.000176	-2.1E-05	-0.00017	-4.1E-05
18	1839.7305	0.000589	0.000239	7.59E-05	0.000164	-0.00012	-0.00024	-0.00028
19	1835.9988	0.000927	0.00026	0.0004	0.000308	0.000295	0.000233	0.000175
20	1832.2671	0.00112	0.000365	0.000567	0.000381	0.000366	0.000376	0.000426
21	1828.5354	0.001019	0.000457	0.000329	0.000243	0.000125	0.000229	0.000222
22	1824.8037	0.000767	0.000366	0.00014	7.26E-06	5.94E-05	-0.00013	4.6E-05
23	1821.072	0.000492	0.0001	-5E-05	-0.00022	-0.0002	-0.00044	-0.00028
24	1817.3403	0.000374	-0.00011	-0.00023	-0.00027	-0.00034	-0.00043	-0.0004
25	1813.6086	0.000341	-4.6E-05	-0.00019	-7.1E-05	-0.00019	-0.0002	-0.0002
26	1809.8769	0.000349	-1.3E-05	-0.0002	-8E-06	-0.00023	-0.00015	-0.00024
27	1806.1452	0.000152	-5.9E-05	-0.00019	-3.2E-05	-0.00011	-9.8E-05	-0.0002
28	1802.4135	0.000112	-1.7E-05	-0.00012	-8E-05	5.51E-05	1.67E-05	-6.1E-05
29	1798.6818	0.000295	0.000208	6.25E-05	5.22E-05	0.000209	0.000276	0.000301
30	1794.9501	0.000326	0.000391	0.000215	0.000247	0.000343	0.000482	0.000572
31	1791.2184	0.000106	9.28E-05	6.89E-06	-5.5E-05	8.09E-05	5.69E-05	0.000151
32	1787.4867	0.000117	4.11E-06	-9.7E-05	-0.0002	-0.00013	-0.00017	-9.8E-05
33	1783.755	0.000426	0.000234	0.00014	9.9E-05	2.59E-05	-5E-05	-2.2E-05
34	1780.0233	0.000404	0.000284	0.000199	0.000391	0.000302	0.000199	0.00021
35	1776.2915	0.000371	0.000486	0.000451	0.000764	0.000805	0.000895	0.000987
36	1772.5598	0.000245	0.000244	0.000312	0.000401	0.000523	0.000637	0.000742
37	1768.8281	3.88E-05	-7.4E-05	3.94E-06	-0.00012	0.000101	0.00011	0.00013
38	1765.0964	-6.3E-05	-2.1E-05	9.21E-06	-0.00015	0.000165	0.00013	0.000171
39	1761.3647	-0.00016	-2E-05	-2.3E-05	-9.5E-05	6.08E-05	6.12E-05	0.000174
40	1757.633	-0.00019	8.03E-05	5.82E-05	0.000166	0.000218	0.000284	0.000409
41	1753.9013	-0.00029	0.000117	0.000191	0.000436	0.000616	0.000827	0.000916
42	1750.1696	-0.00049	-0.00017	9.82E-06	9.82E-05	0.000345	0.000517	0.000566
43	1746.4379	-0.00056	-0.00027	-0.00012	-1.9E-05	0.00025	0.000287	0.000317
44	1742.7062	-0.00051	-8.6E-05	-3.5E-05	0.000333	0.000621	0.000642	0.00077
45	1738.9745	-0.00046	0.00021	0.000433	0.000988	0.001429	0.001708	0.002004
46	1735.2428	-0.00063	0.000101	0.000445	0.000915	0.001478	0.001787	0.001949
47	1731.5111	-0.00103	-0.00055	-0.00038	-0.00015	0.000226	0.00019	0.000184
48	1727.7794	-0.0011	-0.0006	-0.00057	-0.00043	-0.0002	-0.0003	-0.00019
49	1724.0477	-0.00102	-0.00026	-8.8E-06	0.000193	0.000553	0.00063	0.000899
50	1720.316	-0.00096	3.21E-05	0.000646	0.00114	0.001678	0.002053	0.002386
51	1716.5843	-0.00101	-0.00022	0.000232	0.000695	0.001058	0.001399	0.00156

## Salicylic Acid Linearity Raw Data

	L	M	N	O	P	Q	R	S
52	1712.8526	-0.00135	-0.00057	-0.00028	-8.4E-05	0.000218	0.000394	0.000496
53	1709.1209	-0.00169	-0.00061	-0.0004	-8.9E-05	0.000276	0.000494	0.000667
54	1705.3892	-0.00158	-0.00028	0.000105	0.000678	0.001315	0.001761	0.002152
55	1701.6574	-0.00137	-6.4E-05	0.000622	0.001256	0.002196	0.002715	0.003221
56	1697.9257	-0.00151	-0.00049	0.000211	0.000605	0.001399	0.001807	0.00208
57	1694.194	-0.00179	-0.00087	-0.00035	-0.0003	0.000253	0.00053	0.000575
58	1690.4623	-0.00172	-0.00044	0.000117	0.000371	0.001154	0.001581	0.001793
59	1686.7306	-0.00149	6.36E-05	0.000642	0.001131	0.002001	0.002561	0.002855
60	1682.9989	-0.00136	-0.00022	0.000184	0.000488	0.00093	0.001237	0.001419
61	1679.2672	-0.00103	-0.00018	0.000147	0.000437	0.000719	0.001093	0.0014
62	1675.5355	-0.00058	0.000105	0.000503	0.000868	0.001316	0.001638	0.001966
63	1671.8038	-0.00026	0.00024	0.000747	0.001202	0.001627	0.001811	0.001981
64	1668.0721	-0.00024	0.000271	0.000683	0.001076	0.001491	0.001617	0.001777
65	1664.3404	-1.8E-05	0.000317	0.000337	0.000815	0.001329	0.001406	0.00168
66	1660.6087	0.000598	0.000614	0.000603	0.001152	0.001739	0.002054	0.00221
67	1656.877	0.001461	0.001521	0.001783	0.002499	0.003535	0.004215	0.004565
68	1653.1453	0.002052	0.001872	0.001991	0.002544	0.003286	0.003881	0.00432
69	1649.4136	0.002549	0.002015	0.001953	0.002269	0.002765	0.003057	0.003508
70	1645.6819	0.002871	0.001834	0.001371	0.001695	0.002215	0.002284	0.00251
71	1641.9502	0.003484	0.001966	0.001583	0.001557	0.001868	0.001993	0.002262
72	1638.2185	0.004217	0.002804	0.002488	0.002059	0.002582	0.002784	0.003125
73	1634.4868	0.004913	0.003363	0.002566	0.002168	0.002763	0.0025	0.00276
74	1630.7551	0.005507	0.003671	0.002571	0.002323	0.002625	0.002211	0.002611
75	1627.0234	0.005408	0.003017	0.002313	0.0019	0.002059	0.001872	0.002161
76	1623.2916	0.005116	0.00253	0.002077	0.001755	0.002031	0.001956	0.002238
77	1619.5599	0.004863	0.002607	0.002114	0.002018	0.0023	0.002298	0.002563
78	1615.8282	0.004013	0.002211	0.001505	0.001531	0.001478	0.001332	0.001496
79	1612.0965	0.003593	0.002006	0.001433	0.001264	0.00118	0.001062	0.001137
80	1608.3648	0.003529	0.001883	0.001704	0.001158	0.001232	0.00126	0.001033
81	1604.6331	0.003243	0.001683	0.001429	0.000724	0.000871	0.000978	0.00065
82	1600.9014	0.003843	0.001906	0.001293	0.000651	0.000812	0.000723	0.0006
83	1597.1697	0.004418	0.002021	0.001197	0.000801	0.000832	0.000642	0.000628
84	1593.438	0.00446	0.002019	0.001239	0.000974	0.000834	0.000778	0.000709
85	1589.7063	0.004379	0.002145	0.001421	0.001154	0.001034	0.000973	0.000692
86	1585.9746	0.004226	0.001989	0.001427	0.001185	0.001046	0.000976	0.000783
87	1582.2429	0.004503	0.002447	0.002033	0.001804	0.001956	0.001973	0.002109
88	1578.5112	0.00481	0.002972	0.002495	0.002395	0.002826	0.002929	0.003247
89	1574.7795	0.004666	0.002667	0.002121	0.001997	0.00223	0.002352	0.002464
90	1571.0478	0.004259	0.00225	0.001758	0.001532	0.00166	0.001823	0.001755
91	1567.3161	0.003809	0.002204	0.001733	0.001662	0.00187	0.002077	0.002042
92	1563.5844	0.003742	0.002966	0.002804	0.00323	0.00381	0.004369	0.004606
93	1559.8527	0.003015	0.002666	0.002645	0.003158	0.003769	0.004346	0.004669
94	1556.121	0.002047	0.001626	0.001474	0.001614	0.001894	0.00218	0.002324
95	1552.3893	0.001426	0.000998	0.000854	0.000824	0.000991	0.00114	0.001238
96	1548.6575	0.000831	0.000796	0.000863	0.00107	0.001416	0.001524	0.001795
97	1544.9258	0.000738	0.001292	0.001712	0.002334	0.003066	0.003471	0.003976
98	1541.1941	0.000631	0.00126	0.001695	0.002244	0.003061	0.003621	0.003955
99	1537.4624	1.89E-05	0.000407	0.000636	0.00103	0.001535	0.001916	0.001958
100	1533.7307	-0.00042	-8.7E-05	6.67E-05	0.000373	0.000723	0.000964	0.000992
101	1529.999	-0.00041	1.6E-05	0.000245	0.000508	0.001002	0.001193	0.001353
102	1526.2673	-0.00028	0.000454	0.000897	0.001294	0.002015	0.002362	0.002688



## Salicylic Acid Linearity Raw Data

	L	M	N	O	P	Q	R	S
103	1522.5356	-0.00044	0.000371	0.000883	0.001318	0.001992	0.002417	0.002748
104	1518.8039	-0.00067	-0.00012	0.000273	0.000559	0.001058	0.001415	0.00154
105	1515.0722	-0.00072	-0.00024	0.000117	0.000303	0.000764	0.001079	0.001165
106	1511.3405	-0.00043	0.000349	0.000883	0.001316	0.002082	0.002589	0.002924
107	1507.6088	-0.00021	0.000441	0.000982	0.001496	0.002189	0.002707	0.00305
108	1503.8771	-0.0001	0.000149	0.000393	0.000684	0.00108	0.001374	0.001435
109	1500.1454	0.000916	0.000788	0.000863	0.000905	0.001411	0.001686	0.001733
110	1496.4137	0.003357	0.001924	0.001548	0.001223	0.001588	0.001689	0.001733
111	1492.682	0.006785	0.003629	0.002652	0.002147	0.002244	0.002175	0.002169
112	1488.9503	0.007163	0.0037	0.002682	0.002235	0.002164	0.001971	0.001924
113	1485.2186	0.004093	0.001979	0.001384	0.001053	0.001048	0.000952	0.000879
114	1481.4869	0.001505	0.000668	0.000422	0.000392	0.00055	0.000608	0.000618
115	1477.7552	0.000584	0.000497	0.000561	0.00091	0.001281	0.001507	0.001674
116	1474.0234	0.000399	0.000456	0.000678	0.000891	0.001312	0.001515	0.001708
117	1470.2917	0.000651	0.000365	0.000357	0.000312	0.000586	0.000659	0.000713
118	1466.56	0.002771	0.001417	0.001032	0.001008	0.001056	0.001119	0.00106
119	1462.8283	0.006074	0.003346	0.00261	0.002558	0.00258	0.002668	0.002682
120	1459.0966	0.006588	0.003804	0.003064	0.003025	0.003316	0.003477	0.003606
121	1455.3649	0.003853	0.00205	0.001519	0.001511	0.001721	0.001769	0.001768
122	1451.6332	0.001528	0.00068	0.000414	0.000513	0.000609	0.000658	0.000649
123	1447.9015	0.000208	-0.00012	-0.00019	-0.00013	-7.4E-05	3.63E-05	1.82E-05
124	1444.1698	-0.00029	-0.00043	-0.00044	-0.00056	-0.00048	-0.00034	-0.00034
125	1440.4381	-0.00025	-0.00021	-7E-05	-0.00018	9.85E-05	0.000275	0.000414
126	1436.7064	-0.00035	-0.00021	-3.9E-05	-6.2E-05	0.000156	0.000341	0.000446
127	1432.9747	-0.00039	-0.0002	-0.00015	-4E-05	5.78E-05	0.00016	0.000179
128	1429.243	-0.00031	-0.00012	-5.3E-05	0.000113	0.000152	0.000237	0.000254
129	1425.5113	-0.00023	-5.6E-05	7.21E-05	0.000328	0.000428	0.000585	0.000652
130	1421.7796	9.44E-05	0.00021	0.000361	0.000549	0.000894	0.001073	0.001228
131	1418.0479	0.000413	0.000187	0.000263	0.000111	0.000443	0.000471	0.000569
132	1414.3162	0.000783	0.000316	0.000287	5.03E-05	0.000194	0.000178	0.000115
133	1410.5845	0.001229	0.000692	0.000593	0.000356	0.000466	0.000553	0.000449
134	1406.8528	0.001582	0.000908	0.000738	0.000409	0.000584	0.000648	0.00062
135	1403.1211	0.00238	0.001332	0.001071	0.000714	0.000883	0.00092	0.000919
136	1399.3894	0.00411	0.00226	0.001745	0.001243	0.001327	0.001341	0.001324
137	1395.6576	0.00723	0.003786	0.002654	0.001951	0.001754	0.001637	0.001532
138	1391.9259	0.010625	0.005419	0.003711	0.00305	0.002591	0.002352	0.002151
139	1388.1942	0.011517	0.005803	0.003926	0.003387	0.002882	0.002586	0.002351
140	1384.4625	0.009322	0.00456	0.002895	0.002381	0.001961	0.001706	0.001443
141	1380.7308	0.006639	0.003193	0.002056	0.001647	0.001377	0.00123	0.000992
142	1376.9991	0.004745	0.002303	0.001547	0.001224	0.00108	0.000948	0.000799
143	1373.2674	0.003576	0.001644	0.001055	0.0007	0.00067	0.000572	0.000445
144	1369.5357	0.002964	0.00128	0.00069	0.000491	0.000432	0.000437	0.000326
145	1365.804	0.002925	0.001388	0.000801	0.000781	0.000661	0.000687	0.000673
146	1362.0723	0.00319	0.001619	0.001039	0.000897	0.000775	0.000748	0.000727
147	1358.3406	0.003132	0.001462	0.000881	0.000669	0.000565	0.000511	0.00045
148	1354.6089	0.003297	0.001511	0.000896	0.000839	0.000704	0.000643	0.000525
149	1350.8772	0.003966	0.002018	0.001364	0.001218	0.001046	0.000987	0.00081
150	1347.1455	0.004446	0.002376	0.001719	0.001276	0.001274	0.001134	0.001006
151	1343.4138	0.004486	0.002431	0.001752	0.001346	0.001331	0.001206	0.001173
152	1339.6821	0.004391	0.002383	0.001779	0.00129	0.001206	0.001142	0.001097
153	1335.9504	0.003976	0.002084	0.001469	0.000776	0.000744	0.000645	0.000552

## Salicylic Acid Linearity Raw Data

	L	M	N	O	P	Q	R	S
154	1332.2187	0.00338	0.001653	0.001025	0.000664	0.000468	0.000352	0.000257
155	1328.487	0.002996	0.001477	0.000908	0.000941	0.000618	0.000534	0.000424
156	1324.7553	0.002511	0.00119	0.000724	0.000769	0.000566	0.000513	0.00043
157	1321.0235	0.002244	0.001047	0.000652	0.00052	0.000495	0.000449	0.000424
158	1317.2918	0.002288	0.001121	0.000739	0.000519	0.000533	0.000496	0.000473
159	1313.5601	0.002267	0.001008	0.000576	0.000396	0.000379	0.000356	0.000295
160	1309.8284	0.002465	0.001017	0.000567	0.000432	0.000423	0.000394	0.000312
161	1306.0967	0.002911	0.001308	0.000842	0.000661	0.000678	0.000606	0.000501
162	1302.365	0.003314	0.001634	0.001101	0.000778	0.000716	0.000635	0.000505
163	1298.6333	0.003299	0.001693	0.00116	0.000854	0.000696	0.000622	0.000489
164	1294.9016	0.003022	0.001543	0.001068	0.000843	0.000789	0.000736	0.000598
165	1291.1699	0.002832	0.001469	0.001037	0.000822	0.000878	0.000835	0.000737
166	1287.4382	0.002753	0.001452	0.001042	0.000799	0.00074	0.000701	0.0006
167	1283.7065	0.002886	0.001571	0.001151	0.000807	0.000676	0.00062	0.000497
168	1279.9748	0.00303	0.001679	0.00123	0.000866	0.000823	0.000751	0.000679
169	1276.2431	0.00309	0.001643	0.001152	0.000976	0.000917	0.00085	0.000804
170	1272.5114	0.00324	0.001658	0.0011	0.000864	0.000866	0.000768	0.000716
171	1268.7797	0.003783	0.00191	0.001298	0.000783	0.000866	0.000731	0.00064
172	1265.048	0.004695	0.002387	0.001656	0.001061	0.00095	0.000795	0.000701
173	1261.3163	0.005823	0.002982	0.002023	0.001436	0.001121	0.000989	0.000863
174	1257.5846	0.006738	0.003401	0.00223	0.001667	0.001343	0.001195	0.00103
175	1253.8529	0.006747	0.003343	0.002168	0.001566	0.001244	0.001031	0.000874
176	1250.1212	0.005908	0.002911	0.001931	0.001398	0.001088	0.000919	0.000748
177	1246.3894	0.004836	0.00232	0.001482	0.001029	0.000816	0.000698	0.000495
178	1242.6577	0.004405	0.002154	0.001394	0.000901	0.000741	0.000629	0.00045
179	1238.926	0.00419	0.002078	0.001404	0.000894	0.000771	0.00069	0.000548
180	1235.1943	0.003753	0.001813	0.001124	0.000674	0.000462	0.000394	0.000261
181	1231.4626	0.003634	0.001757	0.001095	0.000713	0.000472	0.000368	0.000316
182	1227.7309	0.003853	0.001965	0.001355	0.001022	0.000876	0.000756	0.000738
183	1223.9992	0.00387	0.001951	0.001356	0.001098	0.001005	0.000925	0.000854
184	1220.2675	0.003658	0.001736	0.00111	0.000889	0.000776	0.000738	0.000635
185	1216.5358	0.003675	0.00178	0.001127	0.000979	0.000826	0.000745	0.000679
186	1212.8041	0.003753	0.001899	0.001217	0.001156	0.001025	0.000878	0.000802
187	1209.0724	0.003834	0.001958	0.001254	0.001085	0.000959	0.000814	0.000702
188	1205.3407	0.003864	0.001879	0.001173	0.000842	0.000791	0.000667	0.00056
189	1201.609	0.00397	0.00189	0.001212	0.000742	0.000797	0.000721	0.000614
190	1197.8773	0.004257	0.002126	0.001457	0.000872	0.00093	0.000873	0.000745
191	1194.1456	0.004628	0.002425	0.001697	0.001134	0.001031	0.000931	0.00077
192	1190.4139	0.004976	0.002665	0.001879	0.001307	0.001027	0.000908	0.000793
193	1186.6822	0.005204	0.00272	0.001878	0.001212	0.001006	0.000914	0.000827
194	1182.9505	0.005668	0.002891	0.002031	0.001388	0.001294	0.001153	0.001049
195	1179.2188	0.006234	0.003232	0.002276	0.001674	0.0015	0.001306	0.001194
196	1175.4871	0.006604	0.003391	0.002266	0.001499	0.001286	0.001087	0.000922
197	1171.7553	0.006879	0.003437	0.00217	0.001422	0.001196	0.000999	0.000803
198	1168.0236	0.007416	0.003675	0.00235	0.001609	0.001364	0.001155	0.000954
199	1164.2919	0.008204	0.00413	0.002754	0.00195	0.001723	0.001427	0.00124
200	1160.5602	0.008411	0.004226	0.002832	0.002038	0.001825	0.001501	0.001325
201	1156.8285	0.007971	0.003972	0.002644	0.001869	0.001626	0.00136	0.001185
202	1153.0968	0.007722	0.003877	0.002546	0.001929	0.001639	0.001426	0.001268
203	1149.3651	0.007602	0.003817	0.002446	0.001717	0.001408	0.001198	0.001026
204	1145.6334	0.006491	0.003212	0.002016	0.001224	0.000872	0.000653	0.000515

## Salicylic Acid Linearity Raw Data

	L	M	N	O	P	Q	R	S
205	1141.9017	0.004839	0.002328	0.001445	0.000891	0.000557	0.000403	0.000323
206	1138.17	0.003536	0.001676	0.001013	0.000684	0.000464	0.000377	0.000304
207	1134.4383	0.002521	0.001262	0.000793	0.000473	0.000403	0.000311	0.000272
208	1130.7066	0.001495	0.000742	0.000469	5.25E-05	9.44E-05	-2E-05	-1.9E-05
209	1126.9749	2.45E-05	-0.0002	-0.00031	-0.00054	-0.00044	-0.00054	-0.00052
210	1123.2432	-0.00118	-0.00078	-0.00068	-0.00059	-0.00044	-0.00044	-0.00041
211	1119.5115	-0.00226	-0.00121	-0.00089	-0.00069	-0.00053	-0.00043	-0.00039
212	1115.7798	-0.00371	-0.00194	-0.00142	-0.00106	-0.00092	-0.00079	-0.00075
213	1112.0481	-0.00512	-0.00253	-0.00174	-0.00144	-0.00118	-0.00098	-0.00095
214	1108.3164	-0.0066	-0.00314	-0.00199	-0.00193	-0.00147	-0.00121	-0.00104
215	1104.5847	-0.00868	-0.00424	-0.00274	-0.00242	-0.0019	-0.00161	-0.00133
216	1100.853	-0.0111	-0.00558	-0.00374	-0.00309	-0.00247	-0.00212	-0.00187
217	1097.1213	-0.01326	-0.00669	-0.00451	-0.00357	-0.00277	-0.00233	-0.00204
218	1093.3895	-0.01488	-0.00762	-0.00519	-0.00399	-0.00321	-0.00268	-0.00232
219	1089.6578	-0.01538	-0.00803	-0.0055	-0.00442	-0.00361	-0.00308	-0.00269
220	1085.9261	-0.01451	-0.00762	-0.00525	-0.0044	-0.00348	-0.00299	-0.00261
221	1082.1944	-0.01279	-0.00678	-0.00468	-0.00383	-0.00297	-0.00256	-0.00222
222	1078.4627	-0.01176	-0.00634	-0.00441	-0.0035	-0.00274	-0.0024	-0.00207
223	1074.731	-0.01193	-0.0064	-0.00445	-0.00348	-0.00268	-0.00229	-0.00198
224	1070.9993	-0.01227	-0.00643	-0.0044	-0.00335	-0.00253	-0.00214	-0.00188
225	1067.2676	-0.01213	-0.00637	-0.00438	-0.0034	-0.00266	-0.00229	-0.00205
226	1063.5359	-0.01119	-0.00595	-0.00414	-0.00336	-0.00272	-0.00233	-0.00211
227	1059.8042	-0.00961	-0.00508	-0.00354	-0.0029	-0.00242	-0.00203	-0.00184
228	1056.0725	-0.00791	-0.00409	-0.00286	-0.00223	-0.00191	-0.00157	-0.00139
229	1052.3408	-0.0063	-0.00316	-0.00217	-0.00161	-0.00142	-0.00116	-0.00099
230	1048.6091	-0.00517	-0.00264	-0.00183	-0.00147	-0.00134	-0.00115	-0.00098
231	1044.8774	-0.00415	-0.00211	-0.00148	-0.00134	-0.00115	-0.00099	-0.00085
232	1041.1457	-0.00293	-0.00138	-0.0009	-0.00086	-0.00057	-0.00048	-0.00038
233	1037.414	-0.00193	-0.00091	-0.00057	-0.0006	-0.00037	-0.00039	-0.00029
234	1033.6823	-0.00152	-0.00082	-0.00055	-0.00062	-0.00045	-0.0005	-0.0004
235	1029.9506	-0.00169	-0.00096	-0.0007	-0.0008	-0.00056	-0.00056	-0.0005
236	1026.2189	-0.00176	-0.00099	-0.00075	-0.00076	-0.00054	-0.0005	-0.00046
237	1022.4872	-0.00198	-0.00119	-0.00101	-0.00087	-0.00074	-0.00064	-0.00064
238	1018.7554	-0.00221	-0.00136	-0.00118	-0.00104	-0.00097	-0.00083	-0.00087
239	1015.0237	-0.00208	-0.00112	-0.0009	-0.00069	-0.00061	-0.0005	-0.00051
240	1011.292	-0.00219	-0.0011	-0.00079	-0.00058	-0.00036	-0.0003	-0.00024
241	1007.5603	-0.0027	-0.00139	-0.00093	-0.00095	-0.00074	-0.00064	-0.00055
242	1003.8286	-0.00371	-0.00185	-0.00119	-0.00121	-0.0009	-0.00075	-0.00065
243	1000.0969	-0.00586	-0.00293	-0.00196	-0.00154	-0.00098	-0.00075	-0.00062
244	996.3652	-0.0087	-0.0044	-0.00298	-0.00219	-0.00158	-0.00118	-0.00104
245	992.6335	-0.01057	-0.0054	-0.00367	-0.00278	-0.00222	-0.00173	-0.00152
246	988.9018	-0.00982	-0.00499	-0.00345	-0.00255	-0.00195	-0.00155	-0.0013
247	985.1701	-0.00724	-0.00364	-0.0025	-0.0017	-0.00113	-0.00087	-0.00067
248	981.4384	-0.00489	-0.00257	-0.00178	-0.00125	-0.00083	-0.00071	-0.00055
249	977.7067	-0.00331	-0.0018	-0.00132	-0.00096	-0.00073	-0.00062	-0.00049
250	973.975	-0.00208	-0.00108	-0.00079	-0.00048	-0.00036	-0.00021	-0.0001
251	970.2433	-0.00118	-0.00063	-0.00049	-0.00039	-0.00019	-9.2E-05	-5.6E-05
252	966.5116	-0.00044	-0.00028	-0.00026	-0.00024	-1E-05	7.42E-05	3.01E-05
253	962.7799	0.000815	0.000539	0.00047	0.000491	0.000655	0.000717	0.000705
254	959.0482	0.002108	0.001349	0.001195	0.001016	0.001059	0.001048	0.0011
255	955.3165	0.002958	0.001739	0.001411	0.000979	0.000847	0.000858	0.00087

## Salicylic Acid Linearity Raw Data

	L	M	N	O	P	Q	R	S
256	951.5848	0.003795	0.002052	0.001546	0.000769	0.000633	0.00059	0.000539
257	947.8531	0.004571	0.00237	0.001777	0.001007	0.000903	0.000774	0.000714
258	944.1213	0.004691	0.002306	0.001617	0.001273	0.001165	0.001099	0.000984
259	940.3896	0.004372	0.002068	0.001318	0.001026	0.000997	0.000965	0.000868
260	936.6579	0.004143	0.002079	0.001323	0.000962	0.000931	0.000916	0.000862
261	932.9262	0.003803	0.002096	0.001401	0.001324	0.00126	0.001301	0.001234
262	929.1945	0.003135	0.001903	0.001382	0.001508	0.001561	0.001594	0.001528
263	925.4628	0.002265	0.00147	0.001244	0.001512	0.001764	0.001758	0.001767
264	921.7311	0.001181	0.000692	0.000776	0.001116	0.001422	0.001473	0.001564
265	917.9994	0.000139	7.48E-05	0.000247	0.000604	0.000756	0.000895	0.000993
266	914.2677	-0.00066	-0.00037	-0.0001	0.00043	0.00058	0.00072	0.000773
267	910.536	-0.00111	-0.00055	-0.00018	0.000233	0.000703	0.000826	0.000854
268	906.8043	-0.00145	-0.00048	-0.00016	0.000153	0.000723	0.000877	0.000917
269	903.0726	-0.00203	-0.00074	-0.00027	0.000119	0.000555	0.000717	0.000854
270	899.3409	-0.00255	-0.00114	-0.00047	6.33E-05	0.000483	0.000604	0.000875
271	895.6092	-0.00298	-0.00149	-0.00071	5.53E-05	0.000489	0.000728	0.000813
272	891.8775	-0.00341	-0.00167	-0.00085	-0.0003	0.000225	0.000674	0.000554
273	888.1458	-0.00366	-0.00178	-0.00088	-0.0005	0.000303	0.000795	0.000705
274	884.4141	-0.00371	-0.00176	-0.00093	-0.00054	0.00054	0.001018	0.000964
275	880.6824	-0.00388	-0.00205	-0.00119	-0.00095	2.71E-05	0.000539	0.00056
276	876.9507	-0.00393	-0.00226	-0.00116	-0.00079	-7E-05	0.000362	0.000589
277	873.219	-0.00433	-0.00239	-0.00119	-0.00055	0.000101	0.00032	0.000496
278	869.4872	-0.00487	-0.00264	-0.00157	-0.0008	-8E-05	0.000167	0.000311
279	865.7555	-0.00509	-0.00283	-0.00172	-0.00128	-0.0004	-0.00018	0.000181
280	862.0238	-0.00537	-0.00265	-0.00138	-0.00101	-0.00023	0.000242	0.000488
281	858.2921	-0.00619	-0.00314	-0.00166	-0.00095	-0.00016	0.000614	0.000697
282	854.5604	-0.00725	-0.00408	-0.00256	-0.00151	-0.00072	-0.00019	0.000125
283	850.8287	-0.00788	-0.00415	-0.00262	-0.00135	-0.00058	-0.0001	0.000241
284	847.097	-0.00796	-0.0037	-0.00195	-0.0009	0.00016	0.000811	0.000701
285	843.3653	-0.00754	-0.00338	-0.00168	-0.00072	0.000331	0.000964	0.001029
286	839.6336	-0.0077	-0.00362	-0.00202	-0.00133	-0.00016	0.00029	0.000708
287	835.9019	-0.00812	-0.00387	-0.00244	-0.00186	-0.00039	9.25E-05	0.000235
288	832.1702	-0.00763	-0.00413	-0.00235	-0.00145	1.14E-05	0.000779	0.000564
289	828.4385	-0.00704	-0.00427	-0.00174	-0.00094	0.000403	0.001395	0.001235
290	824.7068	-0.0077	-0.00418	-0.00212	-0.00147	0.000107	0.000949	0.000877
291	820.9751	-0.0082	-0.00388	-0.00268	-0.00202	-0.00054	-0.0003	-0.00029
292	817.2434	-0.00781	-0.00401	-0.00245	-0.00199	-0.00124	-0.00118	-0.00075
293	813.5117	-0.00678	-0.00338	-0.00158	-0.0009	-0.00054	0.000213	0.000371
294	809.78	-0.00636	-0.00321	-0.00153	-0.00048	3.4E-05	0.00109	0.000918
295	806.0483	-0.00736	-0.00368	-0.00201	-0.00164	-0.0004	0.000307	0.000387
296	802.3166	-0.00797	-0.00406	-0.00254	-0.00259	-0.00083	-0.00051	0.000109
297	798.5849	-0.00819	-0.00484	-0.00311	-0.00241	-0.00122	-0.00087	2.94E-05
298	794.8532	-0.0082	-0.0049	-0.00359	-0.00217	-0.00133	-0.00064	-4.4E-05
299	791.1214	-0.00786	-0.00405	-0.00322	-0.00221	-0.00135	-4.8E-05	0.000357
300	787.3897	-0.00714	-0.00339	-0.00148	-0.00058	1.62E-05	0.000994	0.001373
301	783.658	-0.00734	-0.00333	-0.001	0.000207	0.000315	0.001158	0.0018
302	779.9263	-0.00693	-0.00292	-0.00114	-0.00023	-1E-04	0.000946	0.001363
303	776.1946	-0.00613	-0.00272	-0.00141	-0.00076	0.000415	0.001108	0.001337
304	772.4629	-0.00777	-0.00383	-0.00335	-0.00201	-7.5E-05	0.000259	0.000769
305	768.7312	-0.00763	-0.00403	-0.00417	-0.00264	-0.00036	-0.00019	0.00045
306	764.9995	-0.00575	-0.00161	-0.0015	-0.00051	-6.5E-05	0.001896	0.00175

## Salicylic Acid Linearity Raw Data

	L	M	N	O	P	Q	R	S
307	761.2678	-0.00503	-0.00106	-0.00032	0.001092	5.23E-05	0.00358	0.001615
308	757.5361	-0.00629	-0.00331	-0.0015	-0.00044	-0.00015	0.003362	0.001435
309	753.8044	-0.00683	-0.00424	-0.0015	-0.00113	0.000211	0.002343	0.003148
310	750.0727	-0.00725	-0.00467	-0.00072	-0.00203	0.000186	0.000415	0.003189
311	746.341	-0.00736	-0.00409	-0.00072	-0.00209	0.000299	0.000565	0.001658
312	742.6093	-0.00727	-0.0023	-0.00152	-0.00068	0.000539	0.00208	0.001731
313	738.8776	-0.00746	-0.00387	-0.00284	-0.0003	0.000658	0.002007	0.001217
314	735.1459	-0.00653	-0.00268	-0.00376	0.000387	0.001801	0.002261	0.002028
315	731.4142	-0.00631	-0.00243	-0.00418	0.000465	0.001284	0.001984	0.002449
316	727.6825	-0.00448	-0.0036	-0.00271	0.000659	3.79E-05	0.003612	0.002328
317	723.9508	-0.00609	-0.00211	-0.0007	0.002337	0.001633	0.004503	0.002582
318	720.2191	-0.00823	-0.0018	-0.0018	0.003083	0.003483	0.001606	-6.5E-05
319	716.4873	-0.01052	-0.00518	-0.00618	-0.00112	-0.00192	-0.00196	-0.00296
320	712.7556	-0.009	-0.00408	-0.00503	-0.00335	-0.00193	0.000819	0.002041
321	709.0239	-0.00263	0.002016	8.46E-05	0.000322	0.006467	0.00659	0.008253
322	705.2922	0.000411	0.00198	0.000152	0.000988	0.008183	0.007496	0.007357
323	701.5605	-0.00433	-0.00022	-0.00489	0.000451	0.001238	0.008372	0.003532
324	697.8288	-0.00972	0.001882	-0.00648	-0.0021	-0.00287	0.006825	0.000633
325	694.0971	-0.01283	0.001633	-0.00345	-0.00274	0.004553	0.003136	0.005014
326	690.3654	-0.00477	-0.00307	0.001101	0.00155	0.015475	0.008684	0.007746
327	686.6337	0.002714	0.004069	0.008987	0.017488	0.023048	0.017339	0.00774
328	682.902	0.002344	0.008319	0.0125	0.019268	0.012339	0.021648	0.014214
329	679.1703	0.01973	0.009579	0.014092	0.022671	0.006015	0.020514	0.020884
330	675.4386	0.022907	0.027308	0.011454	0.008652	0.013533	0.00993	0.018337
331	671.7069	0.040395	0.047424	0.04506	0.017746	0.03161	-0.00108	0.038309
332	667.9752	0.03742	0.034306	-0.0015	0.211175	0.041259	-0.00308	0.041487
333	664.2435	-0.03673	0.031214	-0.10889	0.176551	-0.01099	-0.01847	-0.01638
334	660.5118	-0.01329	0.05025	-0.07151	0.057809	0.006968	0.009254	-0.00372
335	656.7801	0.045812	0.024709	0.032092	0.047795	0.042077	0.073839	0.0306
336	653.0484	-0.04397	0.004264	0.035975	-0.03612	-0.01248	0.056891	-0.02779
337	649.3167	-0.0637	0.00249	-0.01432	-0.05065	0.00042	0.118745	0.020689

**Figure 7-1      Linearity of salicylic acid in pH 7.4 phosphate buffer (corresponds to Figure 2-1 in Chapter 2)**

The table below contains the raw data collected during the salicylic acid linearity experiment. Eight serial dilutions of salicylic acid reference standards were used during the linearity study. The molar concentrations are displayed in the table. Standard 1 represents about 21 mg of salicylic acid per 900 ml of buffer while Standard 8 represents about 300 mg of salicylic acid per 900 ml of buffer. Since a large salicylic acid peak was observed at  $1388\text{ cm}^{-1}$ , a single-point baseline correction at  $1370\text{ cm}^{-1}$  was used to correct the data.

Description	Flask Volume (L)	Concentration (M)	1388nm	1388-1370
Std-1	0.050	0.03215	0.01152	0.00855
Std-2	0.100	0.01607	0.00580	0.00452
Std-3	0.150	0.01072	0.00393	0.00324
Std-4	0.200	0.00804	0.00339	0.00290
Std-5	0.250	0.00643	0.00288	0.00245
Std-6	0.300	0.00536	0.00259	0.00215
Std-7	0.350	0.00459	0.00235	0.00203
Std-8*	0.700	0.00230	0.00103	0.00118

\* Note: Conc. ~100% of 300mg tablet in actual vessel (900ml) dissolution

**Figure 7-2** Linear regression chart for salicylic acid

The figure below is a linear regression plot for the serial dilutions of salicylic acid reference standards. Since a large salicylic acid peak was observed at  $1388\text{ cm}^{-1}$ , a single-point baseline correction at  $1370\text{ cm}^{-1}$  was used to correct the data.

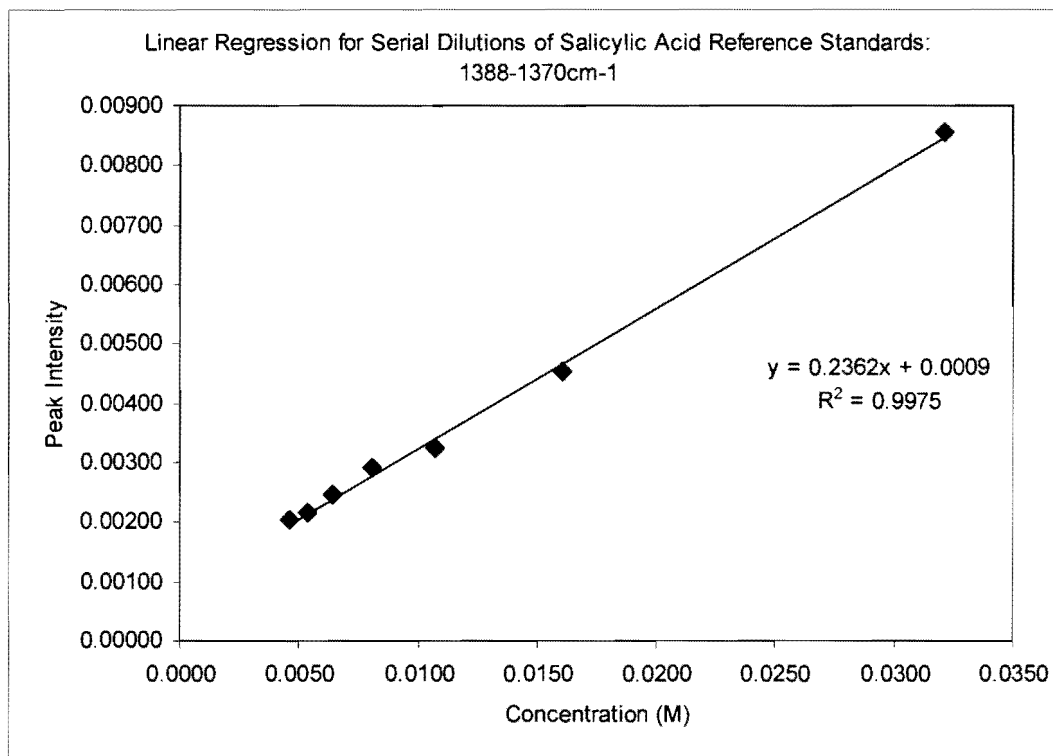


**Figure 7-3**      **Dissolution results for salicylic acid in pH 7.4 phosphate buffer: HPLC vs. IR data (corresponds to Figure 2-2 in Chapter 2)**

The table below corresponds to the percent (%) dissolved data obtained from the salicylic acid dissolution experiment. The table compares ATR-IR to HPLC percent dissolved results. HPLC samples were collected after 30 min, 1 hour, 2 hour, 3 hour, 6.5 hours and finally after 7 hours. Moreover, the samples were analyzed using an Agilent HPLC system. As shown in the table below the maximum absolute difference observed between the IR and HPLC data was found to be 3%.

<b>Time (hh:mm)</b>	<b>% Dissolved (HPLC)</b>	<b>Dissolved by (IR)</b>	<b>Difference</b>
00:00	0.0%	0.0%	0%
00:30	11.1%	14.4%	-3%
01:00	20.9%	23.1%	-2%
02:00	38.2%	38.0%	0%
03:00	52.9%	50.9%	2%
06:30	87.8%	88.3%	-1%
07:00	94.8%	97.8%	-3%



**Figure 7-4      ATR-IR System photo**

The figure below shows a photo of the Mettler Toledo ATR-IR system coupled with a DiComp fiber optic probe. The photo shows the DiComp probe inserted into a standard dissolution vessel. An external electric stirrer was used to control the agitation speed (RPM's).

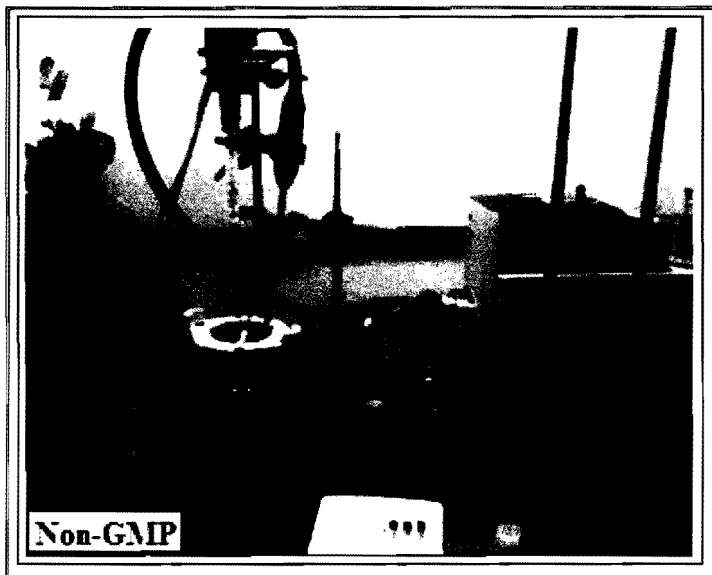


**Figure 7-5      Mettler Toledo ATR-IR/ Dissolution Systems**

The figure below shows a photo of the Mettler Toledo ATR-IR system coupled with a DiComp fiber optic probe. The photo shows the DiComp probe inserted into a standard dissolution vessel. The Vankel six-vessel dissolution system was used for during testing.

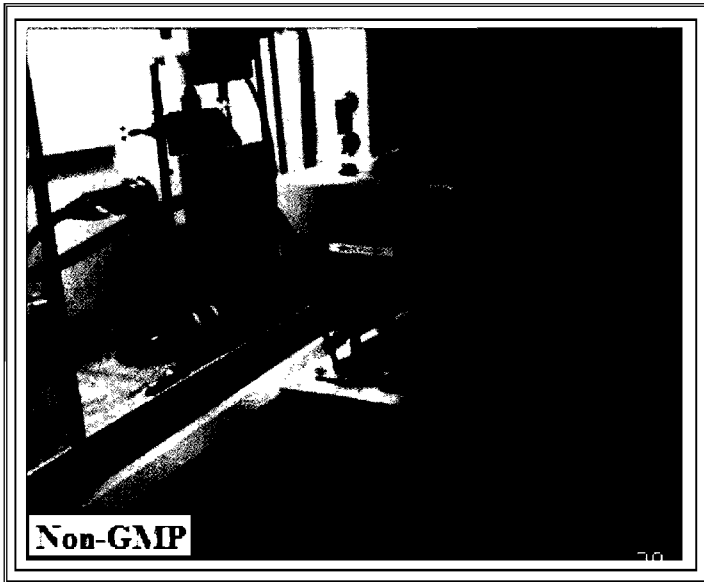


**Figure 7-6      Flow Cell Fiber Optic Probe:**

The figure below shows a photo of the Mettler Toledo ATR-IR system coupled with a Flow Cell fiber optic probe. Plumbing from the Flow Cell was attached to an Agilent six-port valve pump. Also, plumbing from a dissolution vessel was attached to the pump. Thus, a close-loop system was created whereby dissolution samples were drawn to the flow cell via the pump and back to the dissolution vessel. Homogeneous mixing, within the dissolution vessel, was achieved using a stir plate and magnetic stir bar.

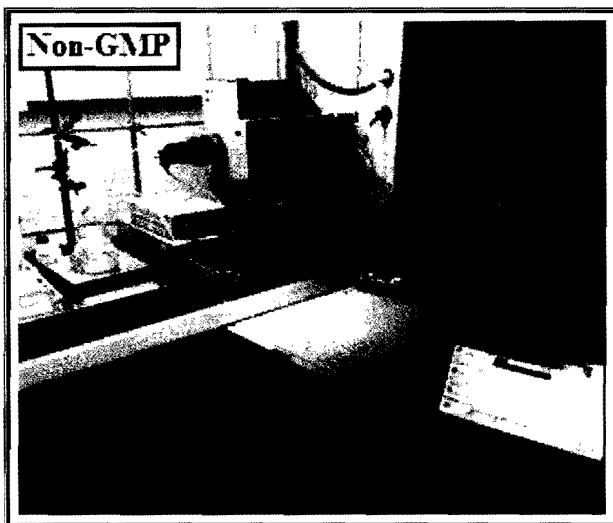


**Figure 7-7      K4 Fiber Optic Probe**

The figure below shows a photo of the Mettler Toledo ATR-IR system coupled with a K4 Conduit fiber optic probe. The photo also shows a dissolution vessel attached to the K4 probe. The dissolution vessel was produced out of a methanol bottle. A valve was attached to the vessel in order to empty the vessel contents during dissolution runs and cleaning.



**Figure 7-8 HPLC analysis for Salicylic Acid calibrator tablets**

**Salicylic Acid Tablets (HPLC Analysis)**

Batch No.: Salicylic Acid calibrator tablets Lot # Q0D200

Sample Name	Vial No.	Injection	Result ID	RT	Area
Standard 1	1	1	2533	0.7	4252948
30min	2	1	2534	0.7	472913
1 hour	3	1	2535	0.7	891091
2 hour	4	1	2536	0.7	1629150
3 hour	5	1	2537	0.7	2259379
6.5 hour	6	1	2538	0.7	3764607
7 hour	7	1	2539	0.7	4064077
Standard 1	1	1	2533	0.7	4252948

Standard-1 Weight (mg):	60.01	Standard-1 Avg Area	4252948
Standard Declared Content (%):	100.0	Std-1Wt/Std-1PA:	1.411.E-05
Vessel Volume (mL)	500.0		
Potency (mg)	300.0		
Standard Volume (mL)	100.0		
Sample (mL)	1.5		

Time (hour)	Vessel Volume
0.5	500.0
1	498.5
2	497.0
3	495.5
6.5	494.0
7	492.5

Time (hour)	% Dissolved (HPLC)
0.5	11%
1	21%
2	38%
3	53%
6.5	88%
7	95%

**Figure 7-9 HPLC Method Parameters: Single Component and Multi Component Experiments**

**HPLC Parameters (HP1050)**

- \* Symmetry 300 C18 5 $\mu$ m column (4.6mm $\times$ 50 mm),
- \* Mobile phase: 60/40/1 (water/methanol/glacial acetic acid),
- \* Flow rate: 2.0 ml/min, isocratic mode, Injection volume = 5  $\mu$ L
- \* UV detector was set at 296 nm.

**HPLC Parameters (Waters 2695)**

- \* Symmetry Shied RP C18 3 $\mu$ m column (3.5mm $\times$ 50 mm)
- \* Mobile phase: 70/30/1 (water/acetonitrile/trifluoroacetic acid (TFA)),
- \* Flow rate: 1.5 ml/min, isocratic mode, injection volume was 5 $\mu$ l. UV detection was set at 296 nm.

**HPLC Parameters (HP1050)**

- \* Phenomenex Intersil ODS C18 5 $\mu$ m column (4.6mm $\times$ 150 mm),
- \* Mobile phase: 60/40/1 (methanol/water/trifluoroacetic acid (TFA)),
- \* Flow rate: 1.0 ml/min, isocratic mode, injection volume : 25 $\mu$ l
- \* UV detection was set at 280 nm.

**Figure 7-10** Typical Excedrin® experiment spectra

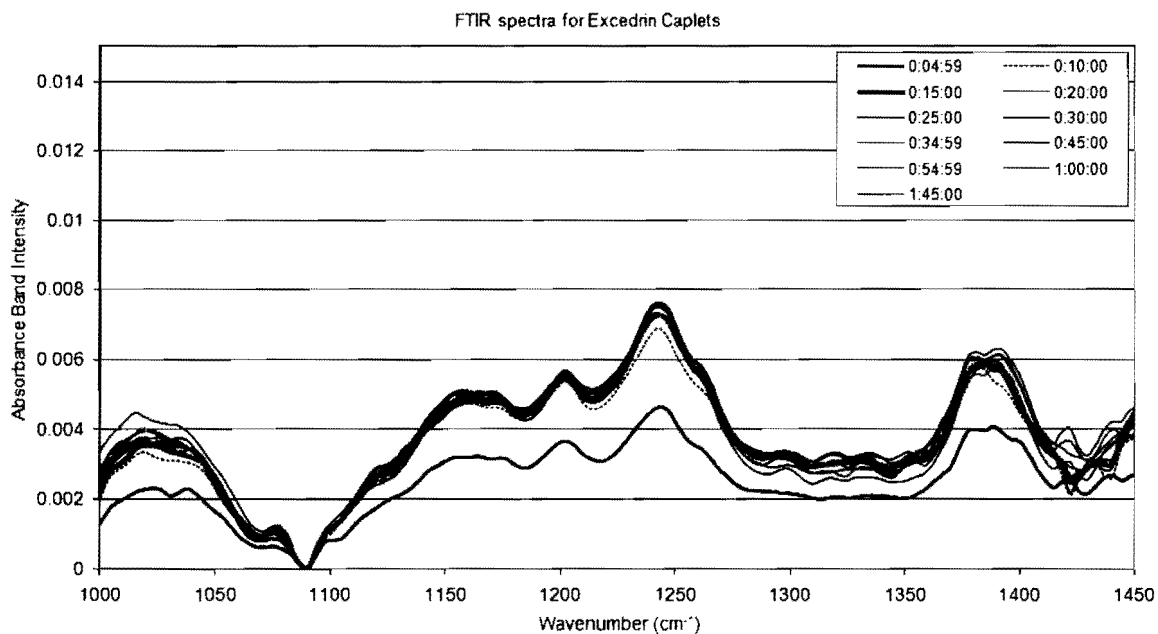
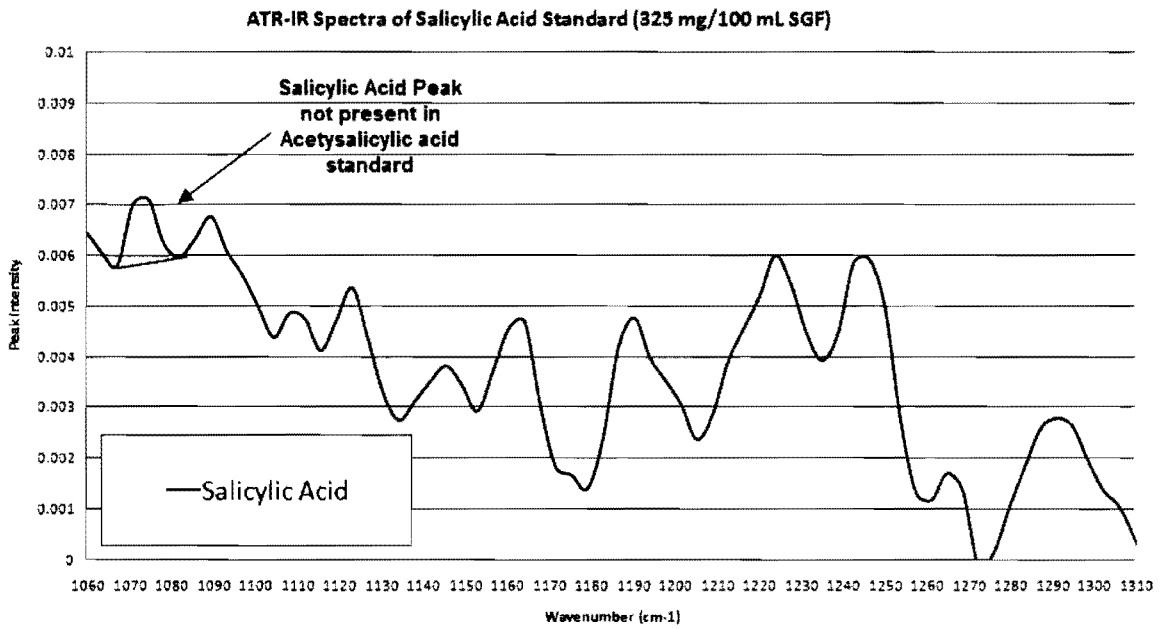


**Figure 7-11** Excedrin® HPLC Data

	Ret time (min)	Area
Acetaminophen	2.033	19015.8
AcetylSalicylic Acid	3.585	9004.3
	Acetaminophen	Acetylsalicylic Acid
10 min	15856.1	8684.1
20 min	16144.8	8848.6
30 min	18301.0	9224.6
1 hour	18868.4	9341.3
	% Acetaminophen	% Acetylsalicylic Acid
0	0	0
10	83.4	96.4
20	84.1	97.3
30	94.3	100.4
60	96.2	100.6

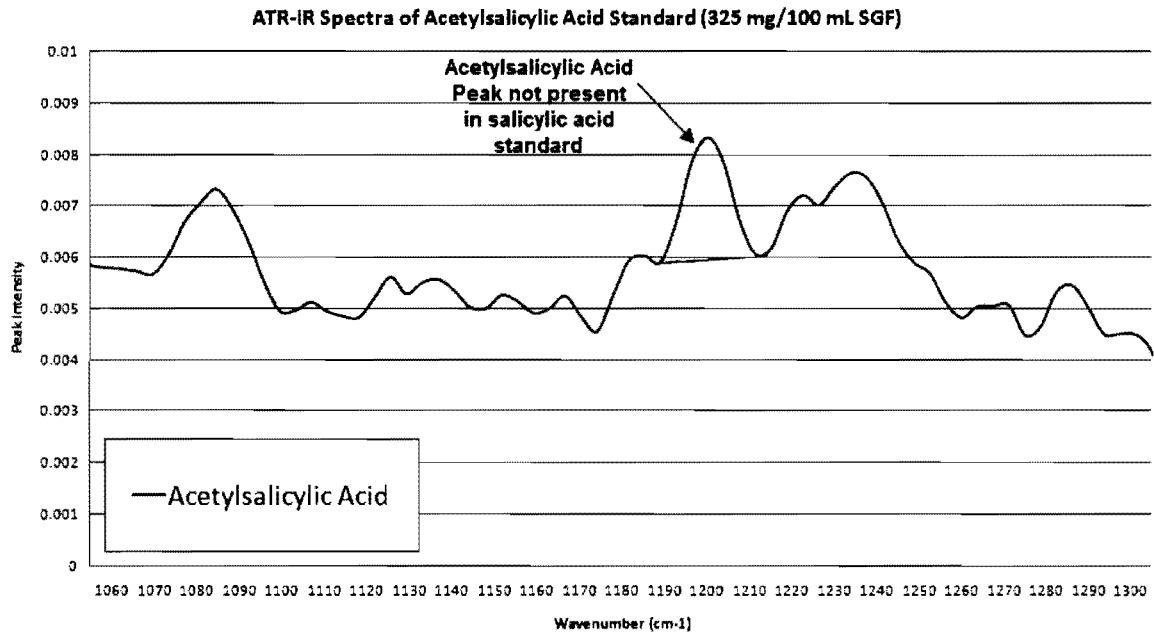
## 8 Appendix [B]: Studying drug kinetics via ATR-IR Spectroscopy

Figure 8-1 Salicylic Acid standard spectra





**Figure 8-2 Acetylsalicylic Acid standard spectra**



**Table 8-1 Aspirin FT-IR Frequencies of Interest**

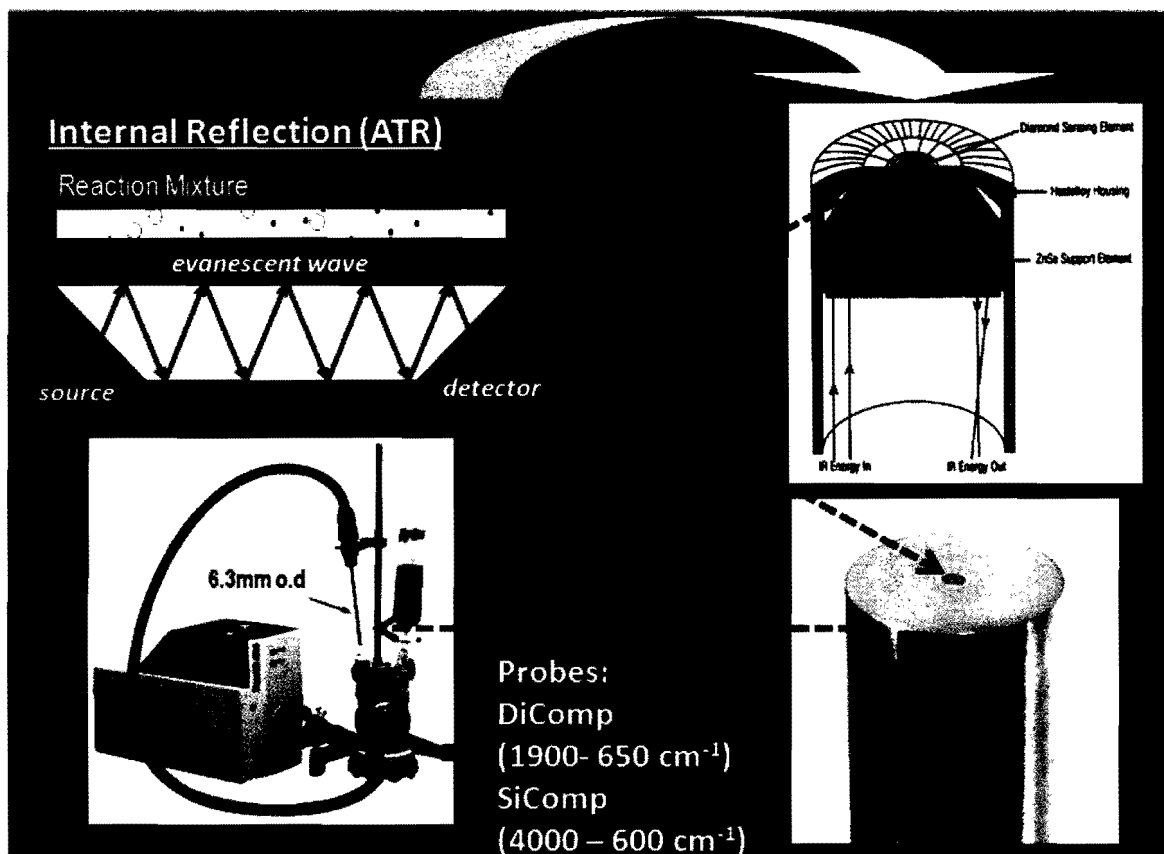
<b>Wavelength (c-m<sup>-1</sup>)</b>	<b>Assignment</b>
2300-2500	carboxyl OH
1760	vinyl ester C=O
1690	aromatic acid C=O
1610	aromatic acid C=O
1580	aromatic C=C stretch
1490	aromatic C=C stretch
1220	=C-O (acid and ester)
1190	=C-O (acid and ester)
760	ortho substituted phenyl C-H bending

**Figure 8-3 Rate Order Formulas and Equations (Reproduced from Wikipedia website on Rate Order)**

	Zero-Order	First-Order	Second-Order	n <sup>th</sup> -Order
Rate Law	$-\frac{d[A]}{dt} = k$	$-\frac{d[A]}{dt} = k[A]$	$-\frac{d[A]}{dt} = k[A]^2$	$-\frac{d[A]}{dt} = k[A]^n$
Integrated Rate Law	$[A] = [A]_0 - kt$	$[A] = [A]_0 e^{-kt}$	$\frac{1}{[A]} = \frac{1}{[A]_0} + kt$	$\frac{1}{[A]^{n-1}} = \frac{1}{[A]_0^{n-1}} + (n-1)kt$ [Except first order]
Units of Rate Constant (k)	$\frac{M}{s}$	$\frac{1}{s}$	$M \cdot s$	$\frac{1}{M^{n-1} \cdot s}$
Linear Plot to determine k	$[A]$ vs. $t$	$\ln([A])$ vs. $t$	$\frac{1}{[A]}$ vs. $t$	$\frac{1}{[A]^{n-1}}$ vs. $t$ [Except first order]
Half-life	$t_{1/2} = \frac{[A]_0}{2k}$	$t_{1/2} = \frac{\ln(2)}{k}$	$t_{1/2} = \frac{1}{k[A]_0}$	$t_{1/2} = \frac{2^{n-1} - 1}{(n-1)k[A]_0^{n-1}}$ [Except first order]

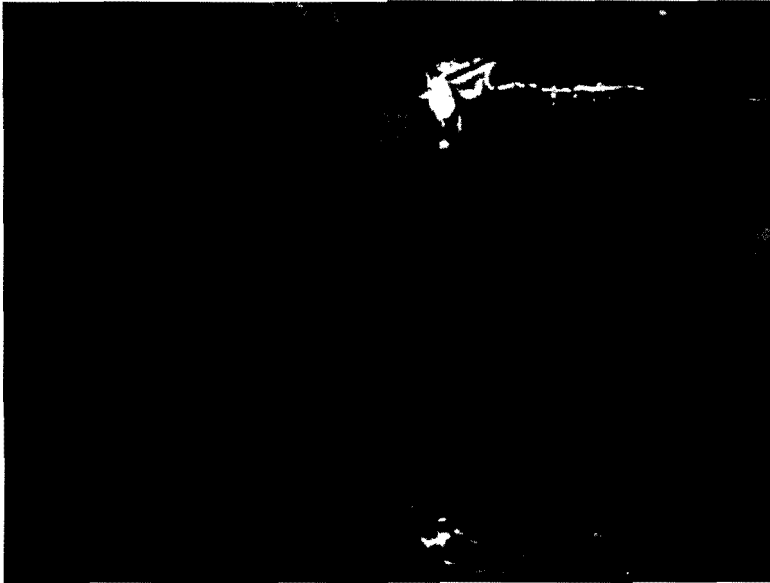
## 9 Appendix [C]: New Instrument Design (“Solv-IR”) attachments

Figure 9-1 ATR-IR Technique Diagram (courtesy of Jian Wang, Ph.D., Mettler Toledo)



## 10 Appendix [D]: BP Gulf oil research attachments

Figure 10-1 Detergents used during BP Gulf oil research





**Table 10-1 Amount of Dawn® dishwashing detergent added**

<b>Time (h:mm)</b>	<b>Volume added (ml)</b>	<b>Total volume in vessel (ml)</b>
0:01	1	1
0:04	1	2
0:06	1	3
0:08	3	6
0:10	3	9
0:13	3	12
0:14	3	15
0:17	3	18
0:19	3	21
0:20	3	24
0:22	3	27
0:24	3	30
0:26	3	33
0:26	3	36
0:28	3	39
0:34	3	42
0:39	3	45
0:41	3	48
1:48	3	51
2:06	3	54

Figure 10-3 Thermo Nicolet 4700: % Transmittance of OIL samples

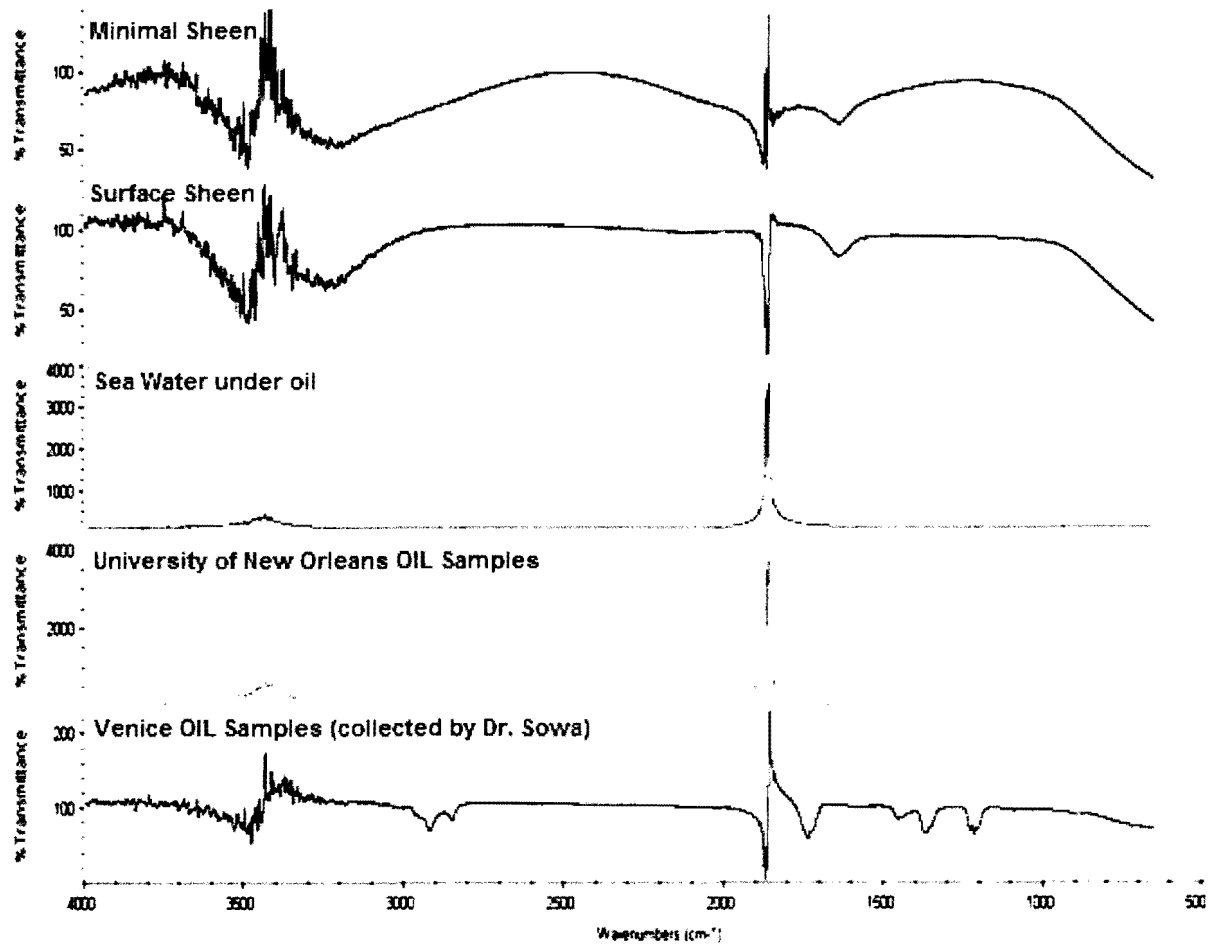




Figure 10-4 Thermo Nicolet 4700: Absorbance of OIL samples

